

# Medium Voltage DC Distribution Systems

## WG C6/B4.37

### Members

James YU, <b>Convenor</b>	GB
A. MOON	GB
G. LI	GB
T. JOSEPH	GB
N. MACLEOD	GB
W. LIU	GB
S. JUPE	GB
P. ATTAVIRIYANUPAP	JP
S. RUPP	DE
P. LURKENS	DE
G. D. CARNE	DE
A. LUKASCHIK	DE
G. KONSTANTINOU	AU

J. LIANG, <b>Secretary</b>	GB
C. LIU	CN
X. WANG	CN
Y. WANG	CN
Z. MA	CN
S. NORRGA	SE
R. MAJUMDER	SE
P. DWORAKOWSKI	FR
D. CORBET	FR
P. MAIBACH	CH
M. CORTI	IT
T. MANNA	US

#### Copyright © 2022

*"All rights to this Technical Brochure are retained by CIGRE. It is strictly prohibited to reproduce or provide this publication in any form or by any means to any third party. Only CIGRE Collective Members companies are allowed to store their copy on their internal intranet or other company network provided access is restricted to their own employees. No part of this publication may be reproduced or utilized without permission from CIGRE".*

#### Disclaimer notice

*"CIGRE gives no warranty or assurance about the contents of this publication, nor does it accept any responsibility, as to the accuracy or exhaustiveness of the information. All implied warranties and conditions are excluded to the maximum extent permitted by law".*



ISBN : [to be completed by CIGRE]

Internal Use

## Executive Summary

**Power Electronics** is a critical enabler for an accelerated transition to achieve a net-zero carbon electricity network. Such technology provides controlled power flow as DC couplers, point-to-point connections as DC links and meshed DC grids with multiple points of connection. **Medium-voltage DC (MVDC)** can be viewed as acting in the same way as high-voltage DC (HVDC) systems in transmission grids, just on a smaller scale and over comparatively shorter distances or at a specific site. Such MVDC systems allow **much more flexible ways of grid operation** beyond the scope of conventional AC systems by flexible power flow control, increased connection capacity on the same infrastructure compared with AC and voltage optimisation, hence a more efficient use of grid resources.



Embedded as part of distribution grids, MVDC systems are expected to facilitate a growing number of distributed renewable energy sources, which require power electronics interfaces largely, and a growing number of DC loads. MVDC systems are envisaged to collect power from renewable resources (such as the collection system of the onshore and offshore wind farms and solar farms) and to distribute power to DC loads such as hydrogen, power-to-gas, high power charging and energy storage systems. In addition to the direct connections, **MVDC distribution systems are envisaged to take on more significant duties** including:

- Enabling more power transfer from the existing assets, to create access to networks for more distributed resources
- Enabling faster power charging for an electrified transport system through DC charging
- Providing a more controllable means to enable a more reliable supply
- Providing a more efficient and sustainable network by reducing overall system power losses
- Enabling more services that distribution system owners and the connected users can provide for the system operation, i.e. Distribution System Operation transition
- Coupling between low voltage (LV, e.g., 400 V) and transmission voltage (higher than 132 kV) to enable a holistic control

Based on the previous efforts from CIGRE working groups of both **C6** (Active Distribution Systems and Distributed Energy Resources) and **B4** (DC Systems and Power Electronics), the working group: C6/B4.37 – Medium Voltage DC Distribution Systems has been set up to produce this technical brochure at the international level, particularly driven by **Angle DC**, an international ground breaking UK flagship **Network Innovation Competition** Project.

In this technical brochure, key findings and engineering standards regarding the **planning and design, project delivery, operation and protection**, and **grid interconnection of MVDC distribution** systems have been discussed. This TB reflects **the latest industrial insights** and the **effective interactions between research communities and the industry at the international level to uplift the readiness of MVDC market**. The potential advantages of MVDC networks as an integrated part of and an alternative to AC distribution networks are explored. MVDC standards are summarised. MVDC drive systems and their applications are also provided.

To achieve a future power electronics based MVDC system, a lot of efforts are still needed: **low-cost, high-efficient and reliable power converters, fast and reliable DC protection** equipment, system **control and protection approaches, holistic planning criteria and tools**, etc. This technical brochure will contribute to promoting the development of DC technology in distribution systems from both research and industrial practices.

# Contents

Executive Summary.....	1
Contents .....	2
<b>1 Introduction.....</b>	<b>7</b>
1.1 Background.....	7
1.2 Scope .....	7
1.3 Structure of this Technical Brochure .....	8
1.4 MVDC Systems: Needs and Drivers .....	8
1.5 MVDC Projects: State-of-the-art.....	9
<b>2 MVDC Distribution System Planning and Design .....</b>	<b>14</b>
2.1 Impact of MVDC on Performance.....	14
2.1.1 Reduction from Three to Two Conductors at Equal Current Density .....	15
2.1.2 Thermal Conditions of AC and DC Lines at the Same Material Budget.....	16
2.1.3 DC Stress on Insulation .....	17
2.1.4 Amount of Insulation Material .....	19
2.1.5 Overall Line Performance .....	19
2.1.6 Summary.....	21
2.2 Economics of MVDC Systems.....	23
2.3 MVDC Bus Architectures and Configuration.....	25
2.4 Experience from DC Microgrid Planning and Design .....	28
2.4.1 Planning and Design Objectives .....	28
2.4.2 Different Solution Models.....	29
2.4.3 DC Microgrid Standards.....	29
2.5 Assessment of MVDC Converter Reliability .....	30
2.6 MVDC Standards.....	32
2.6.1 Factory Tests .....	32
2.6.2 Site and Commissioning Testing .....	34
<b>3 MVDC Network Operation and Protection Requirements .....</b>	<b>37</b>
3.1 Connection of DER and Loads to MVDC Networks .....	37
3.1.1 Power Flow Management .....	40
3.1.2 Voltage Management.....	41
3.1.3 Congestion Management in AC Networks.....	42
3.1.4 MVDC Sub-transmission.....	44
3.2 Dynamic Models of MVDC Converters and Networks .....	44
3.2.1 Converter Dynamic Behaviour - AC.....	45
3.2.2 Converter Dynamic Behaviour - DC.....	46
3.2.3 Converter Behaviour When Operating Between Two Grids .....	48
3.3 Multi-terminal MVDC Grid Operation and Control.....	49
3.3.1 Converter Control.....	50
3.3.2 System Control.....	51
3.4 Operation of MV Networks with MVDC under Fault Conditions .....	54
3.4.1 MVDC Grid Scenarios.....	56
3.4.2 Fault Conditions in AC and DC Grids .....	57
3.4.3 Effects on Fault and Protection of the MV Network.....	59

3.4.4	MVDC Protection Approaches, Fault Detection Algorithms and Settings .....	62
<b>4</b>	<b>Interconnections of MVDC to HV and LV Systems .....</b>	<b>65</b>
4.1	Interconnection of MV and HV to Form Larger Grids .....	65
4.2	Interconnection of MVDC Networks to LVDC .....	70
4.3	LV DER Integration .....	73
4.4	Connection of AC and DC Loads .....	75
4.5	MVDC Power Conversion Topologies .....	80
4.5.1	Modular Multilevel DC-DC Converters .....	80
4.5.2	Dual Active Bridge Based DC-DC Converters .....	82
<b>5</b>	<b>MVDC Drive Systems .....</b>	<b>86</b>
5.1	MV Drive Power Conversion .....	86
5.2	Stability Issues of MV Drive Systems .....	88
5.3	Standards Used for Drive Systems .....	90
5.4	Learnings from Drive Systems .....	90
<b>6</b>	<b>MVDC Applications .....</b>	<b>94</b>
6.1	Offshore Wind Power MVDC Collection Systems .....	94
6.2	Marine Vessels .....	96
6.3	Transportation .....	98
6.4	Microgrids at Mine Sites .....	99
<b>7</b>	<b>Summary and Outlook .....</b>	<b>102</b>
	<b>Acknowledgements .....</b>	<b>103</b>
	<b>Appendix A List of Abbreviations .....</b>	<b>104</b>
	<b>Appendix B Case Studies .....</b>	<b>105</b>
	<b>References.....</b>	<b>112</b>

## Figures and Illustrations

Figure 1.1 Tangjia Bay MVDC distribution pilot project [12].	10
Figure 1.2 The five-terminal MVDC distribution network project in Guizhou University [14].	10
Figure 1.3 Zhangbei AC/DC network [15].	11
Figure 1.4 Jiangdong AC/DC network [16].	12
Figure 1.5 Suzhou AC/DC network [17].	12
Figure 1.6 Wenchang MVDC project AC to DC operation schematic [19].	13
Figure 2.1 Comparison of a 3-phase line (left) with a DC line (right) with equal cross section and insulation stress.	15
Figure 2.2 Thermal conditions shown in correct proportions (o: Max. mantle temperature, o-o: max. temperature difference across insulator)	17
Figure 2.3 Electric field AC vs. DC operation, $V_{0DC}=24.5$ kV, $V_{AC,RMS}=30$ kV.	18
Figure 2.4 Maximum electric field in the DC cable configurations.	18
Figure 2.5 Point-to-point transmission: MVAC (top) and MVDC (bottom) [21].	21
Figure 2.6 Distribution networks under study.	25
Figure 2.7 Network configuration diagrams: (a) point to point, (b) radial, (c) ring, (d) meshed.	26
Figure 2.8 Line configuration diagrams including AC-DC converter and DC-DC converter (isolated or non-isolated): (a) asymmetric monopole, (b) symmetric monopole, (c) bipole, (d) hybrid bipole/symmetric monopole.	27
Figure 2.9 DC-DC converter symbols: (a) DC-DC converter, (b) non-isolated DC-DC converter, (c) isolated DC-DC converter.	28
Figure 2.10 Key requirement to be considered when planning and designing a DC microgrid.	29
Figure 2.11 Comparison of five characteristics of VSCs at different MVDC voltage levels	32
Figure 2.12 Progressive commissioning sequence of an MVDC link post-installation phase.	36
Figure 3.1 MVDC grid operation.	38
Figure 3.2 DC grid connection for DER and loads.	39
Figure 3.3 Options to connect DER and loads.	39
Figure 3.4 DC links and couplers provide controlled power flow.	40
Figure 3.5 DC connections for DER and loads need grid forming converters.	41
Figure 3.6 Grid reinforcement.	43
Figure 3.7 DC Grid forming converters on DC links and couplers.	44
Figure 3.8 MVDC links at sub transmission layer.	44
Figure 3.9 Schematic of a grid-connected converter and, right, the equivalent signal flow diagram.	45
Figure 3.10 Bode diagrams of the MMC ac-side admittance for different control schemes: fixed references (blue); per-phase AC-side current control and circulating current control (yellow); dq frame AC-side current control and circulating current control (red). Results from the measurements on prototype (dots) and the analytical model (lines) are shown [48].	46
Figure 3.11 Bode diagrams of the MMC DC-side admittance for different control schemes: dq-frame AC-side current proportional controller (purple); addition of circulating current proportional controller (yellow); addition of circulating current resonant controller (brown); addition of AC-side current integral controller (red). The analytical models are indicated by the solid lines and the measurements with dots [55].	47
Figure 3.12 Converter forming a DC grid.	47
Figure 3.13 Simplified converter model (DC side).	48
Figure 3.14 Dynamic model of the DC grid.	48
Figure 3.15 Converter model between two grids.	49
Figure 3.16 Multi-terminal MVDC and MVAC grids.	49
Figure 3.17 P-U curve for constant power control.	51
Figure 3.18 P-U curve for constant voltage control.	51
Figure 3.19 Master-slave control.	52
Figure 3.20 Voltage margin control.	52
Figure 3.21 Droop control.	53
Figure 3.22 Example of hybrid AC and DC grids.	55
Figure 3.23 A multi-terminal MVDC grid scenario.	56
Figure 3.24 MVDC fault conditions.	58
Figure 3.25 MVDC operating modes.	60
Figure 3.26 Grid scenario in power feeding mode.	61
Figure 3.27 Grid scenario in grid forming mode.	62
Figure 4.1 Schematic of AC substation connections: (a) point-to-point, (b) multi-terminal.	66
Figure 4.2 Classification of DC-DC converter topologies.	67
Figure 4.3 General diagrams of isolated DC-DC converter topologies: bidirectional, unidirectional step-up and unidirectional step-down.	68
Figure 4.4 HVDC DC-DC converters proposed in CIGRE TB 827: isolated DC-DC converter (left) and non-	

isolated DC-DC converter (right) [70].	68
Figure 4.5 Configuration of the TLC-MMC converter dedicated to MVDC-HVDC power conversion [74].	69
Figure 4.6 Basic bidirectional non-isolated DC-DC converter.	70
Figure 4.7 Series resonant converter (SRC).	71
Figure 4.8 LLC DC-DC resonant converter (LLC).	72
Figure 4.9 Phase-shifted full bridge (PSFB).	72
Figure 4.10 Dual active bridge (DAB).	72
Figure 4.11 Example of power grid modernization [87].	74
Figure 4.12 Example of an MVDC system [88].	75
Figure 4.13 Example of an LVDC system [88].	75
Figure 4.14 Implementation of AC and DC loads in the MVDC grid.	76
Figure 4.15 DC-AC interface with a VSC and a transformer.	76
Figure 4.16 DC-AC interface with a solid-state transformer and an optional energy storage.	76
Figure 4.17 DC-DC interface with isolated and non-isolated DC-DC converter.	77
Figure 4.18 Configuration of bipolar-type DC distribution system with the EV stations [89].	77
Figure 4.19 System layout with solar PV, wind DER; LVDC, MVDC, AC buses [90].	78
Figure 4.20 (a) Magnetic linked MVDC converter-based wind power conversion system; (b) Magnetic linked MV converter for HTS cable-based DC transmission systems [91].	79
Figure 4.21 Schematic of a ZEDS and a generic i-th zone.	80
Figure 4.22 Isolated modular multilevel DC-DC converter [96].	81
Figure 4.23 Isolated resonant mode modular DC-DC converter [97].	81
Figure 4.24 Isolated modular multilevel DC-DC converter consisting of an MMC stage at medium-voltage side connected to an MVDC bus [100].	82
Figure 4.25 LPHR modular multilevel DC-DC converter [101].	82
Figure 4.26 High frequency-link DC transformer based on switched capacitor [98].	83
Figure 4.27 CF-MDAB converters: (a) Single-phase, and (b) three-phase [99].	83
Figure 4.28 Comparison of (a) MDCT, and (b) ADCT [102].	84
Figure 4.29 5-level DAB DC-DC converter [103].	84
Figure 4.30 Isolated double step-down converter [104].	85
Figure 5.1 Two-level converter topology.	86
Figure 5.2 Three-level NPC converter.	87
Figure 5.3 Three-level ANPC converter.	87
Figure 5.4 Five-level cascaded H-bridge converter [105].	88
Figure 5.5 Modular multilevel converter for MV drives [105].	88
Figure 5.6 DC distributed power system [106].	89
Figure 5.7 A typical MV drive system with DC filters [107].	89
Figure 5.8 DC shipboard distribution system [109].	91
Figure 5.9 Structure of VSC-based MVDC TPSS [110].	91
Figure 5.10 Various DC grid configurations and interface: (a) multidrive approach and (b) distributed approach [111].	93
Figure 5.11 The structure of the next-generation MVDC shipboard power system [112].	93
Figure 6.1 MVDC cluster for a wind park [93].	94
Figure 6.2 MVDC cluster for a wind park [118].	95
Figure 6.3 MVDC architecture in an offshore oil-drilling application with a co-located wind farm [119].	96
Figure 6.4 Functional MVDC block diagram [121].	97
Figure 6.5 MVDC used in railway systems, a) classical approach; b) possible future approach [93].	98
Figure 6.6 A VSC-based MVDC traction power supply system [126].	99
Figure 6.7 Dual-voltage locomotive for 24 kV and 3 kV DC catenary voltages [126].	99
Figure 6.8 The schematic of an islanded MVDC microgrid at the mine site [127].	100
Figure 6.9 Block diagram of the control strategy and the power flow [127].	101
App Figure D.1 - Angle DC project.	105
App Figure D.2 - System configuration of the ANGLE-DC project with three-level NPC converters.	106
App Figure D.3 - DC voltages and currents with power flow increasing from 0 to 100%.	106
App Figure D.4 - AC voltages and currents with power flow increasing from 0 to 100%.	107
App Figure D.5 - DC voltages and currents with ramp change of power from 0 to 100% to 0.	107
App Figure D.6 - AC voltages and currents with ramp change of power from 0 to 100% to 0.	108
App Figure D.7 - DC voltages and currents with step change of power flow.	108
App Figure D.8 - AC voltages and currents with step changes of power flow.	109
App Figure D.9 - Interconnections of MVDC to HV and LV systems.	109
App Figure D.10 - Configurations of the DC system.	110
App Figure D.11 - Waveforms of AC voltages and DC.	110
App Figure D.12 - Waveforms of DC voltages and active power of the MVDC systems.	111
App Figure D.13 - Waveforms of DC voltages and active power of the LVDC systems.	111

## Tables

Table 2.1 CapEx and OpEx Benefits of ANGLE-DC .....	24
Table 2.2 Cost-benefit analysis of different scenarios [24]. .....	25
Table 2.3 Summary of applicable testing standards for MVDC factory acceptance testing. ....	32
Table 2.4 Summary of applicable IEC 62501 testing standard clauses cross referenced with inverter drive testing standards. ....	33
Table 2.5 Transferable tests from the HVDC LCC commissioning standard .....	34
Table 4.1 Qualitative comparison of selected isolated DC-DC converter topologies highlighting the main differences (* - bidirectional power flow is possible).....	72

# 1 Introduction

## 1.1 Background

Regional sub-transmission networks and medium voltage (MV) distribution grids play a vital role in controlling the bidirectional power flows that characterize today's, and future, energy ecosystems. The increasing power infeed at the MV level from distributed energy resources (DER) brings additional challenges to the existing infrastructure. Many of the DER being deployed make use of power electronic converters as the interfaces to connect to the AC grid. Wind, solar and battery energy storage systems are examples of such DER.

The conversion to and from AC sources requires additional steps of using power electronics interfaces which can be avoided if DC distribution systems are available, resulting in reduced conversion losses and potentially reduced capital cost. In addition, system losses are reduced, and the distribution operation can be simplified by the deployment of a DC network. The enabling technologies to implement MVDC power systems, such as semiconductor switches and converter topologies are already in place. Converting from one DC level to another is also mandatory in future DC networks with multiple voltage levels, then more power electronics and conversion steps may be involved, which could result in related power losses and costs. Sufficient expertise has been leveraged from the industrial practices (e.g. ANGLE-DC project or Network Equilibrium project) through the involvement of Distribution Network Operators (DNOs) and experts around the world in the conceptualization and delivery of this technical brochure).

## 1.2 Scope

This joint working group (JWG) C6/B4.37 has built upon and leveraged the expertise and knowledge from different Study Committees to present the potential advantages of a DC approach (MVDC networks incorporating DER) as an alternative to AC distribution systems. The scope of this Technical Brochure (TB) is to explore and elaborate on the following topics:

1. Connection of DER and loads to MVDC networks.
2. Operation, control and protection of MVDC systems.
3. Planning, design and standards of MVDC systems.
4. Interconnection of MVDC systems to HV and LV systems.
5. Comparisons of medium voltage AC (MVAC) and MVDC systems.
6. Multi-terminal MVDC networks.
7. Experience and examples of deployments.
8. Guidelines and existing practices, techno-economic challenges and present and future solutions.

The focus of this technical brochure is on the structure, planning, operation and connection of MVDC systems to the existing power system architecture from a technology and benefits point of view. The topologies and structure of MVDC systems provided are reasonably replicable into a generic MV distribution network.

This technical brochure can be jointly read with the outcome of the recent CIGRE WG C6.31 (TB 793, [2]) for information on the feasibility of MVDC grids. Furthermore, other related CIGRE activities currently addressing this topic in detail are listed below for reference.

- CIGRE WG A3.40, "Technical Requirements and Field Experiences with MVDC Switching Equipment", ongoing

- CIGRE TB583, “Guide to the Conversion of Existing AC Lines to DC Operation”, 2014.

### 1.3 Structure of this Technical Brochure

This technical brochure contains seven chapters and two appendices. Further detailed analyses and examples to complement the guidelines and recommendations are provided in the chapters.

**Chapter 2 MVDC Distribution System Planning and Design** – The focus of this chapter is on distribution system planning and operation with MVDC. The economic and reliability analysis of MVDC systems is also discussed. The experience from DC microgrid planning and operation is presented. The efforts for developing MVDC standards is explored.

**Chapter 3 MVDC Network Operation and Protection Requirements** – This chapter identifies the requirements for power management, energy balance, power distribution, and power-sharing among DER and other sources. Distribution network operation with MVDC and co-ordination with other DER, like PV and wind farms, is discussed in this chapter. Typical control approaches of MVDC networks will be investigated. Protection with MVDC and its challenges will be another area which will be explored through this chapter.

**Chapter 4 Interconnections of MVDC to HV and LV Systems** – Future MVDC networks will be the middle layers interconnecting the HV and LV systems (not only DC but AC systems). Power conversion topologies for such interconnections are discussed in this chapter. Furthermore, the connection requirements of MVDC to HV and LV networks to form a cross-connected hybrid and multi-voltage system are explored. Specific focus is on the power conversion topologies, configuration, impact on the hosting of DER, and connection of DC and AC loads.

**Chapter 5 MVDC Drive Systems** – Power conversion technologies in MV drives are explored with particular focus on practical projects, standards, and potential risks, with lessons learned from the solutions implemented to be transferred to MVDC distribution networks.

**Chapter 6 MVDC Applications** – Practical and potential applications of MVDC are introduced in this section, include MVDC collection systems for offshore wind power, marine vessels, transportation and microgrids at mine sites.

**Chapter 7 Summary and Outlook** – Challenges, potential risks, and solutions for the widespread MVDC roll-out are summarized from the learnings of existing projects. Design recommendations and key considerations for MVDC system deployment are provided in this chapter.

### 1.4 MVDC Systems: Needs and Drivers

Power electronics-based network upgrades can solve issues associated with the traditional MV systems such as active control of power flow, independent reactive power compensation, and unbalances. To this end, the existing examples reported in TB 793 and the recent projects involving power electronics installations lead to the possibility of DC system operation in MV and LV networks. These practical examples use different DC technologies and aim to improve the efficiency, reliability and uptake of enhanced renewable and low-carbon sources at the distribution level.

Further to the motivation for MVDC deployment, the key driver for the deployment of such new technologies stems from governments’ commitment to achieving a low-carbon economy and sustainable development. In addition, the aging of the majority of existing electricity networks which were built in the 1950s and 1960s incurs significant investment from network companies to renovate the network while expanding it at the same time to meet the electricity demand growth. For instance,

Great Britain (GB) networks operators have collectively been set to spend over £26 billion between 2015 and 2023 to ensure the GB grid can provide adequate available capacity to allow secure energy transfer to the customers [1].

From the perspective of technology readiness level, in the past decades, the high-voltage direct-current (HVDC) technologies have been well-developed for transferring bulk power over long distances in electricity transmission systems. In particular, voltage source converter (VSC) based HVDC technologies are an appropriate solution for flexible grid interconnections and integration of renewable power sources. Low-voltage direct-current (LVDC) technologies have been used in renewable energy resources (solar and wind), power supply within aircraft and ships, public transport, motor drives, LED lighting, etc. MVDC technologies have been used in motor drive systems (e.g. transportation, marine vessels and more electric aircraft) and partly also in renewable energy resources (wind). However, they have not been widely used in electric power networks due to limited DC sources and DC loads at this voltage level. However, MVDC has potential benefits in solving the problems of power management, quality, operation and control in the existing AC distribution networks. MVDC can be used to form a new layer between future HVDC and LVDC networks.

Moreover, distribution network operators (DNOs) around the world are seeking new solutions and technologies to increase the power infeed from local DER, ways to reduce the footprint of network upgrades, enable connections to remote customers and integrate and stabilise the grid. Power electronics plays a significant role in addressing these challenges at different voltage levels and has received wide interest. However, the development of MVDC systems still faces the challenges associated with the wide application of power electronics devices. For instance, techno-economic MVDC converter design, secure and reliable operation of power electronics at the distribution level, flexible control and operation, fast and reliable protection, etc. Therefore, commercial innovations and engineering advancement alike are required to enable a smarter distribution network to meet the requirements of future electric power networks.

## 1.5 MVDC Projects: State-of-the-art

There have been some MVDC projects worldwide. For instance, the ANGLE-DC and Network Equilibrium projects in the UK, the Flexible Electrical Networks project in Germany, the Eagle Pass Tie project in the USA, the Nanhui, Jinzhai and Baolong projects in China. CIGRE TB 793 has provided an excellent summary of these MVDC projects around the world. Since then, there have been some more MVDC projects, which will be introduced in this section as a supplement of TB 793.

**Zhuhai Tangjia Bay Project** [12]-[13] – The MVDC network consists of three terminals with power capacities of 20 MW, 10 MW and 10 MW. The DC voltage is  $\pm 10$  kV. Hybrid DC circuit breakers are deployed in this MVDC grid for the first time. Dual active bridge (DAB) based DC-DC converters are used in this network to supply DC loads. The configuration of the Tangjia Bay MVDC project is shown in **Fig. 1.1**. The project is in Zhuhai China and was commissioned in 2018.

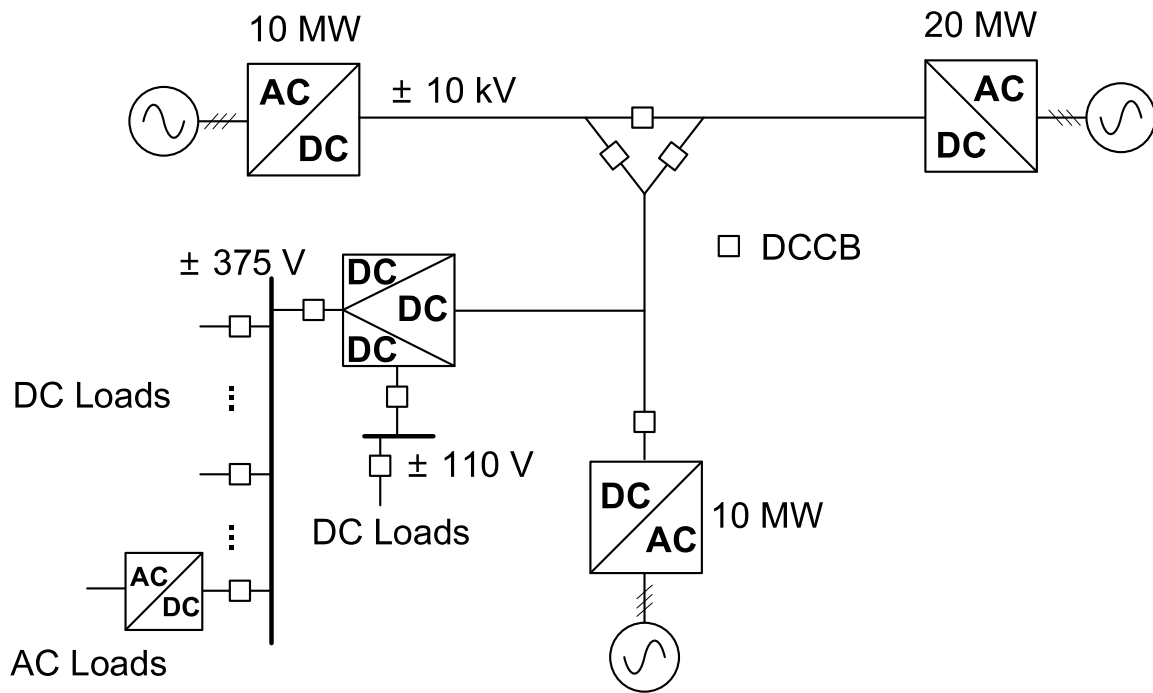


Figure 1.1 Tangjia Bay MVDC distribution pilot project [12].

**Guizhou University Demonstration Project** [14] – This MVDC project is the first five-terminal MVDC distribution project in China. This network consists of three subsystems, which are an MVDC subsystem, an LVAC microgrid, and an LVDC microgrid. The project features hierarchical distributed control based on the idea of ‘local autonomy’ and ‘regional coordination’. The DC voltage is  $\pm 10$  kV. Hybrid modular multilevel converters (MMCs) based on mixed half-bridge and full-bridge submodules, which have the DC fault blocking capability, are used in this project. The MVDC network adopts DC voltage droop control. The system configuration of this project is shown in Fig. 1.2. The project was commissioned in 2018.

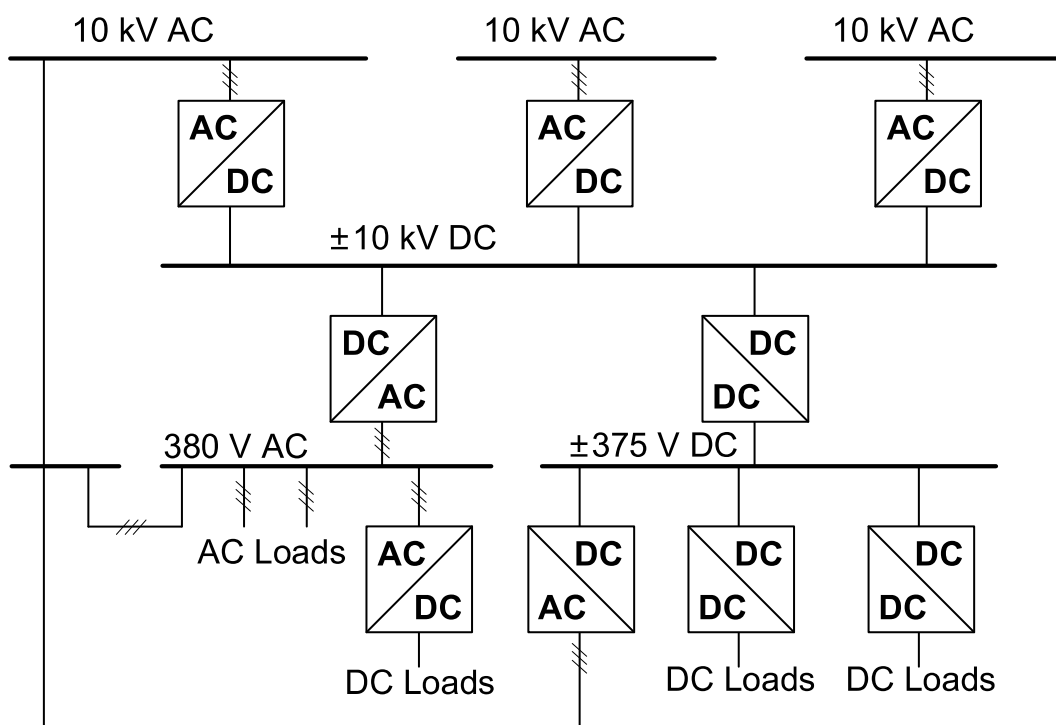
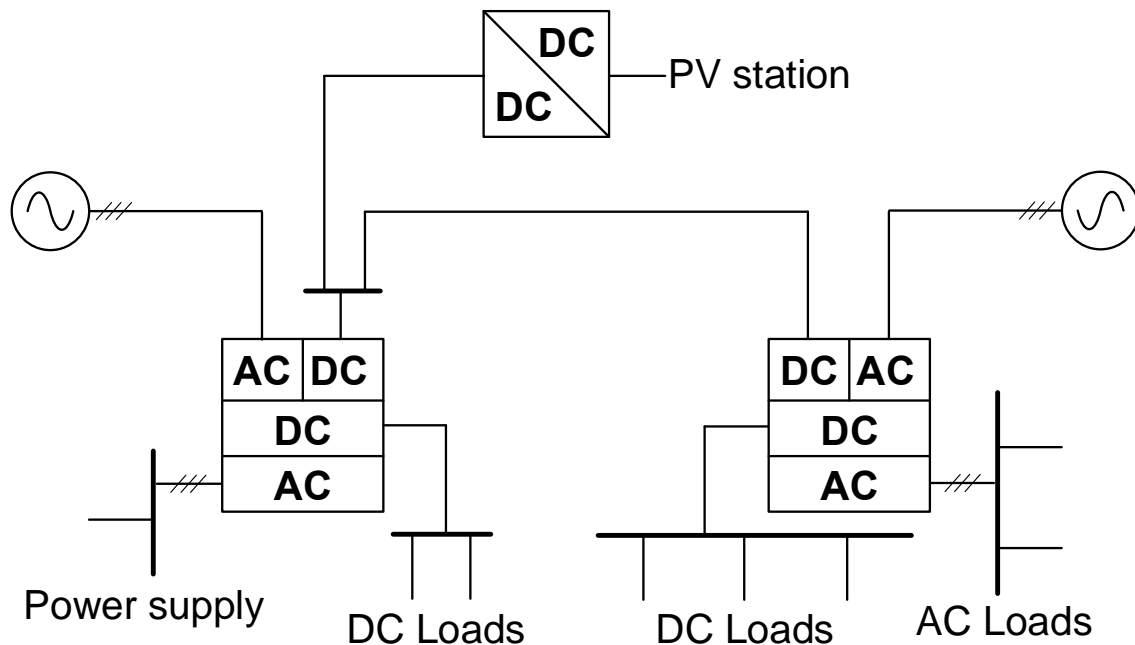


Figure 1.2 The five-terminal MVDC distribution network project in Guizhou University [14].

**Zhangbei AC/DC Demonstration Project** [15] – This MVDC distribution network was constructed from Oct. 2017 and commissioned in Dec. 2018. It is in the low-carbon demonstration zone for the 2022 Winter Olympics. The DC voltage is  $\pm 10$  kV. The feature of this project is the flexible substations. As the control centre of the flexible substations, multifunctional AC/DC power electronics transformers (M-PET) achieve the switching of operation modes as per the actual demand and the system information, realizing constant DC voltage control, DC power control, AC voltage control and AC power control, etc. The double clamp submodule (DCSM) is used in the MMCs in this network. The system configuration of this project is shown in **Fig. 1.3**.



**Figure 1.3** Zhangbei AC/DC network [15].

**Jiangdong MVDC Project** [16] – The MVDC distribution network in Jiangdong New City, Hangzhou is a smart-supply-oriented demonstration project based on the MVDC technique in urban areas, aiming to promote reliability, interaction, and cost-effectiveness. The project is a three-terminal MMC based network that realizes the interconnection of two 10 kV AC lines and one 20 kV AC line, as shown in **Fig. 1.4**. The DC voltage is  $\pm 10$  kV. The capacity of each MMC is 10 MW. DC circuit breakers and DC-DC converters are employed in this project. The project was commissioned in 2018.

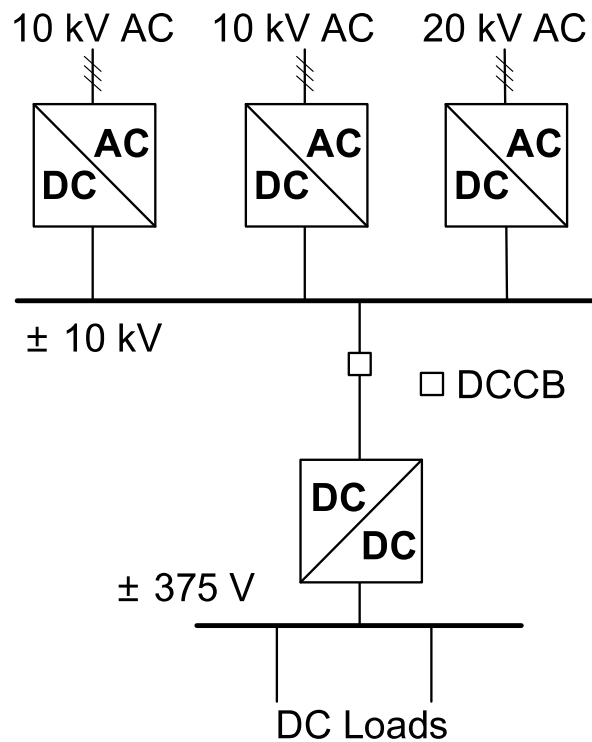


Figure 1.4 Jiangdong AC/DC network [16].

**Suzhou Industrial Park Pilot Project** [17] – This is a four-terminal  $\pm 20$  kV MMC-MVDC network. The DC network connects with four 20 kV AC lines as shown in Fig. 1.5. This topology and setup can flexibly form as two-line, three-line, and four-line connections. The power flow can be flexibly adjusted to achieve optimal power flow. AC circuit breaker based DC protection strategy is used in this project. The project is in Suzhou China and was commissioned in 2018.

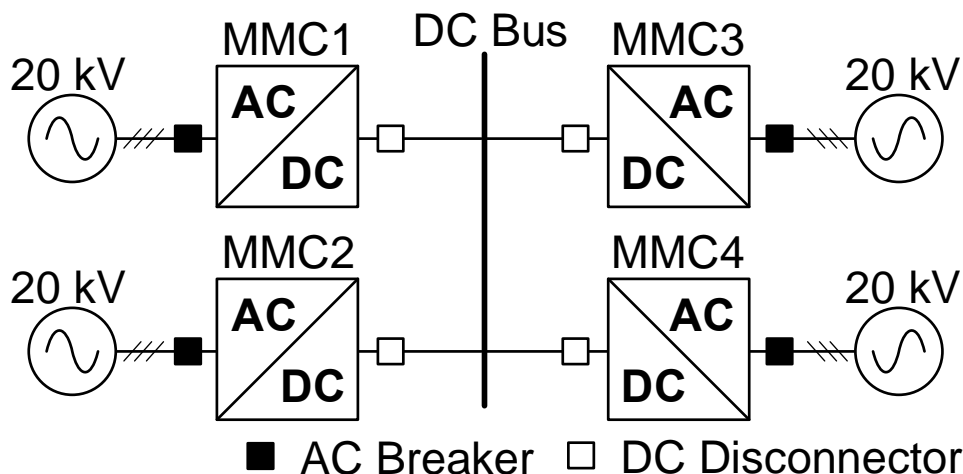


Figure 1.5 Suzhou AC/DC network [17].

**Wenchang Project** [18]-[19] – An MVDC system has been provided for part of the Wenchang platform submarine cable repair project. This was provided by a specialist power electronic equipment manufacturing on a turn-key basis [19]. The Wenchang project was started in 2010 as a product development and engineering departments to help address the urgent loss of supply security. The project aims to convert a faulted 35 kV AC line to a 3 MW,  $\pm 10$  kV DC line with VSC topology as discussed in [18]. A block diagram showing the MVDC system layout is shown in Fig. 1.6. The MVDC solution has been operating successfully since 2013.

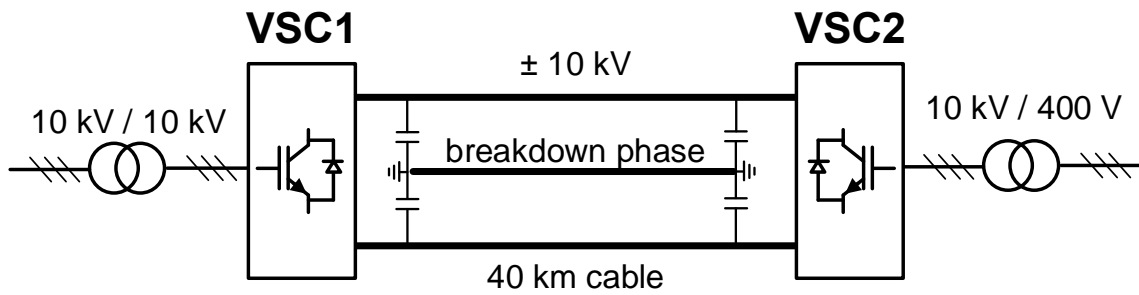


Figure 1.6 Wenchang MVDC project AC to DC operation schematic [19].

**Beichen AC/DC pilot project** – A national-level pilot project for a multi-terminal flexible hybrid AC/DC distribution network was implemented in Tianjin, China. The project aims to improve power supply reliability, optimise power flow of existing distribution systems, and provide appropriate accommodation for the future development of distributed renewable generation in this area. The project has a multi-state switching station which has been constructed for flexible connection of four 10 kV AC feeders at its AC side as well as the simultaneous provision of stable  $\pm 10$  kV and  $\pm 375$  V DC power supply at its DC side.

## 2 MVDC Distribution System Planning and Design

With the strong commitment to achieving a net-zero carbon electricity network, more distributed energy resources (DER) will require access to the network. Most of such connections are at medium voltage (132 kV and below) due to the location and connection costs. In the meantime, customers rightly expect the electricity networks that serve them to be ready to continue supporting their decarbonisation ambitions such as EV charging infrastructure, rooftop photovoltaics and household energy storage. Therefore, medium voltage networks (distribution networks) are critical in linking different vectors of our energy systems in such an accelerated low carbon transition.

This section will discuss the planning and operation of power systems with MVDC. Possible MVDC network configurations will be introduced. The economic and reliability analysis of MVDC systems will be discussed. The experience from the DC microgrid planning and operation will be presented. The efforts for developing MVDC standards will be explored. Although there have been some MVDC projects worldwide, there are no widely accepted MVDC standards and grid codes yet. The planning and operation of these MVDC projects are project-based. The discussion in this section is mainly based on the experience from the AC distribution system and DC microgrid, which are also valuable for the planning and design of MVDC distribution systems.

### 2.1 Impact of MVDC on Performance

Anticipation of advantages of MVDC grid technology is based largely on assumptions on material economy of DC lines in terms of insulation and conductor material use and increase of system voltage. Basically, this approach was also followed in the preceding CIGRE Working Group C6.31 (CIGRE TB793, [2]). There it was applied to a typical MVAC cable from a manufacturer's catalogue and focused on conductor temperature.

It has been discussed whether an increased DC operating voltage of a cable, designed for AC and typically having XLPE insulation, by some factor (“ $k_V$ ”, frequently  $\sqrt{2}$ ) is feasible. A reason for concern is the experience of failures after the introduction of XLPE insulation in cables for HVDC lines, in particular for LCC-HVDC lines. This has been investigated thoroughly and attributed to space charge effects resulting from various mechanisms of DC leakage conductivity and charge trapping in the insulation materials (Khalil [3]), Riechert et al. [4], [5]), and also leading to development of optimized insulation materials for HVDC cables (Kikuchi et al. [6]). Newer experimental studies on MVAC cables, tested in DC operation, however indicate, that common MVAC cables are most likely fit for operation at even higher voltage than a factor of  $\sqrt{2}$ . Schichler and Buchner ([7], [8]) successfully executed adapted LCC prequalification tests according to CIGRE TB 496 for an intended DC operating voltage of 55 kV on commercial XLPE insulated 12/20 kV MVAC cables, far beyond conservative operation at a DC voltage at the level of peak AC voltage. A reason for the promising finding might be that MVAC cables are operating at much lower in-service electric field strength than HVDC cables, whereby thresholds for charge trapping are probably avoided ([9], [10]). An important influencing factor is the temperature difference over the insulation, leading increasingly to inversion of the electric field profile, i.e. the maximum electric field is appearing at the outer diameter of the insulation rather than at the surface of the conductor. This requires a more detailed investigation of temperature conditions than for AC conditions.

Besides the increased voltage rating for the same quantity of insulation material in cables, further favourable properties of MVDC grid technology are anticipated, which differentiate it from AC grid technology. These are based predominantly on assumptions of increased current rating of cables for the same quantity of conductor material and the opportunity to apply medium-frequency converters for providing galvanic isolation and coupling different voltage levels. Using converters with switching

frequencies far above the 50 Hz of AC grids, reduces copper and steel consumption, especially for transformers, in DC grids. **Fig. 2.1** illustrates the increased rating of dc cables by showing a comparison of an AC and a DC cable system in correct aspect ratio for equal conductor cross section and equal maximum electric field in the insulation layer.

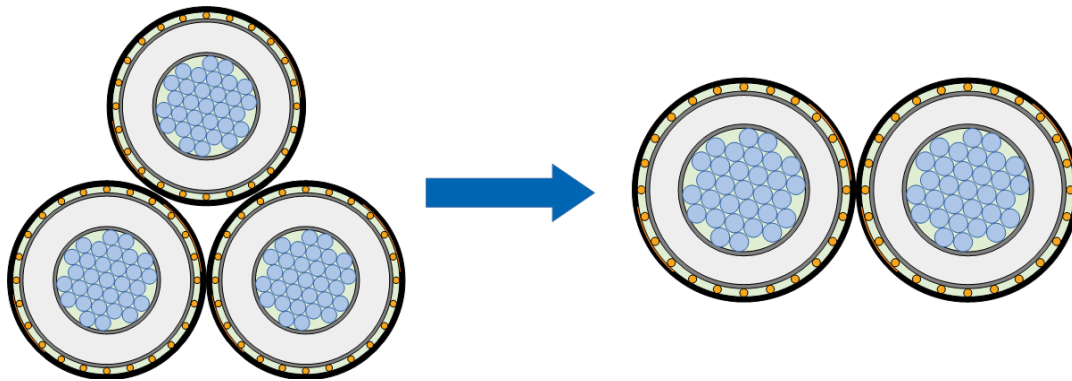


**Figure 2.1 Comparison of a 3-phase line (left) with a DC line (right) with equal cross section and insulation stress.**

In the following the impact of DC on transmission line material use is discussed in more detail, in particular in respect to electric fields in the insulation layer and temperature details. This is exemplified by, but not restricted to, dimensions of a readily available cable, where the material budget of a 3-phase AC line is used for a 2-conductor DC line. The subsequent comparison between AC and DC line performance with the same material budget is based on the following assumptions:

- Reference AC line with
  - line voltage  $V_{AC,RMS}$  (30 kV)
  - current capacity per conductor of  $I_{AC,RMS}$ , conductor cross section  $500 \text{ mm}^2$
  - insulation thickness of AC cable ( $d_{iso}$ , 8 mm)
  - aluminium fill factor 0.88
  - skin, proximity, and sheath losses in AC cable neglected in a first approach
  - AC line power factor  $\lambda = 0.9$
  - soil heat conductivity  $1 \text{ W/(m K)}$ , as in [2]
  - XLPE heat conductivity  $0.3 \text{ W/(m-K)}$
  - maximum temperatures: conductor  $90^\circ\text{C}$  or mantle  $70^\circ\text{C}$ , whatever is exceeded
  - temperature drop across mantle not considered
- The conversion to DC assumes:
  - material use (conductor, insulation) equal or less than that of AC line
  - peak electric field in DC cables equal or less than in AC cables
  - increase of line-to-earth DC voltage by a factor  $k_V$ :  $V_{0DC} = k_V \cdot \frac{V_{AC,RMS}}{\sqrt{3}}$
  - other parameters as AC line

### 2.1.1 Reduction from Three to Two Conductors at Equal Current Density

In a first step, the conductor material of the three AC cables is attributed to the two DC cables, which results in a higher cross sectional area of the individual conductors:

$$\frac{A_{DC}}{A_{AC}} = \frac{3}{2} \quad \left( \frac{R_{CDC}}{R_{CAC}} = \sqrt{\frac{3}{2}} \right)$$

with  $A_{DC}$  and  $A_{AC}$  being the cross sectional areas of the individual conductors and  $R_{CDC}$  and  $R_{CAC}$  the conductor core radii. The ratio of the ohmic resistance per length unit and per conductor of the

individual DC cable over the AC cable is:

$$\frac{r_{DC}}{r_{AC}} = \frac{2}{3}$$

When neglecting some AC related losses such as skin, proximity and sheath losses, the ratio of the allowed total line current, given equal line losses per length unit, would be defined by a current density in the DC conductors equal to the AC current density, just reflecting the ratio of the cross section areas:

$$\frac{I_{DC,RMS}}{I_{AC,RMS}} = \frac{3}{2}$$

### 2.1.2 Thermal Conditions of AC and DC Lines at the Same Material Budget

The concentration of the dissipation into two conductors, rather than three, the larger cable diameter compared to AC, the increased distance between the two conductors and the increased conductor core diameter all influences the thermal situation. To determine the current capacity in all the subsequent configurations, first the power dissipation in the conductor was set such that the temperature limits of the cable were just reached. Then the conductor currents were calculated from the power dissipation and the aluminium conductivity at the individually obtained temperature.

The original AC line determines the reference case for the allowed RMS current in the line, taking as an example a standard NA2XS(F)2Y 18/30kV 500 rm/35 (500 mm<sup>2</sup> conductor cross section and 35 mm<sup>2</sup> screen cross section) cable. Actually, the maximum conductor temperature of 90°C could not be exploited as the mantle temperature limit of 70°C is already reached when the core temperature is still at 79°C. The allowed RMS current is obtained as 702 A per conductor, so the total current load of the AC line calculates to 2106 A. The temperature difference across the insulation is only 9 K, which however is not very relevant for the AC line.

A conversion of the three AC conductors into two DC conductors with the same conductor material results in DC conductors with an effective cross sectional area of 750 mm<sup>2</sup> each and a radius of  $R_{CDC} = 16.47 \text{ mm}$ . For the conversion of the insulation two cases are evaluated here: The first case uses just the same standard insulation thickness of 8 mm as the AC cable (Fig. 2.2, upper right), while the second case uses the entire insulation material of the three AC cables (Fig. 2.2, lower right), resulting into an insulation thickness of 9.8 mm.

In the first conversion case the allowed current per conductor is 1033 A, at maximum temperatures of 70°C for the mantle and 81°C for the conductor, i.e. the total line current load is 2066 A, 1.8% less than the AC line. This difference is less than typical values of skin, proximity and shield losses. The maximum temperature difference across the insulation was obtained as 12 K. This is the temperature difference across the XLPE-Insulation, which occurs at the leftmost surface of the left cable and the rightmost of the right cable. The conductor temperature however is uniform. In the second conversion case the permissible current per cable is 1040 A, at maximum temperatures of again 70°C for the mantle and 83°C for the conductor, thus the total line current load 2080 A, which is 1.2% less than the reference. Here the maximum temperature difference across the insulation is 14 K.

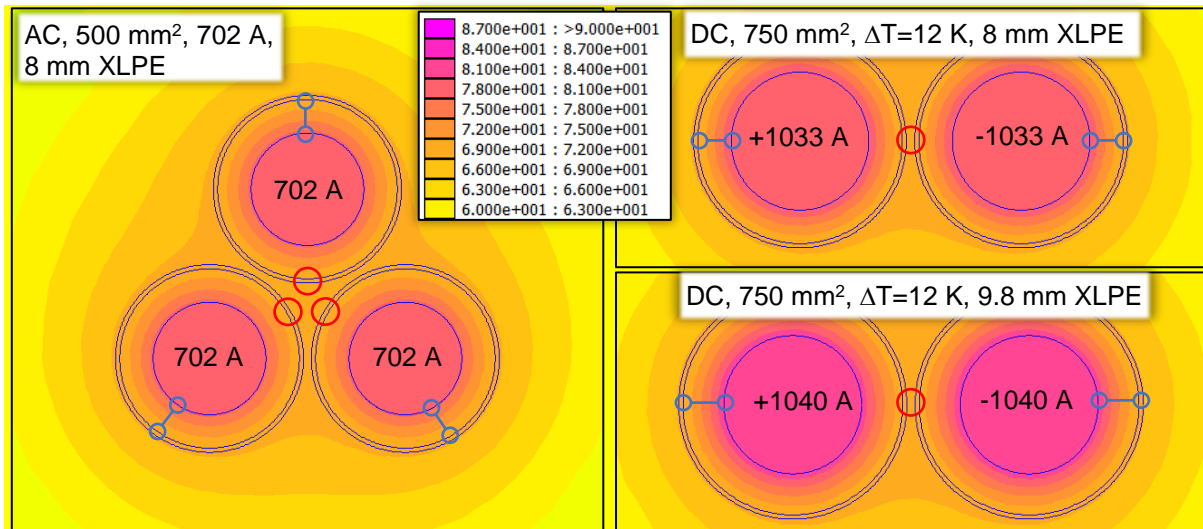


Figure 2.2 Thermal conditions shown in correct proportions (o: Max. mantle temperature, o-o: max. temperature difference across insulator)

The different geometric arrangement with a greater conductor diameter but one less conductor still allows practically the same current density, thus giving justification to the previous considerations. In CIGRE TB793 [2] this was verified a first time by a more simplified thermal simulation. Actually, the minute disadvantage in current density for the DC cases could be more than compensated by the absence of AC losses. The best utilization of conductor material temperature limits occurs with the DC setting with thick insulation.

### 2.1.3 DC Stress on Insulation

The AC reference case operates at a nominal voltage of 18/30 kV with a peak AC field strength of

$$\hat{E}_{AC} = \frac{1}{R_{CAC}} \cdot \frac{\hat{V}_{0,AC}}{\ln(R_o/R_{CAC})} = \frac{1}{13.45 \text{ mm}} \cdot \frac{\sqrt{2} \cdot \frac{30 \text{ kV}}{\sqrt{3}}}{\ln(21.45 \text{ mm}/13.45 \text{ mm})} = 3.9 \frac{\text{kV}}{\text{mm}}$$

at the boundary from conductor to isolation. In DC-operation, however, the electric field develops according to a non-linear and temperature dependent leakage, rather than the electrostatic law. Buchner and Schichler, referring to [11], give in [7] analytic expressions for the electric field in relation to geometry and temperature gradient and coefficients [8] for the dependency on temperature difference ( $\alpha = 0.084/K$ ) and average field strength ( $\beta = 0.0645 \text{ mm/kV}$ ):

$$E_{0DC}(r) = \frac{\delta \cdot V_{0DC} \cdot (r/R_o)^{\delta-1}}{R_o \cdot \left(1 - (R_{CAC}/R_o)^\delta\right)}$$

and

$$\delta = \frac{\frac{\alpha \cdot \Delta T}{\ln(R_o/R_{CAC})} + \frac{\beta \cdot V_{0DC}}{R_o - R_{CAC}}}{\frac{\beta \cdot V_{0DC}}{R_o - R_{CAC}} - 1}$$

with  $V_{0DC}$  equivalent to  $U_{DC}$  and  $E_{0DC}$  equivalent to  $E_{DC}$  in [7]. When operating the just the same AC cable at a DC voltage equal to the AC peak voltage ( $k_v = \sqrt{2}$ ) the resulting peak electric field strength  $\hat{E}_{DC}$  is this evaluates into a peak DC field strength slightly lower than below the AC value at uniform

temperature and a no field inversion. At an assumed temperature difference of 14 K across the insulation the same peak field strength as in the AC case would be obtained with an inverted field profile in the insulation layer (Fig. 2.3). As described by the formula above, the governing factor for field profile inversion is the temperature difference. The conductivity of the insulation material decreases with declining temperature, which leads to an increase of the field strength across the insulation layer.

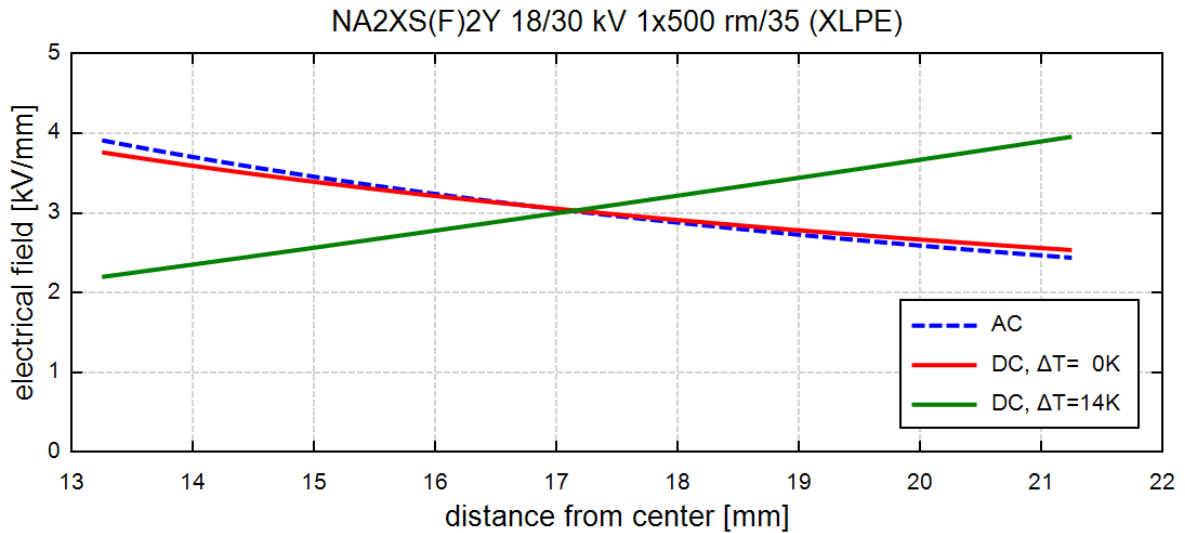


Figure 2.3 Electric field AC vs. DC operation,  $V_{0DC}=24.5$  kV,  $V_{AC,RMS}=30$  kV.

For the first case (equal insulation thickness) of a DC cable with converted cable dimensions, the temperature difference across the insulation of 12 K leads to a slightly lower electric field strength (3.8 kV/mm, Fig. 2.4) than in the AC case. In the second case, using the same insulation material amount as the AC line, the temperature difference across the insulation increases to 14 K. The maximum electric DC field strength reduces to 3.25 kV/mm, because of the thicker insulation of the individual cables. The margin in electric field strength given by the first case compared to the AC case would allow a slight reduction of the thickness, by 2.6% ( $3.8/3.9-1$ ). The second case, however, has a margin of approximately 20% ( $3.9/3.25-1$ ) by which the operating voltage could be increased, before the proposed field strength limit of 3.9 kV/mm is exceeded.

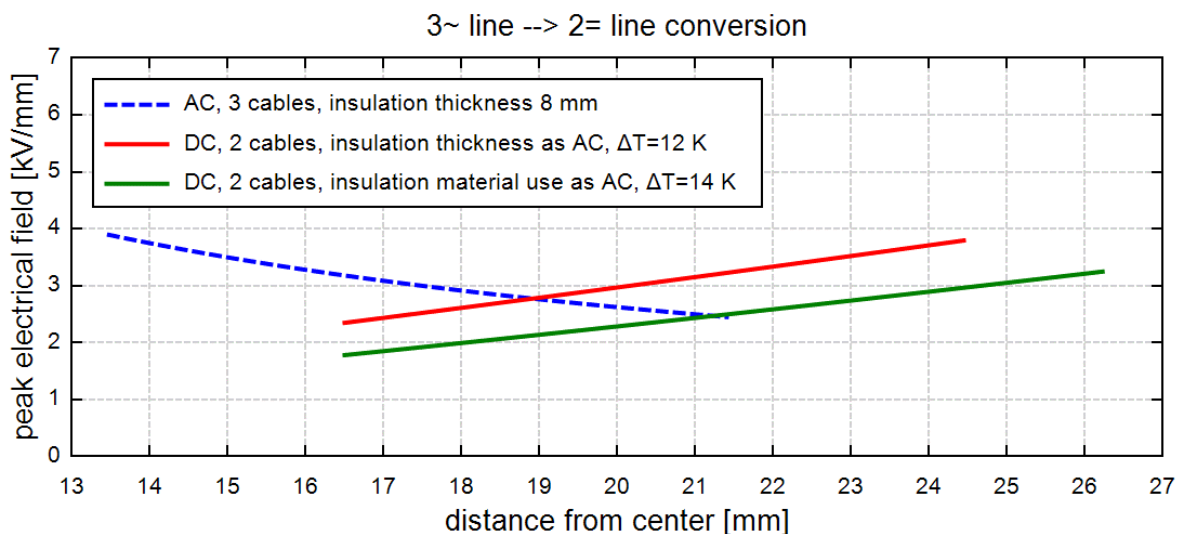


Figure 2.4 Maximum electric field in the DC cable configurations.

As demonstrated in realistic settings and depicted in the figures above, the maximum electric field strength does not necessarily become higher than in the AC case, even under the influence of field

inversion due to temperature and field dependency of the leakage conductance of the insulation material and at the same insulation thickness. Further 20% voltage margin and power capacity could be achieved without increasing the electric field strength over AC cable conditions by using the entire insulation material of the three-phase cable. Thus, voltage increase factors can be in the range of

$$k_v = \sqrt{2} \dots 1.7 .$$

As the in-service electric field strength is substantially lower than in the HVDC design and below charge trapping thresholds, these voltage factors, which would not result in a higher maximum electric field than in the AC case, should at least be feasible.

### 2.1.4 Amount of Insulation Material

The insulation material cross section area per cable for the original AC line was:

$$A_{iso\_AC} = \pi \cdot ((R_{CAC} + d_{iso})^2 - R_{CAC}^2) = 877 \text{ mm}^2$$

Now, utilizing the margin in field strength of the first case as well, the insulation thickness can be reduced slightly and so the cross-sectional area per cable, which calculates to

$$A_{iso\_DC1} = \pi \cdot \left( \left( R_{CDC} + d_{iso} \cdot \frac{3.8 \text{ kV/mm}}{3.9 \text{ kV/mm}} \right)^2 - R_{CDC}^2 \right) = 997 \text{ mm}^2 .$$

This is 14% more per cable than for the cables of the AC line. However, the DC line has only two rather than three cables, so that the total amount of insulation material of the DC line is only

$$a_{isoDC/AC} = \frac{2 \cdot A_{iso\_DC1}}{3 \cdot A_{iso\_AC}} = 76\% .$$

Gradual reduction of the insulation thickness by exploiting field strength margin in the first case and increasing the insulation material thickness by spending the entire insulation material in the second case would, however, lead to non-standard cable dimensions and could require modified manufacturing equipment, maybe leading to a preference for standard AC cable dimensions.

### 2.1.5 Overall Line Performance

As discussed so far, the power capacity of the DC line using the same amount of materials as a reference AC line is mostly determined by an increase in operating voltage and the absence of a power factor. With standard cable dimension the effect of the differences in thermal conditions are small and are not considered here furthermore. By considering the AC power factor  $\lambda$  the ratio of the transmitted DC over the initial AC power is

$$\frac{P_{DC}}{P_{AC}} = \frac{2 \cdot I_{DC,RMS} \cdot V_{DC,RMS}}{\lambda \cdot \sqrt{3} \cdot I_{AC,RMS} \cdot V_{AC,RMS}} = \frac{2 \cdot \frac{3}{2} \cdot \frac{k_v}{\sqrt{3}}}{\lambda \cdot \sqrt{3}} = \frac{k_v}{\lambda} ,$$

and for  $k_v = \sqrt{2} \dots 1.7$  and  $\lambda = 0.9$

$$\frac{P_{DC}}{P_{AC}} - 1 \approx 57\% \dots 88\% .$$

As another effect, the relative ohmic voltage drop  $v$  along the line is lower because of the increased

RMS voltage, as RMS value is practically equal to the peak value at DC. It admits a longer supply range, when the limit is the same relative voltage drop. The ratio of the voltage drop along the DC cable over the AC cable under the previous assumption is obtained as:

$$\frac{v_{DC}}{v_{AC}} = \frac{\frac{r_{DC} \cdot I_{DC,RMS}}{V_{DC,RMS}}}{\frac{r_{AC} \cdot I_{AC,RMS}}{V_{AC,RMS}}} = \frac{r_{DC} I_{DC,RMS}}{r_{AC} I_{AC,RMS}} \cdot \frac{V_{AC,RMS}}{V_{DC,RMS}} = \frac{2}{3} \cdot \frac{3}{2} \cdot \frac{1}{k_v} = \frac{1}{k_v}$$

$$= 71\% \dots 59\%$$

for the same current density as in the AC line. This yields a 41% to 70% extra supply range until the same voltage drop, e.g. 10%, is exceeded, and at a power level 57% to 88% higher than for the AC line. This is mostly the ratio of the DC voltage over the AC RMS voltage to ground. Even more supply range can be gained, when operating the line at the original power level. In this case the current could be reduced to:

$$\frac{I_{DC,RMS@P_{AC}}}{I_{DC,RMS}} = \frac{\lambda}{k_v}$$

with a total resulting supply range gain  $g_s$  of:

$$g_s = \frac{1}{\frac{1}{k_v} \cdot \frac{\lambda}{k_v}} = \frac{k_v^2}{\lambda} = 222\% \dots 321\%$$

In all cases the efficiency of the line is determined by the voltage drop between starting and end point, i.e. 90% representing the limit for the remaining voltage at the end of the line. Different from AC lines, there is no way to adjust the voltage by reactive power injection to given voltage margins. Within the assumed constraints, further range extension would not be possible unless power electronic converters are engaged for voltage adjustment at intermediate positions or the endpoints. Nevertheless, extra efficiency loss would occur and a higher line voltage or conductor cross sectional area may be preferred.

The criteria for an application to switch to DC will depend on the result of a cost-benefit analysis. One of the important performance indicators is the energy efficiency which is a component of the operational expenditure (Opex). Power losses in DC cables are lower than in AC cables, as there is no circulation of reactive current in DC and therefore no corresponding joule losses in the conductors. Moreover, power losses in AC are higher due to the skin effect, which is not negligible for cables and lines with large cross-sections. However, considering that the DC system has to be connected at some point to the existing AC system, a DC-AC converter station is required. This station comes at a given cost and adds some power losses. For high voltage links, it has been demonstrated that a break-even-distance exists, where HVDC becomes advantageous over HVAC. The HVDC/HVAC break-even-distance is approximately 50 km in the case of submarine cables [20]. When considering underground cable point-to-point transmission (**Fig. 2.5**), the MVDC/MVAC break-even-distance according to power loss criteria ranges from less than 10 km at 10 kV to approximately 30 km at 33 kV [21].

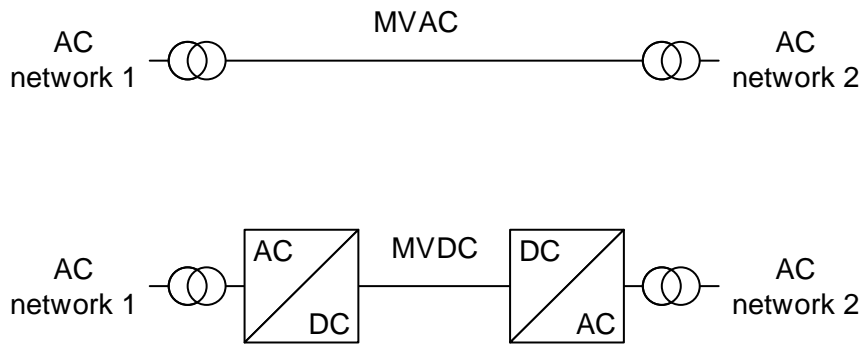


Figure 2.5 Point-to-point transmission: MVAC (top) and MVDC (bottom) [21].

While high voltage DC is already a standard option for electric power grids, medium voltage and low voltage DC with a relevant proliferation in the field are yet to emerge. So currently high voltage DC is concentrating on point-to-point connections between high voltage AC grid nodes. Very few high voltage grids with multi-terminal topology are in operation, not having left a prototype state yet. Aside from a seamless DC power grid, advantages of DC technology could also help to address challenges in hybrid grid situations. The anticipated advantages are:

- phase and frequency immunity
- higher possible RMS voltage at the same peak field strength
- zero reactive power
- lower losses or higher power capacity
- almost zero leakage losses (no losses due to capacitive leakage)
- significantly less zero corona losses for overhead lines
- zero steady-state induced sheath current and zero capacitive leakage (cables)

These properties allow various applications of this technology in utility grids, which in part, will be set forth in following sections. The opportunities arising from the above-mentioned properties are:

- Exchange of power without changing fault current level
- Direct coupling of (distribution) grid segments divergent in phase or frequency
- Longer supply range
- Higher power capacity with same material
- Lower idle losses
- Controlled power dispatch

These allow direct connections between AC grid segments at MV voltage level in the sub-transmission domain, which otherwise are connected only on transmission voltage level (“horizontal” vs. “vertical” coupling). Power levelling directly between adjacent distribution grid areas becomes possible, without interfering with the transmission grid. MVDC lines have less voltage drop at the same material effort and power load, which allows around two times longer supply range. MVDC can allow connections in the remote terminal of the MV feeders to relieve the heavily loaded one.

### 2.1.6 Summary

DC line configurations would have better material exploitation in terms of power capacity, supply range or efficiency, but not for all of it to the full extent at the same time. The main effects here are mainly due to higher utilization of the insulation material by increasing the exploiting the peak AC voltage as system voltage at equal insulating layer thickness or even 20% higher by using the entire insulation material budget of the AC line, and the absence of an AC power factor ( $\lambda$ ). This yields into power capacity gain calculated at least as 157% at the same insulation layer thickness and up to

188% when using the entire material budget. If the admissible current density is exploited fully, then the resistive voltage drop per km remains the same in absolute numbers ( $V/km$ ). Because of starting at an operating voltage higher by a factor  $k_v$ , this leads to a supply range extended by the same factor for a given limit of a resistive voltage drop (e.g. 10%) for AC and DC line and the same efficiency loss occurs. When operating at the same power level as the AC line, the DC operating current would be reduced by the factor  $k_v / \lambda$ , such as the longitudinal voltage drop, and the supply range increases by the inverse of the factor again. At  $\lambda = 0.9$  it could reach 222% of the AC line at  $k_v = \sqrt{2}$  and up to 321% at  $k_v = 1.7$ , then making full use of the insulation material of the AC line. The differences in the thermal conditions between 3-phase AC and 2-phase DC installations are only little as shown in [2] and also here. Sheath, skin and proximity losses, occurring in the AC line, were not taken into account in the presented considerations and would easily offset the small differences in thermal conditions.

It is found, that standard MVAC cables are designed at a practical peak field strength much lower than of HVDC cables (and also of HVAC cables), giving substantial margin against insulation failure. Recent work by Schichler, Buchner et al. demonstrated successful testing according to adopted principles of CIGRE TB 496, adapted to DC operation at 55 kV on a regular 12/20 kV AC cable at standard insulation thickness of 5.5 mm which results in a factor of  $k_v = 3.2$ . It appears however, that with 10 kV/mm under normal operation at 55 kV published thresholds for charge trapping might be reached and at 15 kV/mm during long term testing possibly exceeded.

While high voltage DC is already a standard option for electric power grids, medium voltage and low voltage DC with a relevant proliferation in the field has yet to emerge. So currently high voltage DC is concentrating on point-to-point connections between high voltage AC grid nodes. Very few extra high voltage grids with multi-terminal topology are in operation, not having left a prototype state yet. Aside from a seamless DC power grid advantages of DC technology could also help to address challenges in hybrid grid situations. The anticipated advantages are:

- phase and frequency immunity
- higher possible RMS voltage at the same peak field strength
- zero reactive power
- lower losses or higher power capacity
- almost zero leakage losses
- zero corona losses for overhead lines
- zero steady-state induced sheath current and voltage and zero capacitive leakage (cables)

These properties allow various applications of this technology in utility grids, which in part, will be set forth in following sections. The opportunities arising from the above-mentioned properties are:

- Exchange of power without changing fault current level
- Direct coupling of (distribution) grid segments divergent in phase or frequency
- Longer supply range
- Higher power capacity with same material effort
- Lower idle losses
- Controlled power dispatch

These allow direct connections between AC grid segments on MV voltage level in the sub-transmission domain, which otherwise are connected only on transmission voltage level (“horizontal” vs. “vertical” coupling). Power levelling directly between adjacent distribution grid areas becomes possible, without interfering with the transmission grid. MVDC lines have less voltage drop at the same material effort and power load, which allows up to three times longer supply range, depending

on operating conditions. MVDC can allow connections in the remote terminal of the MV feeders to relieve the heavily loaded one.

## 2.2 Economics of MVDC Systems

DC technology is now widely used for high voltage power transmission (HVDC) and there are a few examples of stations operating at medium voltage levels. Additionally, there are some applications of DC which are mainly back-to-back (BtB) and point-to-point topologies or niche power supplies to off-shore oil and gas installations, e.g. ANGLE-DC project [22], Network Equilibrium project [23], Wenchang project [19]. To date, there are only a few applications for MVDC links in distribution networks. The use of DC technology can bring a number of benefits to the operation of the medium voltage network and hence to the consumer, as outlined in the following:

- Enhanced power supply capacity and power flow management of an existing network;
- More precise control of the flow of power in the distribution circuit;
- No risk of overload of the circuit;
- Control of AC voltages at the ends of the distribution circuit;
- Control of reactive power flow at both ends of the distribution circuit;
- Lower losses in the wider distribution network due to the improved voltage control;
- Rapid support to the system voltage during faults;
- Fault level decoupling between distribution systems;
- Facilitating accelerated access to the network for renewable energy integration.

In the particular case of the ANGLE-DC project in the UK [22], DC makes better use of the conductor than AC: DC allows more current to flow and the transfer power will be greater with higher DC voltage. ANGLE-DC enhances the thermal rating of the existing circuit by around 23% from 24.8 MVA (operating in AC at 65°C) to 30.5 MVA (operating in DC at 50°C) by conversion to DC operation. A potentially higher capacity release could be achieved [22].

To be specific, the MVDC investment should take into account the following benefits:

- Establishing an existing power transfer corridor interconnecting two distribution systems which might not be possible using AC due to the voltage angle difference and offers an avoided capital investment and enables the transport of low-carbon generation between two distribution systems (A 17% factor is assumed based on the generation load factors published by UK's Department of Energy & Climate Change on renewable resources and the generation portfolio on Anglesey);
- Providing additional thermal capacity on the existing infrastructure to avoid/defer the capital investment;
- Enhancing voltage and reactive power controllability at both ends of an MVDC link and subsequently reducing losses.

Other factors need to be considered in the business application include: MVDC converters have a lower lifespan than AC transformers. As mentioned in [19], the lifetime of MVDC equipment would be ~15-25 years compared to 30-40 years. The converters will undergo regular planned maintenance to ensure the secure operation in a long lifetime, which will incur greater replacement costs. Moreover, MVDC losses may be higher than its AC counterpart. The power losses should be considered at the whole system level.

The ANGLE-DC project demonstrated the tangible financial benefits from capital expenditure (Capex) and operational expenditure (Opex) perspectives, as shown in **Table 2.1**. Based on this example, the

payback time is about 7-10 years.

**Table 2.1 CapEx and OpEx Benefits of ANGLE-DC**

	2030	2050
<b>CapEx (MVDC equipment)</b>	-£8.08m	-£8.08m
<b>OpEx benefits (Losses)</b>	£7.57m	£15.77m
<b>Avoided capital investment</b>	£10.98m	£10.98m
<b>Total benefits</b>	<b>£10.47m</b>	<b>£18.67m</b>

At the planning stage, the benefits and costs of different grid options should be studied to select the best techno-economic solution. In [24], several scenarios including the AC grid, AC grid with BtB converter and MVDC network converted from AC have been compared in terms of system capacity, power transfer capability, power losses, cost benefits, etc. The study uses a 12-node double-circuit AC distribution network as the base case, as shown in Fig. 2.6. Detailed parameters can be found in [24]. The existing AC line 1 is converted to DC line 1. VSC power losses considering the vary with load can use the following equation:

$$P_{loss} = aI^2 + bI + c .$$

where  $I$  is the DC current of the VSC,  $a, b, c$  are curve fitting coefficients based on measurement. Generally, the power losses of a VSC are about 1.5-2%, which is accurate enough for system level analysis.

The results are included in the below Table 2.2. Detailed calculation and parameters can be found in [24]. It can be concluded that the capital cost of using the technique of converting the existing medium-voltage AC lines is much lower than the cost of building new AC lines. However, it should be mentioned that the analysis needs to be carried out case by case due to the use of different types of VSCs, distributed generation (DG), loads and transmission lines, etc.

By converting existing AC lines to MVDC operation, a huge amount of costs can be reduced by removing or deferring the need of building new AC lines. Most importantly, building a new line would be impossible in some urban areas due to very limited spaces. In addition, building a new AC line can only increase system capacity which might not be fully used due to the lack of flexible control. With VSC control, power quality including voltage and harmonic performance can be improved.

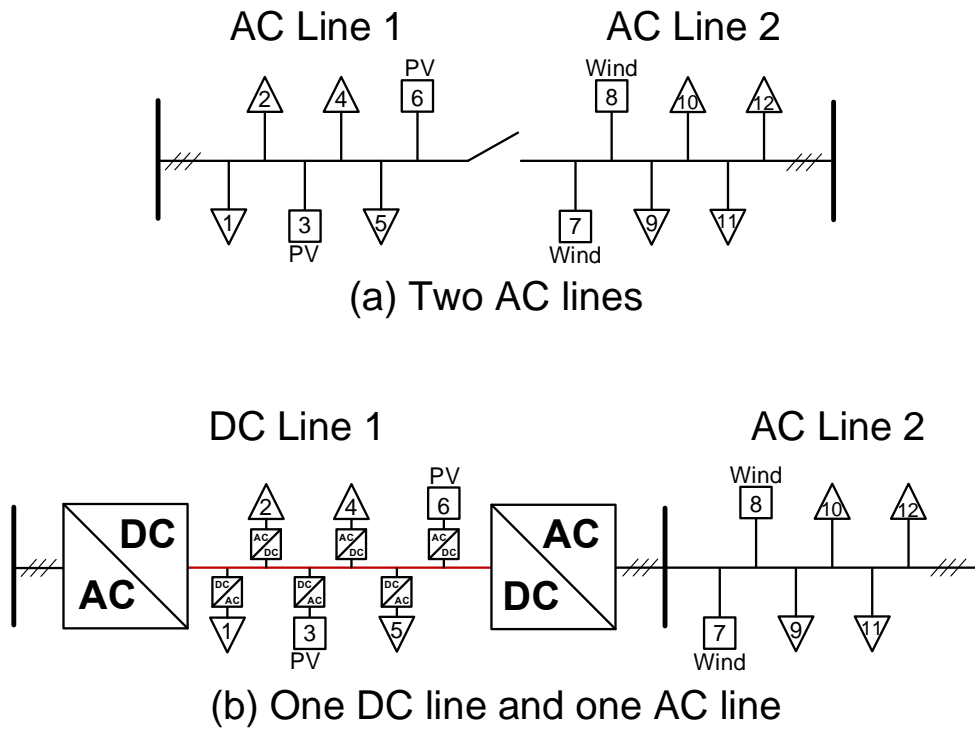


Figure 2.6 Distribution networks under study.

Table 2.2 Cost-benefit analysis of different scenarios [24].

Cases	AC (Base Case)	AC (Reconfiguration)	AC (with BtB)	Hybrid AC/DC
Line capacity	Low (17 MW)	Low (17 MW)	Low (17 MW)	High (21.2 MW)
Power transfer capability	Low (10.5 MW)	Low (12 MW)	Low (15 MW)	High (21.2 MW)
Power losses under a load of 10.5 MW	High (4911 kWh/day)	High (4013 kWh/day)	High (1735 kWh/day)	High (1733 kWh/day)
DG integration	Low (8.4 MW)	Low (8.4 MW)	Low (11.2 MW)	High (14 MW)
Requirement of new lines	High	High	Low	Lowest
Power quality	Low	Low	High	High
VSC cost	--	--	Low (€1.6 M)	High (€6.4 M)
DC line operation and monitoring cost	--	--	Low	High

## 2.3 MVDC Bus Architectures and Configuration

Suitable DC configurations for an MVDC system should be selected during the design and planning stage. CIGRE TB 793 identified different network and line configurations [2]. They are recalled and extended in this brochure.

The possible DC network configurations are:

- point to point transmission (**Fig. 2.7 (a)**),
- radial network (**Fig. 2.7 (b)**),
- ring network (**Fig. 2.7 (c)**),
- meshed grid (**Fig. 2.7 (d)**); this can include loads and sources as well.

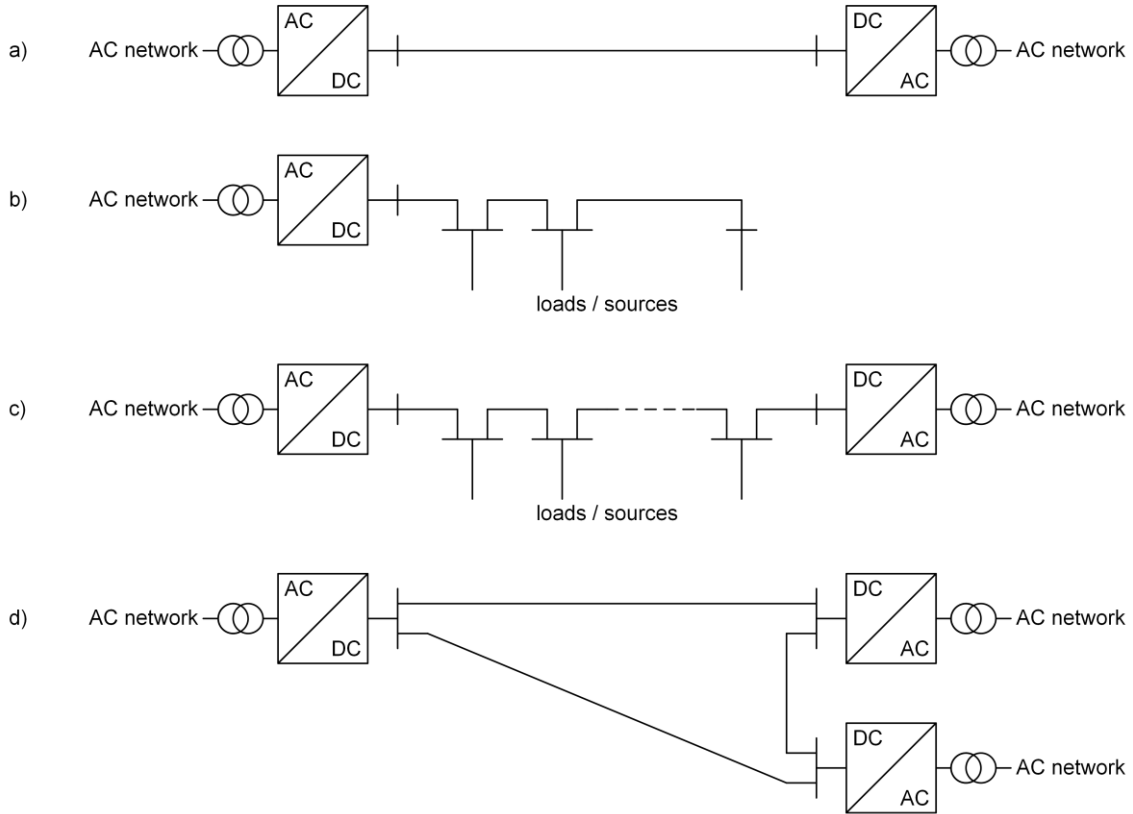


**Figure 2.7 Network configuration diagrams: (a) point to point, (b) radial, (c) ring, (d) meshed.**

The point-to-point transmission is a specific case of the radial network. It is mentioned here as an independent network configuration because it is the most common network configuration in DC systems, HVDC in particular.

The line configurations have been well studied for the point-to-point transmission. The possible line configurations are:

- asymmetric monopole (**Fig. 2.8 (a)**),
- symmetric monopole (**Fig. 2.8 (b)**),
- bipole (**Fig. 2.8 (c)**).

However, considering the MVDC distribution systems some hybrid line configurations are possible as well, for example, bipole / symmetric monopole (**Fig. 2.8 (d)**).

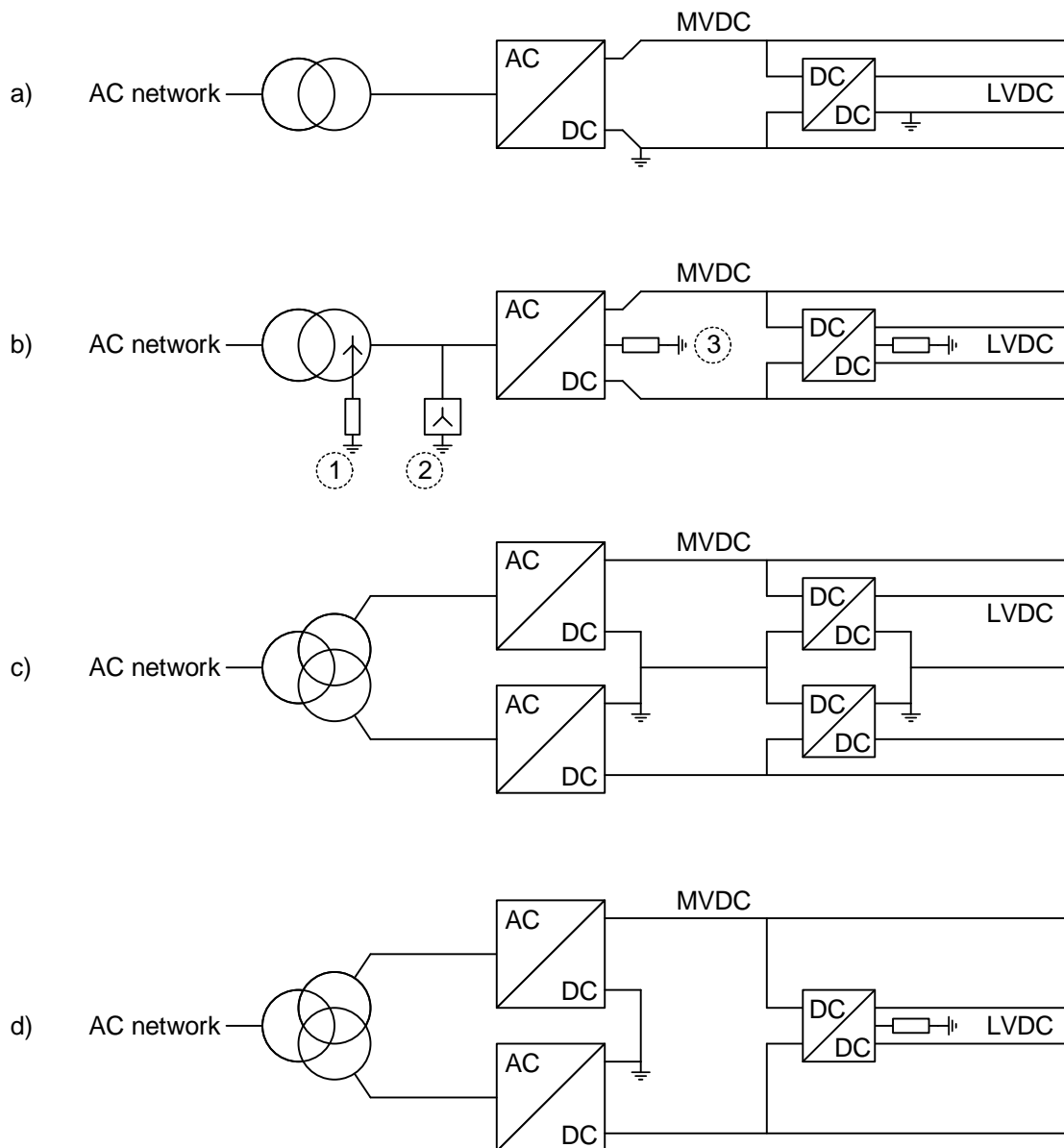


**Figure 2.8 Line configuration diagrams including AC-DC converter and DC-DC converter (isolated or non-isolated): (a) asymmetric monopole, (b) symmetric monopole, (c) bipole, (d) hybrid bipole/symmetric monopole.**

Different grounding schemes are possible. The asymmetric monopole is commonly realised with a directly grounded metallic return wire. Three grounding schemes are possible for the symmetric monopole:

1. AC grounding of the transformer star point - this is the preferred solution if the transformer star point is available on the converter side winding,
2. AC grounding with a star point reactor - this the preferred solution if the transformer star point is not available on the converter side winding,
3. DC grounding - this a preferred solution if neither of the above is possible or if the grounding point is normally present within the converter.

Furthermore, the grounding can be realised through:

- high impedance - this limits the line-ground fault current but results in transient overvoltages,
- low impedance - this allows high fault currents, which facilitates the selectivity of the

protections.

The bipole can be realised with different DC grounding schemes:

- metallic return,
- rigid bipole,
- ground return (not recommended because of risk of corrosive ground currents).

The line configuration diagrams presented in **Fig. 2.8** include the DC-DC converters because they are likely in the MVDC distribution systems for interfacing with the LVDC systems or HVDC systems. One of the major differences of DC-DC converters when compared to the function of the transformer in AC systems is that the DC-DC converter may provide galvanic isolation or not. Symbols of DC-DC converters are presented in **Fig. 2.9**. The line configuration diagrams presented in **Fig. 2.8** include a DC-DC converter but it is not defined whether it is an isolated or non-isolated DC-DC converter. In order to choose the appropriate type of DC-DC converter, a detailed analysis has to be performed for each application. The analysis should take into account the voltage levels and grounding schemes of the two DC systems, and the power electronics constraints. This is further discussed in Chapter 4.



**Figure 2.9 DC-DC converter symbols: (a) DC-DC converter, (b) non-isolated DC-DC converter, (c) isolated DC-DC converter.**

## 2.4 Experience from DC Microgrid Planning and Design

### 2.4.1 Planning and Design Objectives

When planning a DC microgrid one of the key objectives is to design a network that can operate economically in both the short-term and long-term. In other words, for economic operation, investment and operational costs are required to be kept minimal [26], [27]. One important and salient feature of microgrids is that they enhance reliability with their islanding capability. This allows DC microgrids to be disconnected from the main grid in the presence of faults, disturbances or voltage fluctuations in the upstream network [28]. However, after disconnecting from the main grid, the degree of resilience of the DC microgrid is required to be considered during the initial planning process. Therefore, the DC microgrid should be designed to be tolerant to faults or disturbances in upstream networks, which would enhance the customers' reliability and system resilience [29]. In other words, the DC microgrid network structure should be robust enough to maintain security of supply. **Fig. 2.10** highlights the key requirements that need to consider when planning and designing a DC microgrid.

The planning model with the objective of minimizing the microgrid total cost is required to consider a) the optimal DER size and generation mix, b) the point of connection of DER and c) optimal energy storage sizing. The total planning cost is composed of three parts: the investment cost, the operation cost, and the reliability cost. The investment cost is long-term and calculated annually while the operation and reliability costs are short-term and should be calculated hourly for each day of the planning horizon [26].



Figure 2.10 Key requirement to be considered when planning and designing a DC microgrid.

## 2.4.2 Different Solution Models

A mixed-integer programming optimization model has been proposed in [26] to identify threshold ratios of DC loads which made the DC microgrid a more economically viable solution than the AC microgrid. The objective is to minimize the total planning cost subject to various planning and operation constraints. The study in [27] proposes an operation planning model considering load/generation changes for a low voltage DC microgrid including DC sources such as batteries, fuel cells and PVs. The objective of the study is to minimize daily operation costs.

In [30], a mixed-integer linear procedure using a multi-path dynamic programming approach has been used for determining optimal operation planning of DC based electric vehicle supply infrastructure. The procedure aims at optimizing daily operational costs, based on the forecast of photovoltaic production and EV exploitation. In [31], a microgrid planning problem to determine the optimal size and type of DER to be installed with combined heat and power (CHP) systems is studied. The model aims at simultaneously minimizing the total planning cost and carbon dioxide emissions.

As discussed above, when planning and designing a DC microgrid the key objective is to optimize the total investment and operation costs while maintaining the security of supply. This is applicable to MVDC system planning and designing as well. One difference is that there is still no agreement on which types of converters to use for MVDC distribution systems. The modular multilevel converter (MMC) has been widely accepted for voltage source converter based high voltage DC (VSC-HVDC) transmission systems. In the DC microgrid, two-level and three-level VSCs are widely used. Therefore, the selection of optimal converters for MVDC distribution systems should be considered in the planning and design stages, which will be discussed in the following sections.

## 2.4.3 DC Microgrid Standards

Whenever a new technology emerges, technical standards are required to maintain the quality of the technology. This can range from retaining compatibility of products from different vendors to design guidelines to which adherence is required in order to provide a quality service to consumers.

The draft IEEE 2030.10 standard targets sustainable DC off-grid and remote power, in both the developed and developing world [32]. This standard discusses the design and operation of a dc microgrid for rural or remote applications based on extra low voltage dc (ELVDC) to reduce cost and simplify stability. The proposed architecture includes a scalable network of sources, storage, power management and loads. The architecture can support a home, a network of homes, and joint use

buildings.

In [33], existing international power quality standards and metrics specified in IEC 61000 and IEEE Std 1159 has been reviewed in terms of applicability and required modifications. It is concluded that most existing definitions of power quality are sufficiently general to encompass DC microgrids. Voltage transients, short- and long-term variations, noise, notching, and voltage fluctuations are highly similar to the existing AC power quality issues. However, the power quality issues of DC offset, inter-harmonics and imbalance are different.

Due to the existence of different levels of fault current in microgrids, new protective schemes need to be developed that can monitor changes in the microgrid and calculate the operating conditions at any given time. Logical nodes available in IEC 61850-7-420 communication standards can be used to design such versatile schemes [34]. In [35], it is demonstrated that the utilization of IEC 61850-based communication in low voltage microgrid protection is needed to ensure a fast and reliable protection.

Further, the recommendations of CIGRE working groups in the field of HVDC grids such as:

- CIGRE TB 604, "Guide for the development of models for HVDC converters in a HVDC grid", 2014.
- CIGRE TB 699, "Control methodologies for direct voltage and power flow in a meshed HVDC grid", 2017.
- CIGRE TB 713, "Designing HVDC grids for optimal reliability and availability performance", 2017.
- CIGRE TB 739, "Protection and local control of HVDC-grids", 2018.

will be useful to elaborate a complete design guideline describing clear functional requirements for all relevant aspects of DC microgrid systems and associated equipment.

The International Electrotechnical Commission (IEC) standards for HVDC systems such as IEC 62199 (withdrawn and replaced by IEC/IEEE 65700): Bushings for D.C. application, IEC 62271: High-voltage switchgear and control gear, and IEC TR 62543: High-voltage direct current (HVDC) power transmission using voltage sourced converters (VSC) and IEEE standards such as P2656 - Guide for Functional Specification of Voltage-Sourced Converter for HVDC Stations, IEEE Std. 1240-2000 IEEE Guide for the Evaluation of the Reliability of HVDC Converter Stations, P2832 - Guide for Control and Protection System Test of Hybrid Multi-terminal High Voltage Direct Current (HVDC) Systems should also be referred.

Various studies have shown different heuristic optimization techniques can be used to design an optimal DC microgrid structure. Although there are several draft standards for DC microgrids, a complete standard is yet to be developed.

## 2.5 Assessment of MVDC Converter Reliability

Reliability analysis is an important tool for assisting the design phase of a power electronic converter to fulfil its life-cycle specifications. This helps identification of optimal preventive maintenance strategies and required improvements in the design, such as optimum redundancy levels. Further, the lifetime of an MVDC converter depends on the topology and individual failure rates of different sub-systems.

The typical life-cycle of a power electronic component is characterized by the well-known "bathtub" curve. When estimating the total lifetime of a converter, not only the useful life of individual components but also the wear-out phase should be considered. As discussed in [36]-[37], the lifetime

of a power electronics converter is influenced by its mission profile and ambient temperature. Therefore, depending on the MVDC application (MVDC distribution systems, shipboard and traction applications, large scale solar PV generation systems, etc.), the reliability of the converter will be different.

To estimate the reliability of a converter there are several different handbook methods available. The most commonly used method relies on MIL-HDBK-217. However, the data provided in this handbook has been considered as out-of-date for new technologies as it was last updated in 1991. IEC 61709:2017 provides guidance on the use of failure rate data for mission profile-based failure rate prediction of electric components. The most recent update of MIL-HDBK-217 is the FIDES guide, which considers the component physics of failures [38].

Once the component failure rates are obtained, the converter system-level reliability can be obtained using methods such as the Reliability Block Diagrams (RBD), Fault Tree Analysis (FTA), and the Markov Chain (MC) [36]. The RBD method focuses on the success combinations whereas the FTA is based on the failure combinations. However, the MC technique can only be used if the converter component failures only hold Markov properties.

From the pool of voltage source converter topologies, MMC has been used for recent HVDC projects due to lower power losses and scalability compared to other VSCs such as two-level and three-level VSCs. At low-voltage DC (LVDC) levels, two-level VSC has been used due to simplicity and less control complexity. However, at MVDC levels it is still not clear which VSC topology is most suitable in terms of reliability, DC voltage level, power levels and lifetime cost.

For reliable operation of power converters, redundant designs may be required. In [39], a guideline to select the optimal multi-level MVDC VSC at various power and DC voltage levels has been proposed. To obtain the optimal redundancy level, an RBD based method can be used considering the anticipated availability level of the whole converter system. With the knowledge of different converter sub-systems (cooling system, controller, VSC topology, filters, etc.) in terms of functionality and configuration, sub-system RBDs can be developed to obtain the final RBD of a certain VSC topology. Once the overall reliability function of a VSC is obtained, different topologies can be compared to select the most reliable topology at a certain MVDC voltage level and power level. Additionally, a return-on-investment (ROI) analysis is required to be performed, considering different annual energy losses of converters with its mission profile and capital investment.

For instance, **Fig. 2.11** illustrates how different decision variables i.e., ROI, efficiency, B10-life (which is defined as the time taken to reach the availability level of 90%), total cost of ownership (TCO) and component redundancy vary at three different MVDC voltage levels for three multi-level converter topologies - namely three-level neutral point clamped converter (3L-NPC), cascaded 3L-NPC (C3L-NPC) and MMC. In general, higher converter efficiency, ROI, B10-life and lower TCO and redundancy is preferred. However, due to the unique characteristics of each VSC, there is always a trade-off between these five characteristics. For instance, among the converters considered in **Fig. 2.11**, MMC shows a higher efficiency at all the MVDC voltage ranges between  $\pm 10$  kV and  $\pm 50$  kV but its TCO is the highest. Further, it can be observed that the B10-life decreases with the increase of MVDC level irrespective of the topology due to the higher part count. However, in general, with the increase of MVDC voltage level and power levels, the results in [39] highlight that MMC would be the most economic and reliable option whereas at lower MVDC levels and power levels three-level NPC VSC topology could be a better choice. To select a suitable converter topology at a certain MVDC voltage level, project engineers could use their experience and knowledge combined with the above calculated factors.

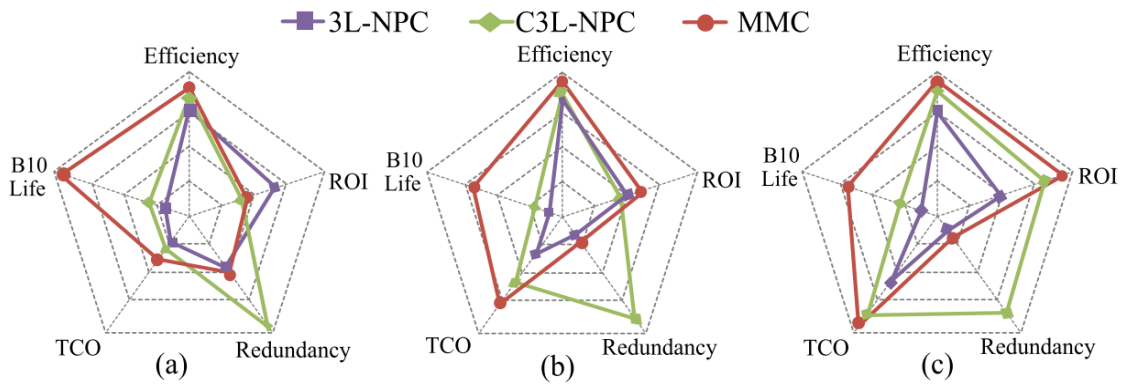


**Figure 2.11 Comparison of five characteristics of VSCs at different MVDC voltage levels (a) ±10 kV; (b) ±27 kV; and (c) ±50 kV [39].**

The examples of the modelling of the reliability of different VSCs can be found in [39].

## 2.6 MVDC Standards

At the time of writing, no specific MVDC testing and commissioning standards exist. For power transmission applications, testing standards exist for line commutated converter (LCC) based HVDC and guidance technical papers and brochures on commissioning are available for LCC and VSC HVDC installations. MVDC systems will have some major differences compared with their HVDC counterparts, so not all testing and commissioning steps will be desirable. One main area of difference is the criticality and typical restoration times of an MVDC system when compared with HVDC.

### 2.6.1 Factory Tests

Some elements of the MVDC system tests will be based on standard items of passive network equipment. These are usually: AC disconnectors and breakers, line reactors, capacitor banks, transformers, and AC and DC filters. The testing standards for these elements do not generally change because they are being applied to an MVDC application and the details can be found within the appropriate international and national standards. For the power electronic valves or modules, applicable MVDC testing standards come from either MV drive or VSC-HVDC applications, which are summarised in **Table 2.3**.

**Table 2.3 Summary of applicable testing standards for MVDC factory acceptance testing.**

Standards	Title
IEC 62501	Voltage sourced converter (VSC) valves for high-voltage direct current (HVDC) power transmission – Electrical testing
IEC 60060-1	High-voltage tests techniques – Part 1: General definitions and test requirements
IEC TR 60919-2	Performance of high-voltage direct current (HVDC) systems with line commutated converters – Part 2: Faults and switching
IEC 61975	High-voltage direct current (HVDC) installations – System tests
IEC 60146-1-1	Semiconductor converters - General requirements and line commutated converters - Specification of basic requirements
IEC 61800-4 (Replaced by IEC 61800-2)	Adjustable Speed Electrical Power Drive Systems – Part 4: General Requirements - Rating Specifications for AC Power Drive Systems above 1 000 V AC and not Exceeding 35 kV
IEC 61800-5-1	Adjustable speed electrical power drive systems – Part 5-1: Safety requirements – Electrical, thermal and energy

Of the standards listed in **Table 2.3**, not all clauses should be used for factory acceptance. For other topology types, not all clauses are universally applicable and there is some overlap with other testing

standards for drive applications.

**Table 2.4 Summary of applicable IEC 62501 testing standard clauses cross referenced with inverter drive testing standards.**

Clause	Title	Application to MVDC
<b>IEC 62501</b>		
6.4	Maximum continuous operating duty	Inverter Module Routine Test at LOAD at test voltage and 1.05 pu current. Max continuous temperatures recorded; IGBT, Diode, snubber and freewheeling diode. <i>Overlap with IEC 61800-2 &amp; IEC § 7.3.1</i>
6.5	Maximum temporary over-load operating duty test	Test initiated at thermal equilibrium with 6.4 test as initial conditions. Test conducted at current OVERLOAD value for 1.2 times the in-service OVERLOAD duration.
6.6	Minimum DC voltage test	Test only applies where valve electronic circuits voltage is extracted from the voltage appearing between the valve terminals.
7.3.1 & 7.3.2	Valve support DC & AC voltage tests	Initial condition 0.5 times of test voltage. Rapid rise to min test voltage and hold for 1 minute. Reduce to specified test voltage and hold for 3 hrs (DC) or 30 mins (AC). Record partial discharge, must remain within testing limits.
7.3.3 & 7.3.4	Support impulse tests: Switching and lightning	3 applications of positive and negative polarity impulse voltage between main terminals (IEC 60060 waveshape).
8.3.1 & 8.3.2	Dielectric tests: Multiple valve unit DC voltage test	Initial condition 0.5 times of maximum MVU test voltage. Rapid rise to min test voltage and hold for 1 minute. Reduce to specified test voltage and hold for 3 hrs (DC) or 30 mins (AC). Record partial discharge, must remain within testing limits. <i>Overlap with IEC 60060-1 § 6.3.1, IEC 61800-2 § 10.2.2.1, IEC 60146-1-1 §7.2, IEC 61800-5-1 § 4.3 &amp; 5.2</i>
8.3.1 & 8.3.2	Multiple valve unit support impulse tests: Switching and lightning	Test only relevant if valves or module share support structure.
10	IGBT overcurrent turn-off test	Worst combination of voltage stress and instantaneous junction temperature are conditions for the test. Control and protection system used to detect test overcurrent. IGBT current should not rise above maximum safe turn-off limit.
11	Short-circuit current test	System fault level event should be carried out for a duration of the time it takes for protection to operate e.g. 50 ms.
12	Test for valve insensitivity to electromagnetic disturbance	Test monitors for spurious switching of IGBTs erroneous signals sent to the converter control and protection systems during tests under clauses 6-11.
13.4.3	Voltage grading check	Ensure that voltage division between series-connected voltage levels will be correct for applied voltages.
13.4.4	Control, protection, monitoring checks	Check the function of any control, protection or monitoring circuits that form an integral part of the module or valve. <i>Overlap with IEC 61800-2 § 10.2.2.1 &amp; IEC 60146-1-1 §7.5</i>
13.4.5	Voltage withstand checks	Check that the valve components can withstand the voltage corresponding to the maximum value specified for the valve.
13.4.6	Partial discharge tests	To be carried out throughout testing on critical components.
13.4.7	Turn on/off check	IGBT(s) in each valve level turns on and turns off correctly in response to switching commands
13.4.8	Pressure test	Check that there are no coolant leaks <i>Overlap with IEC 60060-1</i>

## 2.6.2 Site and Commissioning Testing

As for the factory testing standards, there is no MVDC VSC commissioning standard, but the LCC HVDC testing standard that does exist is a useful framework for identifying which commissioning tests should be used and the sequence in which they should be conducted. **Table 2.5** summaries the transferable tests from the HVDC LCC commissioning standard.

**Table 2.5** Transferable tests from the HVDC LCC commissioning standard

Clause	Title	Application to MVDC
<b>IEC 61975</b>		<b>System Testing</b>
5.3	Energisation of Reactive Components	Energisation of the interface transformer windings from the AC side, with DC switch open. <i>Equivalent with CIGRE TB 697 § 7.5</i>
5.7	Open Line Test	Progressive energisation test from the DC side of the converter station with AC network disconnected. DC circuit energised for 30 minutes <i>Equivalent with CIGRE TB 697 § 7.6</i>
<b>TB 697</b>		<b>STATCOM Commissioning Tests</b>
8.2	Open Circuit Tests	Progressive STATCOM test, Q=0 MVar for 30 minutes followed by a shutdown and disconnection and inspections.
8.3	Protective Action Tests	Tests to verify protective tripping sequences and blocking actions of the converter station control and protection systems.
8.5	Reactive Power Control Tests	Progressive STATCOM test for Q control. Q setpoint is varied between 0 – 0.2 Q <sub>rated</sub> MVar; each Q setpoint held for several minutes followed by a shutdown and disconnection and inspections.
8.6	AC Voltage Control Tests	Progressive STATCOM test for V <sub>ac</sub> control. V <sub>ac</sub> setpoint is varied between 0 - V <sub>ac,max</sub> ; each V <sub>ac</sub> setpoint held for several minutes, followed by a shutdown and disconnection and inspections. Stable ramping of Q should be demonstrated.
8.7	Step Responses and Simulated Fault Ride Through Tests	Demonstration of stable operation following system disturbances. Testing the control response and dynamic behaviour in reactive power and voltage control modes. First tests to be carried out under 0.2 pu. Result to be compared with software and factory system simulations and tests. <i>Equivalent with IEC 91975 § 6.5.2 &amp; 6.6</i>
<b>TB 697</b>		<b>Distribution System Tests</b>
9.2	Energisation of DC Cable and Overhead Line	Demonstration that the condition of the DC circuit is as expected. No power is transmitted. The initial voltage is set to V <sub>DC,min</sub> for 5 minutes. V <sub>DC</sub> incrementally increased to V <sub>DC,max</sub> , holding setpoint for 5 minutes at each step. V <sub>DC,max</sub> held for 1 hour, followed by a shutdown and disconnection and inspections. <i>Equivalent with IEC § 91975 5.7</i>
9.3	First Power Distribution	Low power distribution tests up to 0.2 pu. Power is increased in incremental steps, from P <sub>min</sub> to 0.2 P <sub>rated</sub> . For each power setpoint, the flow direction should be changed in the opposite direction and observe ramping of active power through the zero-crossing. Power setpoint should be held for 5 minutes. AC network load flow studies should be performed ahead of testing to verify setpoint profiles are allowable. <i>Equivalent with IEC § 91975 6.1.2</i>

Clause	Title	Application to MVDC
9.4	Active Power Control and Steady State Tests	<p>Verification of stable active power transfer within the PQ envelope of the MVDC system up to <math>S = 0.2</math> pu. Setpoints should be held for 5 minutes and a few ramps of active power through the zero-crossing should be observed with transfer of reactive power. Ramping to new setpoints should be interrupted (stopped) to test control response. AC network load flow studies should be performed ahead of testing to verify setpoint profiles are allowable.</p> <p><i>Equivalent with IEC § 91975 6.1.4</i></p>
9.6	Step Responses	<p>Demonstration of stable operation following system disturbances. Testing the control response and dynamic behaviour following:</p> <ul style="list-style-type: none"> <li>• Active power order step change.</li> <li>• Reactive power order step change.</li> <li>• Power factor step change.</li> </ul> <p>First tests to be carried out under 0.2 pu and repeated at full power rating. Result to be compared with software and factory system simulations and tests.</p> <p><i>Equivalent with IEC 91975 § 6.5.2 &amp; 6.6</i></p>
9.7	High Power Distribution Tests	<p>This test verifies:</p> <ol style="list-style-type: none"> <li>1. control stability and accuracy at the limits of the MVDC link PQ envelope.</li> <li>2. The capability of the AC network to distribute the maximum active power levels</li> </ol> <p>Power is increased in incremental steps, from <math>P_{min}</math> to <math>P_{rated}</math> at each reactive power or p.f. setpoint, each setpoint should be held for 5 minutes. AC network load flow studies should be performed ahead of testing to verify setpoint profiles are allowable for the time period of testing.</p> <p><i>Equivalent with IEC 91975 § 6.8.2</i></p>
9.9	Heat Run Tests	<p>Demonstrate that all components of the MVDC system are capable of continuously running at the load levels of <math>S_{rated}</math> without exceeding their maximum design temperatures at the maximum allowable ambient temperature. The maximum power level should be held for a duration of 90 minutes.</p> <p><i>Equivalent with IEC 91975 § 6.8.4</i></p>

Not all clauses of each document are used, due to the differences between HVDC and MVDC and some modifications are required to suit the application. **Fig. 2.12** shows the progressive commissioning sequence of an MVDC link post-installation phase. The converters in the system will firstly start with the STATCOM operation mode and then switch to their target operation modes.

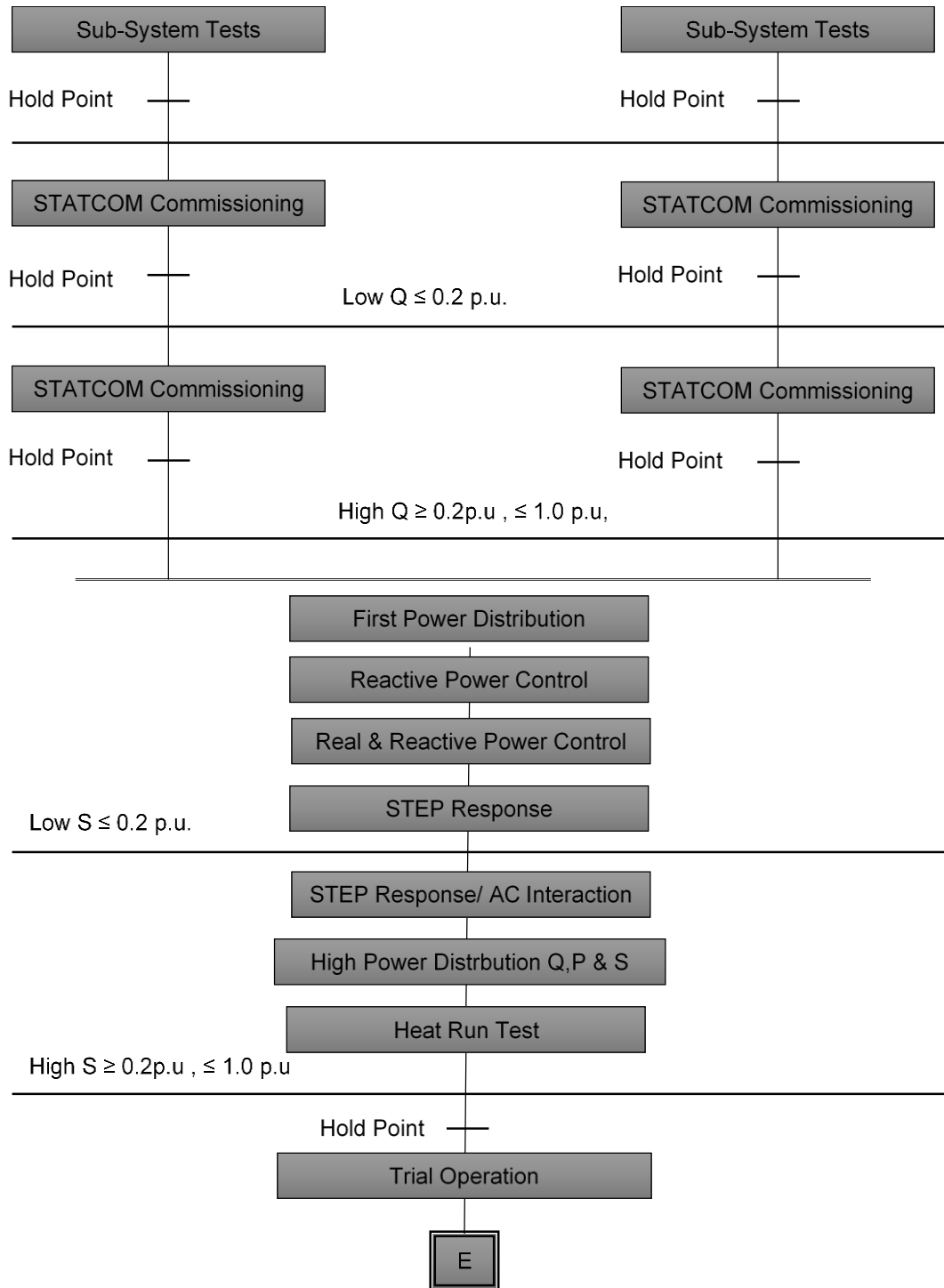


Figure 2.12 Progressive commissioning sequence of an MVDC link post-installation phase.

## 3 MVDC Network Operation and Protection Requirements

In current installations, MVDC links provide controlled power flow as DC couplers or DC links in meshed MV AC grids. This way, MVDC systems today act in much the same way as HVDC systems in transmission grids, just on a small scale and over comparatively short distances. Concerning operation and protection, they essentially represent point-to-point connections providing power transmission. Such MVDC systems allow much more flexible ways of grid operation beyond the scope of conventional AC systems by a controlled power flow and hence a more efficient use of grid resources.

Being located in distribution grids, the role of MVDC systems is expected to grow due to a growing number of distributed renewable energy sources, which largely represent DC sources and a growing number of DC loads. MVDC systems are envisaged to collect power from renewable resources (such as wind farms and solar farms) and to distribute power to DC loads such as power-to-gas, high power charging and energy storage systems. Currently, conversion from DC to AC and hence the point of interconnection to the AC grid is predominantly located at low voltage levels. With a growing number of installations and growing demand on power, it is expected that the point of interconnection will move to higher voltage levels.

The point of interconnection from MVDC may be located in the distribution grid, or directly connect to the transmission grid with a conventional AC transformer. Such a scenario leads to a distributed MVDC grid with multiple voltage levels. In terms of operation and control, such MVDC systems will need to cover functions that are currently beyond the scope of HVDC systems engaged in point-to-point power transmission. The functional set for MVDC systems includes: (1) power transmission to grids, (2) grid forming operation to sources and loads, (3) multi-terminal connectivity, (4) grid forming operation in grids.

Chapter 3 of this TB summarizes the requirements on the operation and protection for MVDC systems. Representing active systems, the operation is largely based on converter control. Protection may be based on the specific capabilities of active systems, which allow to react fast, but with limited fault currents. A sample grid is used to illustrate the case and to show different scenarios and associated fault conditions. Main drivers of multi-terminal capabilities of MVDC systems are the need to distribute and collect power, and the need to interconnect systems of different supplies. MVDC systems represent a part of the grid rather than a system connected to the grid, this results in the need for MVDC grid codes.

In comparison to conventional AC grids, DC grids represent active systems, which allow new ways to identify and to handle fault situations. It is expected that new capabilities, which allow a more flexible operation and more efficient use of grid resources, will become the key differentiators for DC grids.

In summary, MVDC systems in public grids are just emerging. There are references in different areas of application such as marine vessels and railway power grids (described in Section 4.6 of the TB). Concepts for operation and protection can be based on such references, although their scope for emerging utility power grids is as limited as their scale in terms of power, grid supporting and grid forming capabilities. Hence, the deployment of MVDC systems in public grids will need deeper analysis by grid simulations and trial installations. This section only attempts to summarize the state of the art and to identify some areas of interest for deployment and field trials.

### 3.1 Connection of DER and Loads to MVDC Networks

MVDC grids may represent a convenient way for grid operators to integrate an increasing number of renewables (DER), storage systems and loads. The grid side converters represent grid resources in much the same way as transformers or HVDC systems, supporting grid operation. This way, the grid interface becomes a DC interface, instead of the current AC interface. The following scenario is intended to motivate the modes of operation for power converters. A more detailed view on interconnecting MVDC grids is provided in chapter 4.

Most likely innovation and competition would benefit from a DC grid code to connect DER and loads. In comparison to current AC grid codes, the grid-side converter could integrate much closer into the grid and take the role of conventional power plants. The DER-side converter (MVDC to LVDC) may replace the currently inefficient chain of {LV-DC/AC converter, LV/MV transformer and MV-AC/DC converter}.

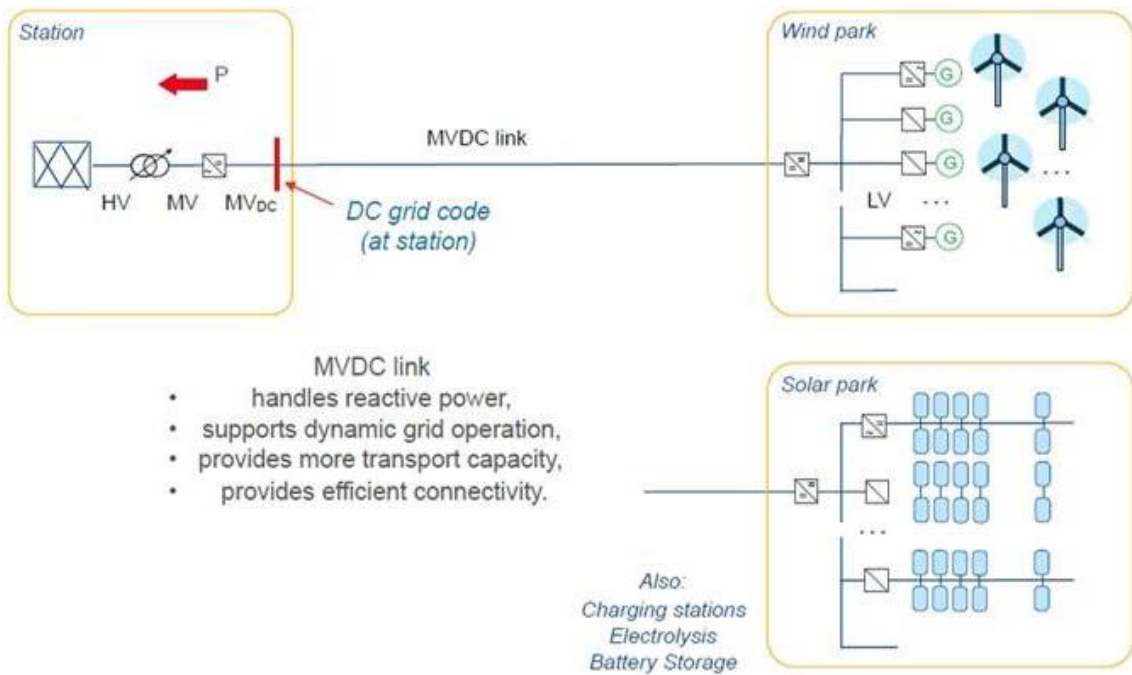


Figure 3.1 MVDC grid operation.

As of today, most DER and loads, such as charging infrastructure, electrolysis for H<sub>2</sub> production as well as battery storage, represent DC sources or sinks. Still, they connect via DC/AC converters to the AC grid. At power beyond 1 MVA, AC transformers are used to connect to the MV AC grid.

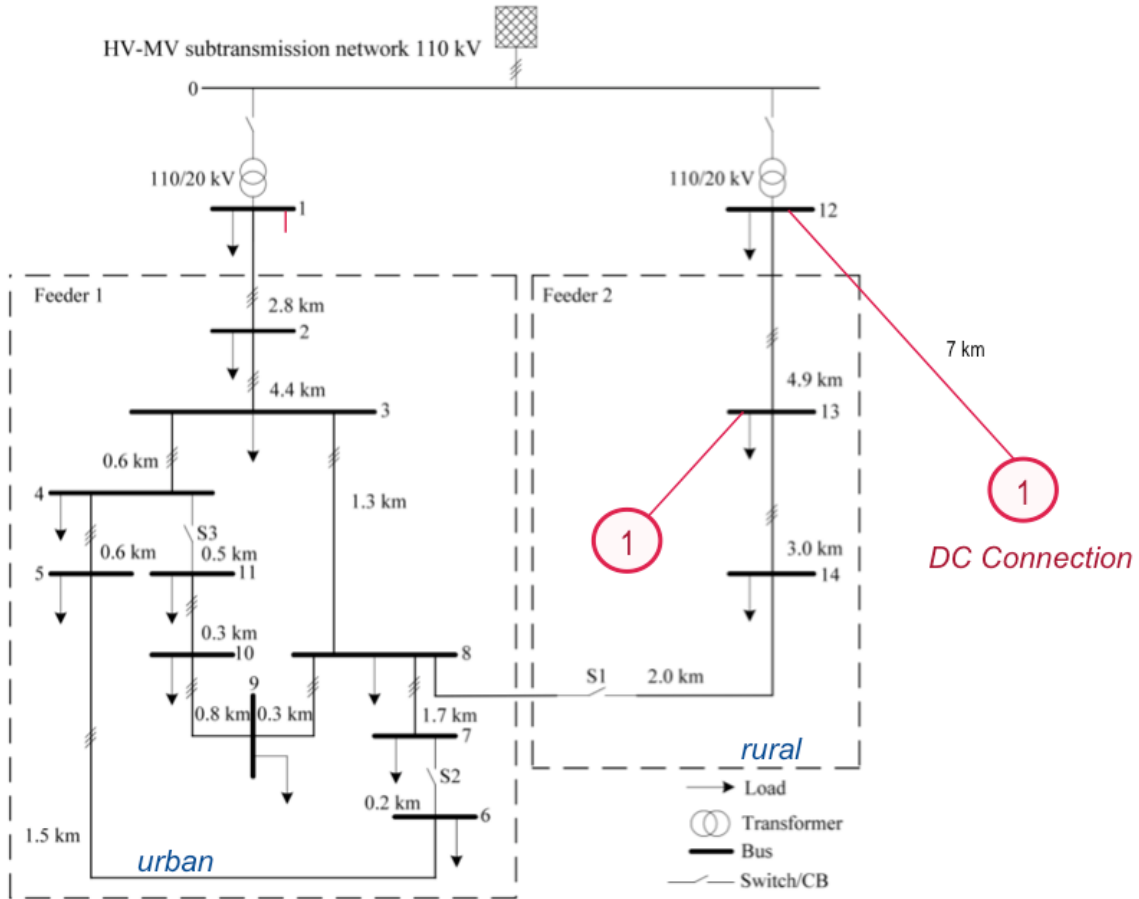


Figure 3.2 DC grid connection for DER and loads.

As shown in Fig. 3.3, an MVDC link is used to connect DER and loads, consisting of a grid-side converter (on the left), and a system-side converter (on the right). The system-side converter connects DER and loads collected over AC transformers. The grid-side converts to the grid according to an AC grid code. It is not part of the grid, but a system on the grid.

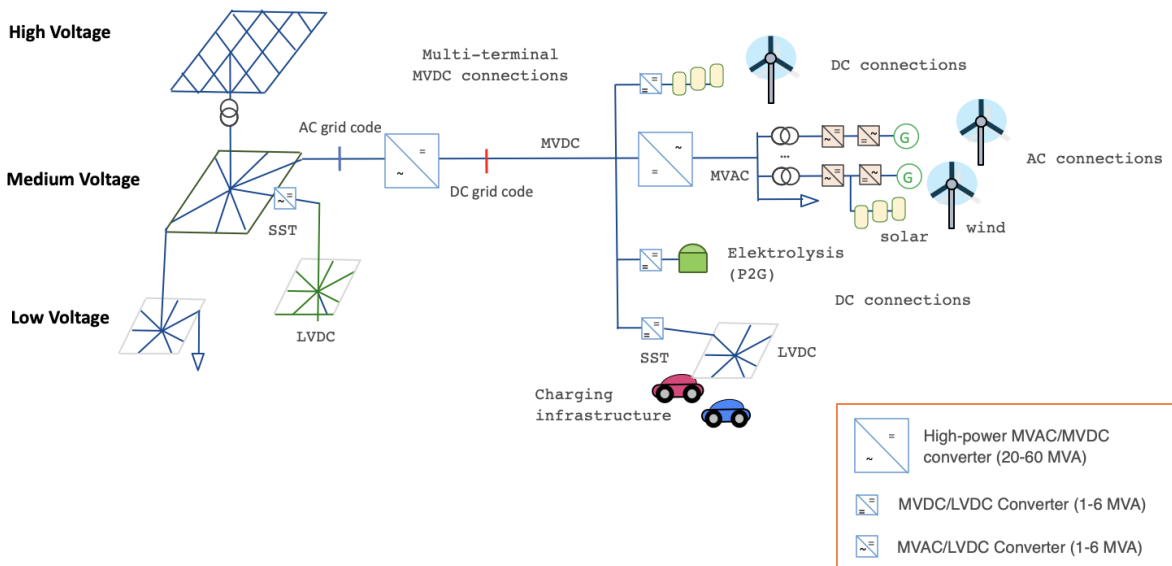


Figure 3.3 Options to connect DER and loads.

The growing number of DER and emission free loads may lead to the following developments:

1. The **grid-side converter** becoming part of the grid and is closely involved in grid operation. It will need to perform more than the current supporting functions demanded by AC grid codes, such as Q(U), Q(P), fault ride through u(t), harmonic distortion and P(f). Being a grid component, it will

need to support power and voltage management in a dynamic way. Most likely, grid operation will follow curative measures to achieve higher grid utilization.

2. The **system-side converter** for traditional **AC** connections. The combination of both converters follows the current practice in HVDC links, with the system-side converter being a grid-forming type. The systems-side converter collects AC sources and AC loads over an MVAC grid.
3. **System-side converters** for **DC** sources and sinks. The system side converters represent solid state transformers (SSTs) by implementing the combination of {MVDC/MVAC converter + transformer + LVAC/LVDC converter} into one system acting as a transforming converter for MVDC/LVDC, respectively MVAC/LVDC. DER and loads are collected over an MVDC distribution grid in much the same way as current over MV AC grids, but with different protection mechanisms.
4. The grid-side converter becoming part of the grid, the grid interface is becoming the **DC grid connection**. Among the implications are: the need for a (1) DC grid code for systems connecting at MVDC, including (2) ways to handle multi-terminal connections including protection. Another impact of the DC grid connection is clearing the way for more efficient and innovative implementations of system side converters in a competitive environment. The current AC grid codes block such options.

### 3.1.1 Power Flow Management

Conventional DC transmission systems like HVDC links or MVDC links and MVDC couplers provide controlled power flow between grids or within a mesh in the grid.

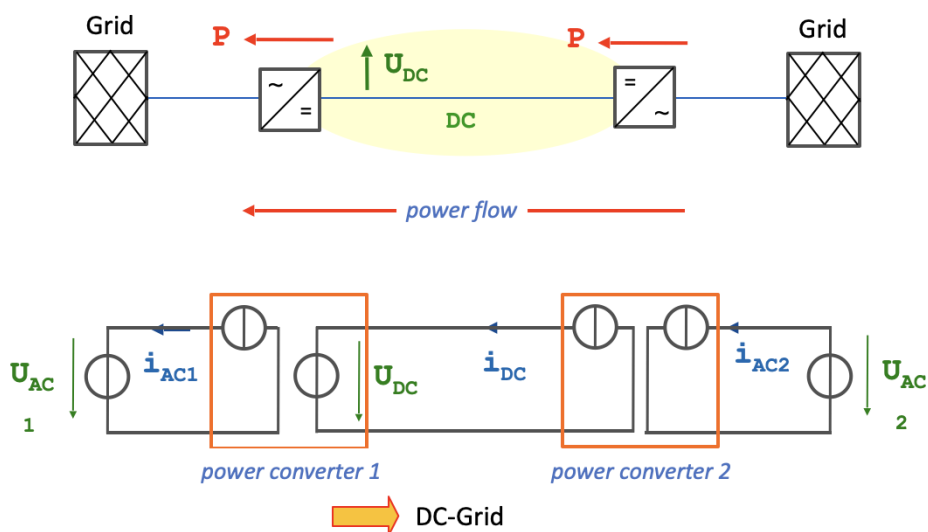


Figure 3.4 DC links and couplers provide controlled power flow.

In such configurations, the DC link handles power flow between the grids by acting as a current source on each grid, as shown in the lower part of Fig. 3.4. Load flow is bi-directional. On the DC link, one of the converters is maintaining the DC voltage, thus forming a DC grid.

A continuing growth of DER in relation to conventional power plants will need to meet the following future demands, as regards functions of the grid-side converter:

- Projected increase in DER with power electronic converters connected at distribution levels will also present challenges to the grid operators particularly with respect to reduction in short circuit levels and system inertia which are common measures of system strength. Future grid

codes will require changes to ensure DER will not compromise grid stability and security. The requirements will demand similar characteristics/behaviour to conventional power plants in terms of: grid inertia response, power oscillation damping characteristics, and fault current contribution to aid system voltage stability and facilitate protection. As such, these requirements will have to be met by the AC/DC converters that connect the MVDC systems to the AC grid systems.

- Inertia support requirements may necessitate the need for energy storage capability on the MVDC system to aid AC grid system rate of change of frequency (RoCoF) restrictions. Requirements on the size and rating of inertia support & inertia time constant (MWh/MVA) will need to be defined for a given system rating.
- Fault current contribution both in terms of amplitude, phase, rate-of-rise and duration of fault current contribution of the AC/DC converters interfacing to the AC grid will need requirements to be defined.
- To address these challenges, the AC/DC converters will need to exhibit virtual synchronous machine characteristics and act as true voltage sources capable of establishing and controlling grid voltage and frequency independent of grid status, that is “grid forming”.
- Reductions in AC grid short circuit ratios (SCR) will also impose requirements on the AC/DC converter control requirements to guarantee stability. Traditional phase locked loop (PLL) based control systems pose stability challenges particularly in weak grids with low SCRs, say  $<1$ .

### 3.1.2 Voltage Management

Connecting DER and loads via DC or AC requires a different functional set for the power converters, as shown in Fig. 3.5.

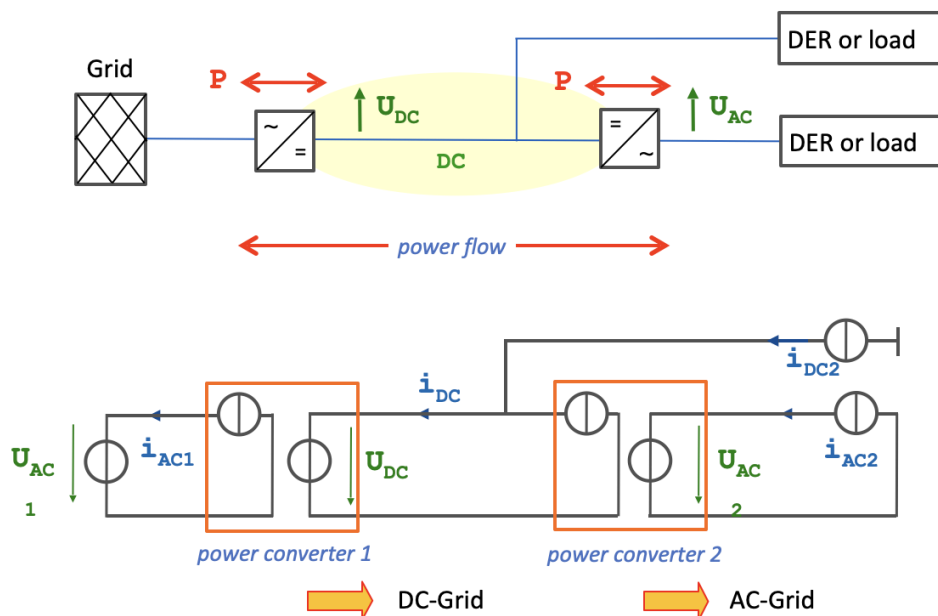


Figure 3.5 DC connections for DER and loads need grid forming converters.

Most likely, DER and loads are constant-power controlled and inject currents into the grid, or demand currents from the grid. Hence, the connecting converters in a wind farm or solar farm need to be grid forming; it is represented by a voltage source. In this configuration, both converters are grid forming:

one spans a DC grid, the other an AC grid for DER and loads.

Another major difference to current DC links or DC couplers is the fact that the DC link is not a point-to-point connection, but represents a multi-terminal system in much the same way as AC distribution grids. Voltage management in a distributed configuration is more challenging.

Among the key requirements for operating grid-forming AC and DC connections are:

- Power and voltage on the MVDC link
  - Unlike traditional AC links, MVDC links inherently allow power flow control owing to the use of power electronic converters in the grids. Requirements of power controllability will need to be defined to enable equipment from various manufacturers to be interfaced without compromising grid stability and security.
  - Standardized voltage levels will need to be defined to facilitate MVDC grid equipment specification, procurement, design and manufacture.
  - Common standards for system grounding, galvanic isolation, stray dc ground currents, corrosion issues, etc. will need to be defined
- Definitions of standard ratings for voltages and currents, maximum voltage, voltage withstand, rated current, short circuit capability, overload ratings, peak repetitive voltages, applicable tolerance limits, etc. and standard ranges to facilitate equipment specification, design and manufacture.
- Protection
  - Short circuit current limit capability of converters on fault discrimination may require departure from traditional definite time or inverse time grading (owing to bidirectional current and high rate of rise of DC fault current), technical guidelines and requirements for protection coordination will be necessary. Protection strategies and fault detection/discrimination algorithms with guidelines on selectivity, speed, sensitivity, and independence from converter control will need to be defined.
  - Communication protocols for intelligent electronic devices (IEDs) performing the fault detection and discrimination and protection devices (ACCBs, DCCBs, converters, switches) will be needed.
- Functions of the system side converters.
- Black start recovery.
- Harmonics and interference with conventional protection devices and existing sensitive infrastructures, e.g. rail signalling etc. in urban areas.
- Preventive and curative measures for (n-1) operation.

This results in new requirements on the grid-side converters and requirements for system-side converters at the DC grid connection.

### 3.1.3 Congestion Management in AC Networks

Reinforcing and extending the grid may lead to meshes with unwanted power flows. The introduction of MVDC couplers or MVDC links allows handling of congestion and controlling power flow. Such

measures need to be compared with other ways of handling load flows, such as UPFCs (i.e. FACTS). Representing full power converters, MVDC couplers and MVDC links provide full control of active power between the grid sections, and reactive power on both ends.

Unlike measures from FACTS, full converters decouple grids in terms of reactive power and frequency and thus allow individual setups for reactive power in each grid or part of the grid.

Conventional DC links and DC couplers (as shown in Fig. 3.6), including HVDC act as power controlled or current controlled systems. Growth of DER in relation to conventional power plants will demand future DC links and DC couplers to be grid forming (i.e. voltage controlled). Among the reasons is the need to provide more short circuit power and an increasing grid impedance, which renders current controlled devices increasingly difficult. This condition applies to HVDC connections and MVDC grids, irrespective of the voltage level.

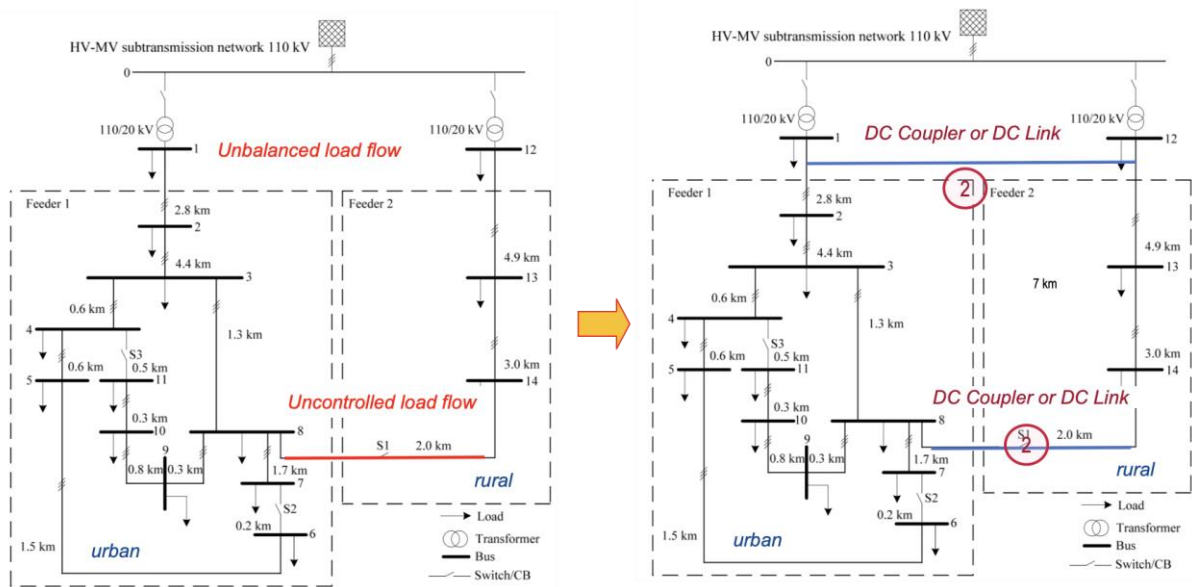
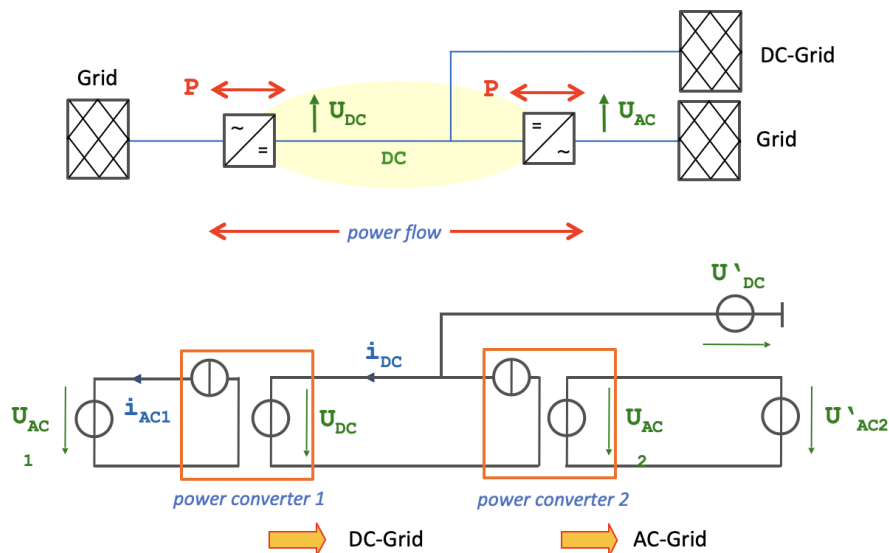


Figure 3.6 Grid reinforcement.

Fig. 3.7 shows a DC link of a DC coupler with:

- Grid forming converters on DC and the second AC connection;
- A multi-terminal link on the DC transmission.



**Figure 3.7** DC Grid forming converters on DC links and couplers.

The right hand grids are represented as voltage sources, which in reality may contain a variety of power sources and loads. Without any voltage controlled generators in the right hand grids, this case is identical to the connection of DER and loads shown in **Fig. 3.5**.

When at least one of the grids on the right contains voltage sources, the grid-forming converters need appropriate control algorithms. Among the challenges are:

- load flow in a multi-terminal configuration;
- recovery from faults including black start capabilities;
- fault detection and protection.

### 3.1.4 MVDC Sub-transmission

MVDC provides measures to reinforce the grids and provision for extra connectivity for DER and loads. A reinforced and extended MV grid (distribution grid) may also off-load the transmission grids by:

- Using high capacity MVDC links over larger distances;
- Using high capacity MVDC links instead of (say) 110 kV AC sub-transmission links.

The possible feasibility of 50 kV DC transmission over AC underground cable may allow MVDC connections over longer distances. Given the better public acceptance of underground cables in comparison to overhead wire, this may facilitate grid reinforcements.

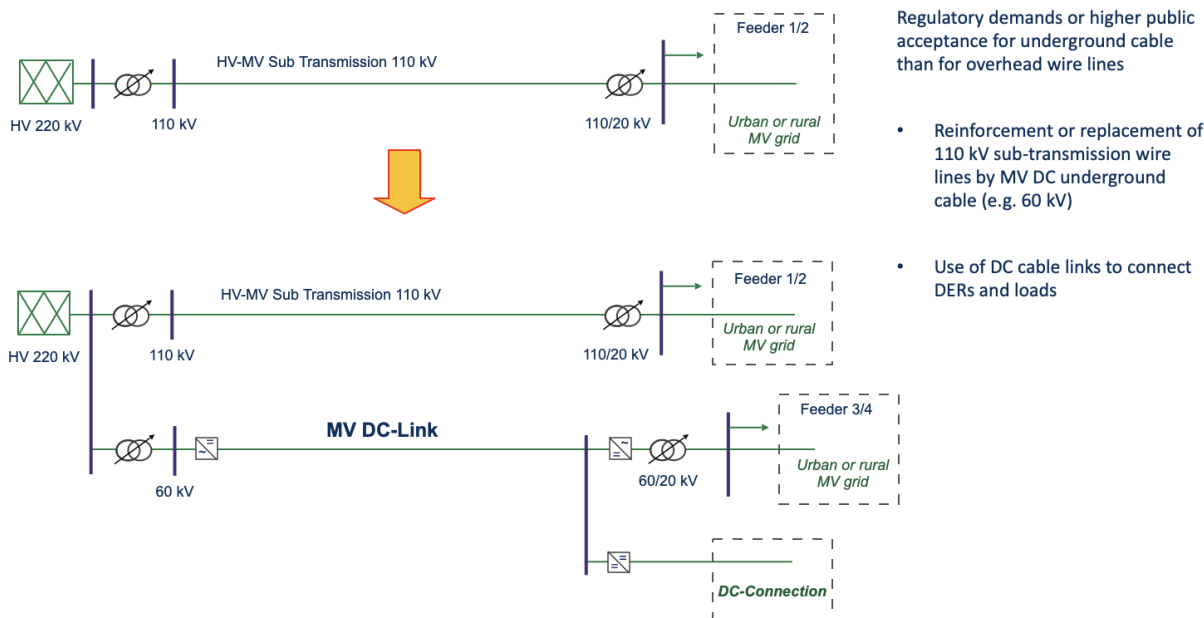


**Figure 3.8** MVDC links at sub transmission layer.

Whether DC systems over conventional AC cables may provide a higher transport capacity than AC systems and allows to replace 110 kV/138 kV sub transmission lines at a commercial benefit remains to be investigated.

## 3.2 Dynamic Models of MVDC Converters and Networks

The dynamic behaviour of converter systems can be described in the frequency domain. By this

method power converters are represented by current sources and voltage sources (or, alternatively, Thevenin or Norton circuits) to show their essential properties as power sources, power sinks and grid-forming converters. The same methods apply to AC grids and DC grids.

### 3.2.1 Converter Dynamic Behaviour - AC

The frequency domain behaviour of a converter connected to an AC grid is crucial for analysing the performance and stability of the combined system. The stability of the inter-connected system can be analysed using the impedance-based stability criterion [40] or the passivity-based stability assessment [41], which are based on the converter impedance, or admittance, measured at its AC terminals. The former can be understood by observing how the converter-grid-combination can be interpreted as a closed-loop control system, see Fig. 3.9. Thus, conventional theory for the dynamic properties and stability of feedback systems can be used, if the converter admittance  $1/Z_c$  is known.

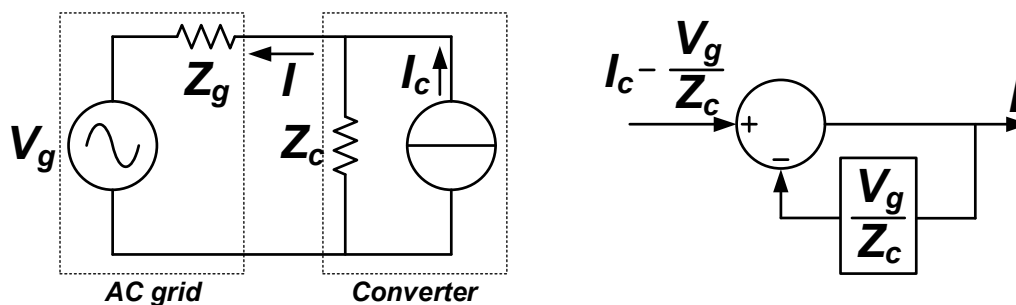


Figure 3.9 Schematic of a grid-connected converter and, right, the equivalent signal flow diagram.

The behaviour of power converters is inherently non-linear due to the switching action, which amounts to the multiplication of voltage and current by a switching function. An applied current or voltage harmonic will therefore generally cause a response in the form of several harmonics at different frequencies. This implies that deriving the converter admittance is challenging, and generally only small-signal analysis on a linearized system is possible. Furthermore, the converter admittance is heavily influenced by the control system of the converter so any meaningful analysis must include exact information about the control scheme and the control parameters. A straightforward way of determining the admittance is to apply a perturbation signal and measure the response. This can either be made in a simulation or on a physical system [42]. However, such methods do not provide a deeper insight into how the system parameters affect the admittance characteristic, and analytical methods also have an important role to fill.

Several methods are known from the literature for analytically deriving the AC-side admittance of voltage source converters. For two-level VSCs, examples are reported in [43] and [44]. For MVDC applications, MMCs [45] are also optional candidates, to handle the voltage. Analytical models of the MMC AC-side admittance by using small-signal analysis in the time domain, which is then shifted to the Laplace domain where the admittance expressions are derived, are documented in [46]. A sequence impedance model for MMCs is presented in [47], based on multi-harmonic linearization. This methodology is comprehensive and can easily take the impact of different control schemes into account. However, it involves significant matrix manipulation and implies significant complexity. It, therefore, offers few hints as to how changes in the system affect the admittance.

A further approach is the use of a linear model obtained by analysing the main perturbation frequency components of the converter variables individually. This method reaches a good balance between accuracy and complexity while making it possible to consider different control schemes. Fig. 3.10 shows results from the latter approach [48], where analytically derived admittances are compared to measured values from an MMC prototype. The results for three different control

schemes are illustrated in the figure.

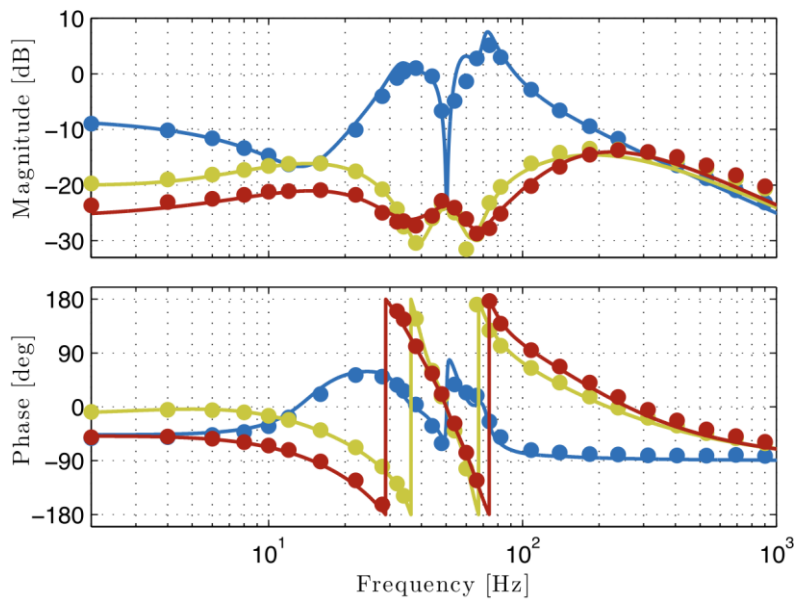


**Figure 3.10** Bode diagrams of the MMC ac-side admittance for different control schemes: fixed references (blue); per-phase AC-side current control and circulating current control (yellow); dq frame AC-side current control and circulating current control (red). Results from the measurements on prototype (dots) and the analytical model (lines) are shown [48].

A further common way of assessing stability in converter-grid interaction is the eigenvalue-based method. It is based on state space models and to examine the eigenvalues of the system matrix [49].

### 3.2.2 Converter Dynamic Behaviour - DC

In a multi-terminal connection, involving several voltage source converters connected in parallel on the DC side, such as in an MVDC distribution system, the DC side dynamic properties of a converter will also be of importance. Similar methodologies as discussed in the previous section can be used for analysing stability and dynamic properties but, instead, the DC side converter admittance is required. Several studies have been made over the years to analyse how the choice of topology and the controllers influence the DC side behaviour. In [50] and [51], the DC-terminal impedance of a two-level VSC has been analytically derived and the stability of the VSC-HVDC system is analysed. The DC-side admittance modelling of MMCs has also been studied extensively and both analytical solutions [52] and methods based on harmonic linearization [52]-[54] are reported.

**Fig. 3.11** shows the DC-side admittances of an MMC under various control schemes. A combination of harmonic linearization and frequency domain representation has been used to model the converter admittance [55] and the results have been verified experimentally. Similar results have been reported in [53] and [54] with different levels of model complexity.

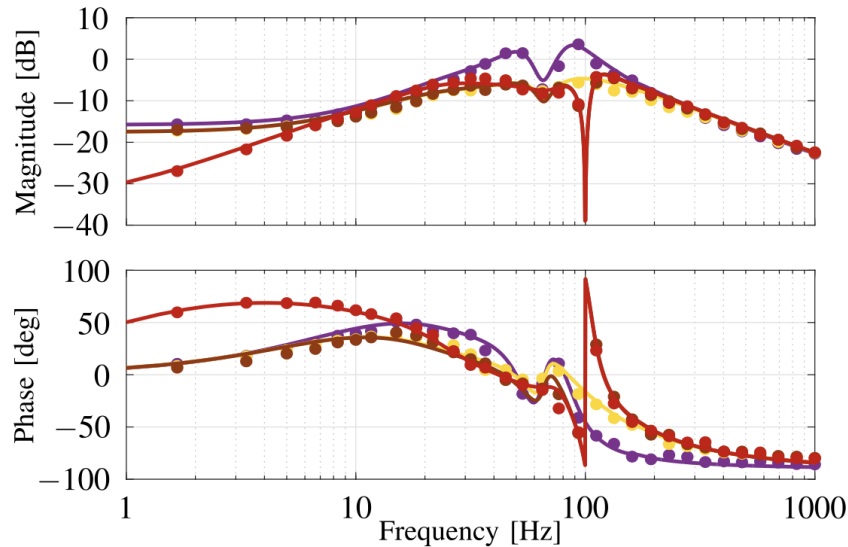


Figure 3.11 Bode diagrams of the MMC DC-side admittance for different control schemes: dq-frame AC-side current proportional controller (purple); addition of circulating current proportional controller (yellow); addition of circulating current resonant controller (brown); addition of AC-side current integral controller (red). The analytical models are indicated by the solid lines and the measurements with dots [55].

In the DC side, converters may be grid forming or feeding into a grid. In the most simple case, the DC side and AC side are coupled by active power, as indicated in Fig. 3.12. This way, active power at AC is determined by the power feeding into the DC grid (respectively power taken from the DC grid). AC control still covers reactive power; DC control represents provisioning DC voltage, i.e. DC grid forming. Converter control is based on  $Q$  and  $V_{DC}$ . In the DC grid, other converters are feeding in as DER or loads.

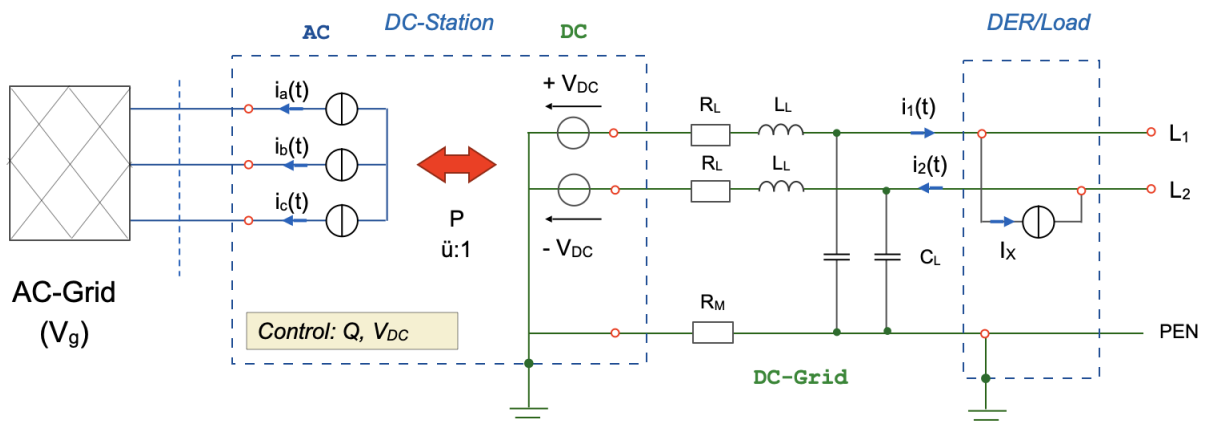


Figure 3.12 Converter forming a DC grid.

In the DC side, the circuit may be simplified as shown in Fig. 3.13. While the transient behaviour in the time domain is of most interest, the system may still be analysed in the frequency domain in order to describe its dynamic behaviour. Thus, the structure remains the same as on the AC side, with the converter now representing the grid and other sources or loads feeding in as current sources. The DC voltage of the DC grid now represents the dynamic behaviour of a grid forming converter in much the same way as the current at the point of interconnection for a converter feeding into the grid.

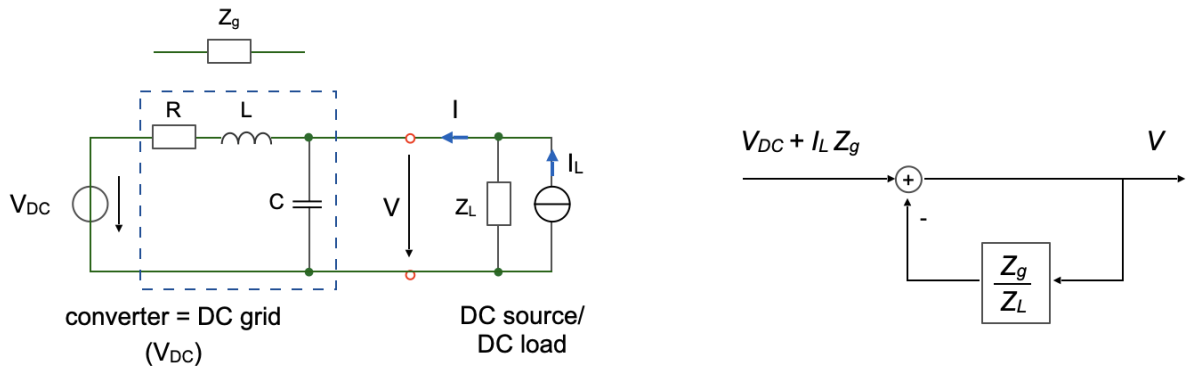


Figure 3.13 Simplified converter model (DC side).

In a multi-terminal configuration, multiple DC sources and DC loads are connected to the grid-forming converter. A distributed configuration is essentially described by its line of cable impedances (which are mainly inductive under load in a cable based grid), and the input capacitors of the connected loads and sources. Hence, each load or source represents a resonant circuit, i.e. an LC filter with the load representing the attenuation R. For the total dynamic behaviour, the resonances accumulate on the system.

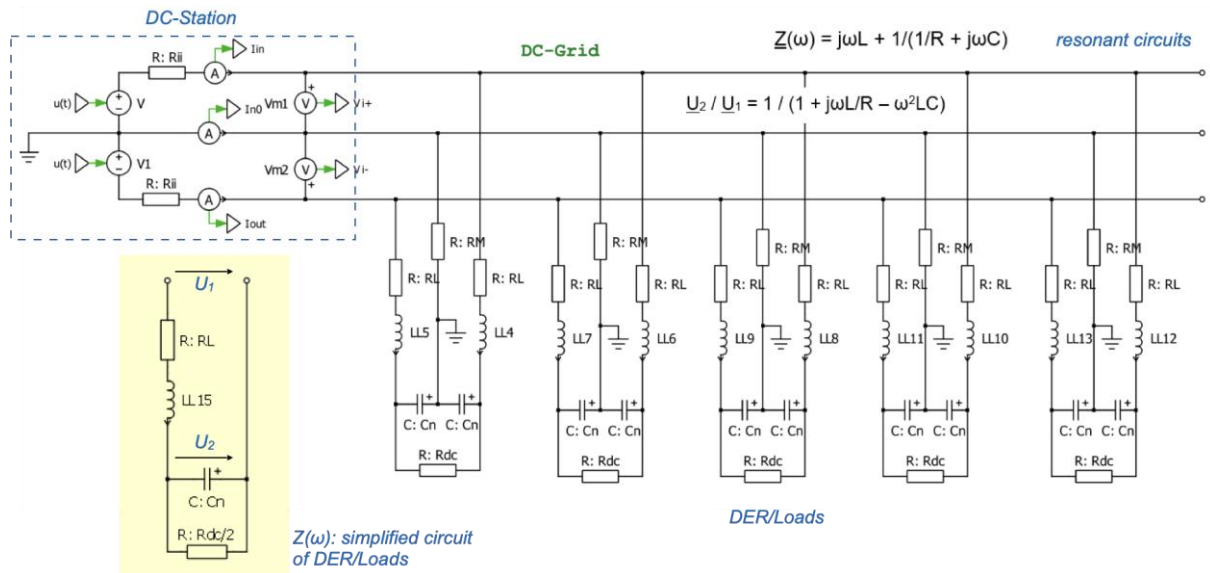


Figure 3.14 Dynamic model of the DC grid.

The same methods apply for analysing the dynamic behaviour and stability of AC and DC systems. Depending on the role of the converter, it is represented as a current source on an AC grid or DC grid, respectively a voltage source for a grid forming converter. Multi-terminal configurations require the specification of converter dynamics depending on the specific properties of the grid.

### 3.2.3 Converter Behaviour When Operating Between Two Grids

For a converter operating between two grids, e.g. between an AC grid and a DC grid, balance of power is maintained: the converter is nearly free of losses and does not contain a power source. This way, incoming power in grid 2 is equal to the outgoing power in grid 1, as shown in Fig. 3.14.

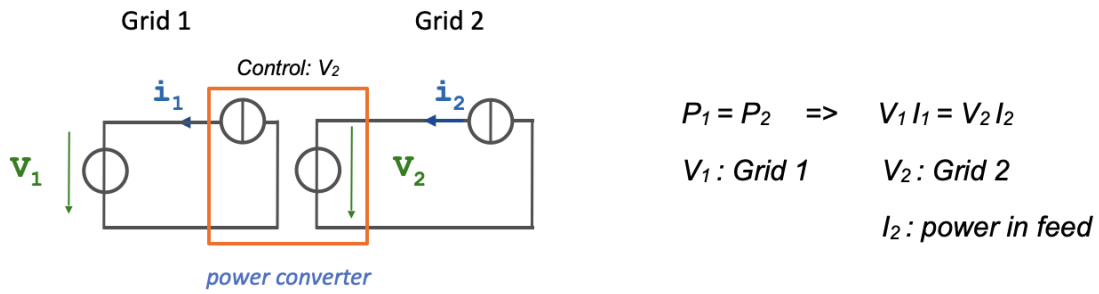


Figure 3.15 Converter model between two grids.

If the voltage  $V_1$  is determined by Grid 1, the power converter provides the voltage  $V_2$  of Grid 2. The power in-feed or load in Grid 2 determines the current  $i_2$ . This way, the current  $i_1$  in Grid 1 follows the power, which the power consumes from Grid 2 by maintaining the grid voltage  $V_2$  in grid-forming mode.  $i_1$  is fixed by the balance of power ( $P_1 = P_2$ ).

In the examples shown in this section, Grid 1 is represented by an AC grid, and Grid 2 by a DC grid, i.e. the converter transforms DC/AC. The converter model is not limited to this choice: Grid 1 could be a DC grid, where the converter feeds power from an AC grid and transforms AC/DC. In the same way, the converter may operate as a DC/DC converter or AC/AC converter. Voltage levels in both grids may be different. In this model, both grids are coupled by active power.

### 3.3 Multi-terminal MVDC Grid Operation and Control

Unlike HVDC systems, MVDC systems may not exactly apply to off-shore wind farms, where the MVDC could achieve important cable lengths if this type of DC link is developed. The main objective for DC systems at MV is to collect DER and DC loads in an efficient way. At some point, DC systems need to be converted into AC in order to connect to the grid. With MVDC systems, this point moves from LV level to MV level. Connecting multiple DER and DC loads leads to multi-terminal MVDC grids.

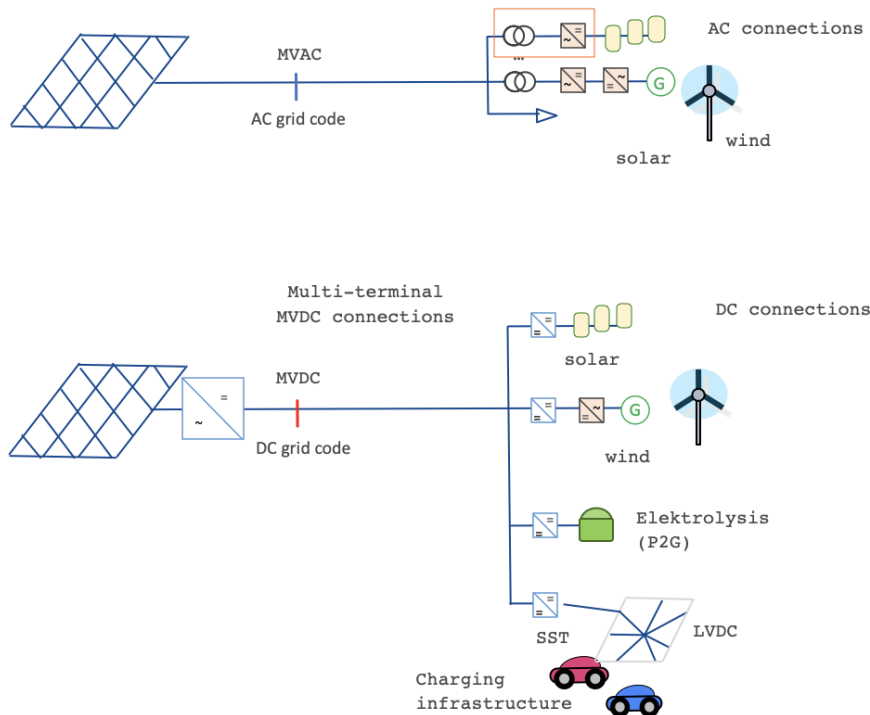


Figure 3.16 Multi-terminal MVDC and MVAC grids.

The DC grid connects distributed systems in the same way as an MVAC grid. In comparison to AC

links, DC links allow a simplified converter structure and the benefits of decoupling reactive power. However, power converters introduce power losses. For the configurations indicated in **Fig. 3.16**, the power losses are:

- Cable or overhead line:
  - Under the condition of the same peak voltage (which roughly corresponds to  $1.4 \approx \sqrt{2}$  of the RMS value), and under the condition of the same RMS-current (i.e. equivalent thermal conditions), an MVDC link loses 2/3 of the power of an MVAC link when operated at same power (using 2 wires instead of 3 wires).
  - Total losses depend on the distance and type of cable or conductor.
- Chain of converters:
  - AC: (1) transformer + (2) LV AC/DC converter
  - DC: (1) MVAC/MVDC converter + (2) MVDC/LVDC converter

In such a configuration, one power converter at the point of interconnection to the AC grid is inevitable. Using a centralized MVAC/MVDC converter (DC case) for the same total power can be expected to provide a more efficient solution than the use of multiple transformers and LV AC/DC converters (AC case). However, the DC case needs an MVDC/LVDC converter instead of a simple MV/LV transformer. This case needs to be justified in terms of costs, overall efficiency and the benefits of a more flexible way of operating the grid.

Hence grid operation and control are becoming the key differentiator for MVDC grids.

In summary, a multi-terminal MVDC grid may provide lower losses than conventional MVAC grids, if the distances between systems and the grid are significant and if operated at the same power and RMS currents. In terms of capacity, the MV DC provides better utilization of cables or conductors, and may provide a higher transport capacity, when operated at a higher voltage level (i.e. beyond the peak AC-voltage). However, multi-terminal operation has implications on the control of converters.

### 3.3.1 Converter Control

**Viewpoint:** The control of a multi-terminal MVDC grid can adopt the traditional multi-layer structure more similar to HVDC, but it should pay more attention to its expandability and compatibility due to the specific features of distribution networks. Usually, more time-variable loads and DER are integrated into the distribution network. The multi-layer structure of DC grid control includes three layers which are: system control, converter control and valve control. System control coordinates each converter in the grid by giving the voltage or the power reference in accordance with the operational objectives. Converter control mitigates the deviation between the measured and the reference values in real time, thereby tracking the power and voltage orders. Valve control produces the pulses through an appropriate modulation to trigger the valves.

Converter control receives the power and voltage orders as the reference values which the system control gives to each converter station. Depending on the algorithm of PI control, it reduces the deviation between the measured values and the reference. The control methods are generally illustrated as power-voltage curves [49]. The typical converter controls are introduced in this section.

#### 3.3.1.1 Constant power control

Constant power control is represented as a vertical line segment in the  $P-U$  plane as shown in **Fig. 3.17**.  $P_{ref}$  denotes the power reference. The vertical line in the figure is the possible working points of the converter station.

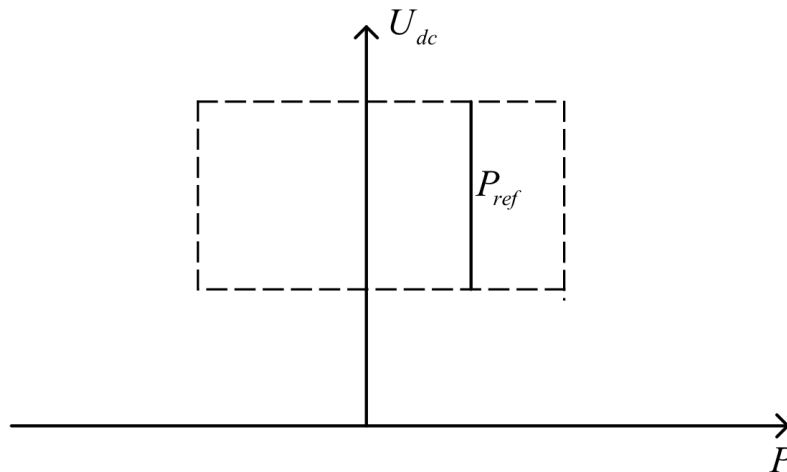


Figure 3.17 P-U curve for constant power control.

### 3.3.1.2 Constant voltage control

Similarly, constant voltage control can be represented as a horizontal curve in the  $P-U$  plane (**Fig. 3.18**).  $U_{dcref}$  denotes the voltage reference. The horizontal curve consists of the possible working points of the converter station. The converter with this type of control is often selected as a DC “slack bus” to balance the active power in the DC grid.

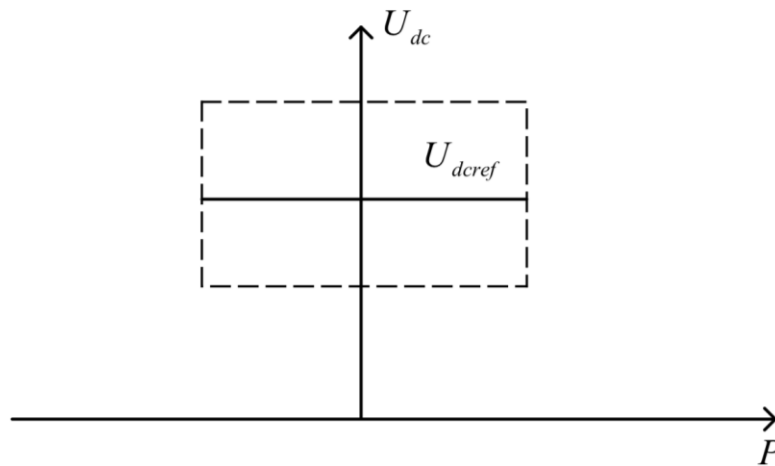


Figure 3.18 P-U curve for constant voltage control.

## 3.3.2 System Control

Nowadays, most control schemes for multi-terminal MVDC are adapted from HVDC transmission systems, including the system-level control and the converter-level control. The converter-level control is usually based on the double close-loop structure, tracking the reference power or voltage. The system-level control coordinates the converters in the grid by giving the voltage or the power reference in accordance with the operational objectives. The system control is achieved by optimizing the real-time DC voltage and active power from the aspects of the entire grid. Nowadays, mature methods include master-slave control, voltage margin control and voltage droop control. MVDC controls need to be integrated into station control and control centres in much the same way as other grid resources.

### 3.3.2.1 Master-slave control

In master-slave control, a converter station is designated as the master control station, which usually regulates the DC voltage of the network. Other stations control their power, as shown in Fig. 3.19. The master station acts as a DC “slack bus” to maintain the DC voltage stability and balance the active power within the DC network. The DC voltage of the grid is determined by the master station, and the working points of the slave stations are determined by both the DC voltage and the power, as shown by the intersection point in Fig. 3.19. This control method features its simple structure and easy implementation. However, it requires enough backup capacity in the master station. With increasing system capacity and complexity, the feasibility of master-slave control becomes limited.



Figure 3.19 Master-slave control.

### 3.3.2.2 Voltage margin control

Voltage margin control is a kind of modification on the master-slave control. A converter with voltage margin control normally operates in constant power control (as long as the voltage is within the normal operation voltage margin). If the voltage deviation goes beyond the limit of the voltage margin, the converter controller will switch to constant voltage control mode, clamping the voltage at the margin limit to prevent further voltage deviation. This type of control is illustrated in the Fig. 3.20.

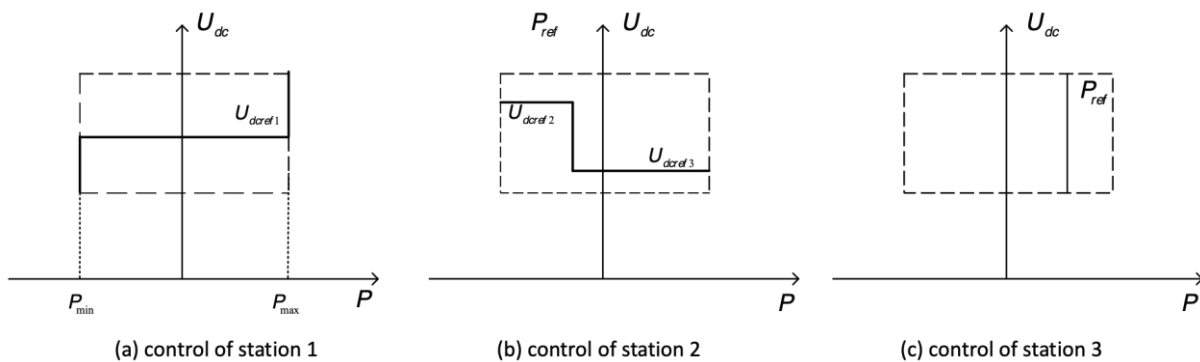


Figure 3.20 Voltage margin control.

The limits  $P_{\min}$  and  $P_{\max}$  are the minimum and the maximum active power of Station 1.  $U_{dcref1}$  is the DC voltage reference.  $U_{dcref2}$  and  $U_{dcref3}$  are the highest and the lowest values of the voltage margin set by Station 2. The reference active power is  $P_{ref}$ . In the case that the power of Station 1 reaches the limits or Station 1 fails, Station 1 cannot control the DC voltage and the DC voltage will no longer remain at  $U_{dcref1}$ . When the voltage reaches  $U_{dcref2}$  or  $U_{dcref3}$ , Station 2 will switch from constant power control to constant voltage control, clamping the voltage at the margin limit to prevent further deviation.

When the master station reaches its power capacity limit in the master-slave control, the master station will not be able to maintain the DC voltage, which may lead to unstable operation. However, the voltage margin control can manage to avoid this situation. The voltage margin control is more reliable as more than one converter can be switched to maintain the DC voltage. But it may lead to

conflicts and perform in an unexpected manner, especially in a large network. Additionally, when the number of terminals increases, it will be challenging to configure their voltage margins to satisfy both the steady-state and dynamic requirements [50].

### 3.3.2.3 Droop control

This control method is suitable for systems with multiple converter stations, which can enable the voltage and power control to be realized in a distributed manner. When the system is disturbed, the converter stations using droop control balance the active power according to their  $P$ - $U$  curve and stabilize the DC voltage. The larger the droop slope, the larger the power change. The control is illustrated in Fig. 3.21.

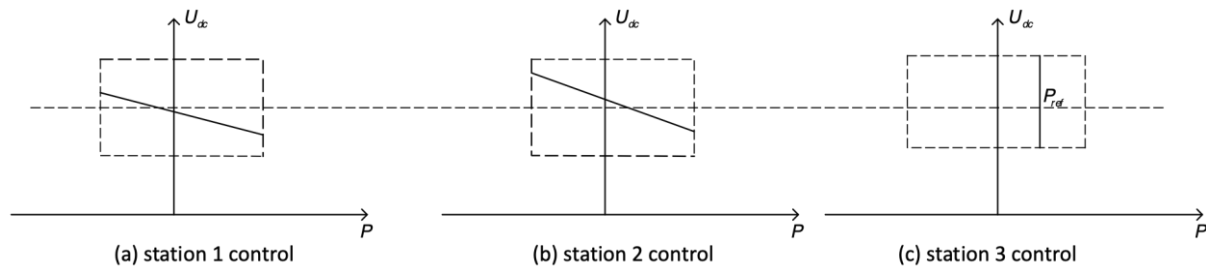


Figure 3.21 Droop control.

In droop control, more than one station maintains the voltage of the DC grid, so it shows better stability. In the extreme situation that one station quits, the grid might not collapse as the remaining stations share the DC voltage control by adjusting their power. Besides, it is easy to configure the droop control scheme without modifying the control system of other converter stations. The main drawback of droop control is the inherent trade-off between the DC voltage deviations and the power sharing accuracy. It is difficult to choose the droop slope. Besides, the DC voltage working point in the droop strategy is not fixed hence the power flow can't be controlled precisely [57].

### 3.3.2.4 Adaptive droop control

The MVDC distribution network usually supplies more time-variable loads than the transmission grid. In addition, more DER are integrated in the distribution network. All these challenges make the working mode in MVDC change frequently. In traditional droop control, the margin of the converter station cannot be fully utilized when the system operation frequently changes with more uncertainty. Hence the adaptive droop control method has been proposed. It is an improvement of droop control, which adjusts the droop slopes in real-time to make full use of the power margin of the converter station. Therefore, it has a good application prospect in MVDC control.

[58] proposes a 10 kV radial multi-terminal MVDC distribution network in PSCAD/EMTDC with solar PV integration. The preliminary study is carried out involving the modelling and comparison of the master-slave, voltage margin and droop control. The results show that droop control is the most responsive and flexible in the MVDC distribution network. However, MVDC contains many renewable energy sources. It is impossible to take into account all their operating conditions in droop control. This will cause the station power to change significantly, making it difficult to achieve the balance between DC voltage deviation and power distribution accuracy. Meanwhile, the proper droop slope is difficult to choose.

Consequently, many adaptive droop control methods have been proposed in the literature to simultaneously and effectively fulfil the constraints on DC voltage and power deviations [59]-[61]. An example of adaptive droop control that changes the droop slope is described below.

The droop slopes  $k_i$  and  $k'_i$  of voltage droop control and adaptive droop control are as follows :

$$(1) \quad k_i = \frac{P_i^{\max} - P_i^{\min}}{U_{dci}^{\max} - U_{dci}^{\min}} = \frac{2P_N}{U_{dci}^{\max} - U_{dci}^{\min}}$$

$$(2) \quad k'_i = \alpha k_i \frac{P_i^{\max} + \text{sgn}(U_{dci} - U_{dci}^{\text{ref}})P_i}{2P_i^{\max}}$$

where, for the  $i$ th converter station,  $P_N$  is the rated power,  $P_i^{\max}$  is the maximum power,  $P_i^{\min}$  is the minimum power,  $U_{dci}^{\max}$  is the maximum voltage,  $U_{dci}^{\min}$  is the minimum voltage,  $U_{dci}$  is the DC voltage,  $P_i$  is the power,  $\alpha$  is the scale factor,  $\text{sgn}(x)$  is the sign function.

When the total power changes  $\Delta P$ , the power change of the  $j$ th converter station is  $\Delta P_j$

$$(3) \quad \Delta P_j = \frac{K_j \Delta P}{\sum_{i=1}^n k_i}$$

where  $k_j$  is the droop slope of the  $j$ th station,  $n$  is the total number of the station used voltage droop control,  $k_i$  is droop slope of the  $i$ th converter station.

It can be seen from equation (3) that when  $\Delta P$  is constant, the larger the droop slope  $k_j$ , the larger the power change  $\Delta P_j$ . When droop control is used, in the case of large power fluctuations, some converter stations with large droop slopes may be fully loaded or even overloaded. In adaptive control, the droop slope can be adaptively changed with the change of active power, thereby slowing down the trend of power change and preventing the converter station from being fully loaded or even overloaded due to excessive unbalanced power. Therefore, adaptive droop control can benefit the access of renewable energy to MVDC, and will not cause the converter station to be fully loaded or even overloaded due to the unreasonable droop slope setting.

### 3.4 Operation of MV Networks with MVDC under Fault Conditions

DC systems connected to MV networks or MVDC grids embedded in MV networks need to perform under fault conditions. Fault conditions vary depending on the types of interconnection. To classify different cases, a generalized grid is used, as shown in **Fig. 3.22**.

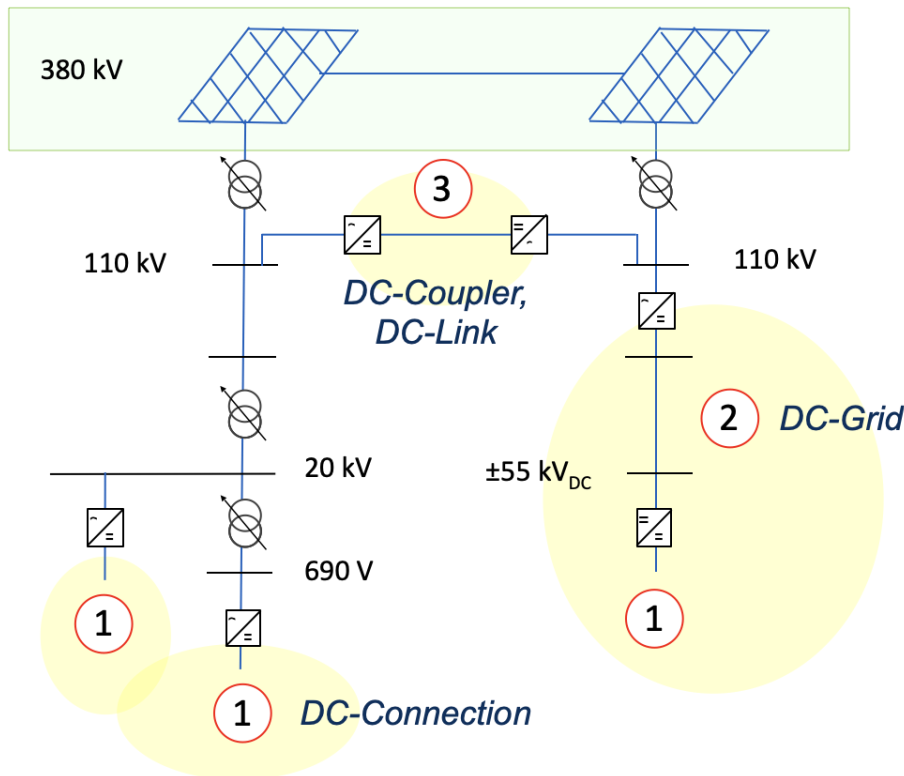


Figure 3.22 Example of hybrid AC and DC grids.

The following cases may be differentiated:

- **DC-Connection:** In this case, a system representing a DC source (DER) or DC load connects to the AC grid. This case is well described in the current AC grid codes. At the point of connection (POC), systems need to comply with (1) requirements on reactive power (such as  $Q(U)$ ,  $Q(P)$ , load factor  $\cos\phi$ ); (2) requirements on active power (such as  $P(f)$  supporting the grid depending on the load situation); (3) requirements on harmonics, and (4) over-voltage fault ride through and under-voltage fault ride through. The latter represents common practice for fault conditions in the AC grid.
- **DC-Grid:** In this case, systems representing DC sources (DER) or DC loads connect to the AC grid via DC links and DC grids. Concerning the POC, this case is identical to the case of a DC connection above. The same grid codes apply and are common practice. This way, the DC grid is part of a system connecting to an AC grid. For a grid operator, the DC grid is entirely out of scope. The situation changes if the grid operator is offering a DC grid connection for systems to interconnect to the grid. In this case, a DC grid code is required to define the system requirements including the behaviour in case of faults. It is obvious that the existing AC grid codes are of limited value in this case: reactive power does not exist, a grid frequency does not exist. Remaining from an AC grid code are requirements on harmonics and requirements on fault ride through. At the same time, systems will need to support the grid depending on the load situation, so an equivalent of  $P(f)$  is in demand. DC grid codes still appear far from common practice and represent a valid area for field trials and standardization.
- **DC Coupler or DC Link:** In this case, MVDC converters are used to couple two MV grids or grid sections with or without a DC transmission link. This situation corresponds to HVDC systems implemented in transmission grids. DC links and DC couplers allow a horizontal exchange of power below the transmission level and represent a way to reinforce power grids. There are in-service installations and field trials, so common practice is emerging. Like in HVDC transmission, the DC links in current installations are point-to-point connections and represent proprietary systems with both ends of the link implemented by the same supplier. There are no specifications or grid codes on the DC link yet. Because the MVDC link is embedded into the grid, common AC

grid codes usually do not apply. Thus, the behaviour in fault conditions remains the property of the grid operator.

In summary, operation under fault conditions is:

- **well defined** in common AC grid codes for DC systems connecting at the AC interconnection point,
- **entirely in the hands of the grid operator** in case of DC links or DC couplers, or
- **entirely open** in the case of DC systems connecting on a DC interconnection point or DC systems connecting to a DC grid.

An implication of the current lack of standardized DC grid codes for DC systems is that connecting DC systems remains a project-specific exercise. There is no easy way to achieve interoperability between systems from different suppliers. For further studies on operation under fault conditions, connecting DC systems to an MV grid is analysed in a sample grid containing different scenarios for interconnection.

### 3.4.1 MVDC Grid Scenarios

The sample grid shown in **Fig. 3.23** connects different DER and loads to the grid: power stations with high power chargers replacing petrol stations, solar farms, and wind- and gas farms which allow to store surplus power and feeding it in from storage devices. In the sample grid, the POC to the AC grid has been moved into the MV level: a DC grid connects directly to the transmission grid over an AC transformer or via an HVDC system. This sample depicts a possible future scenario for the purpose of investigations. As of today, MVDC and HVDC converters have not been integrated in the field yet, according to the knowledge of the authors. In order to connect DER and loads on the other ends, a future DC grid will need to provide several voltage levels in much the same way as AC grids do.

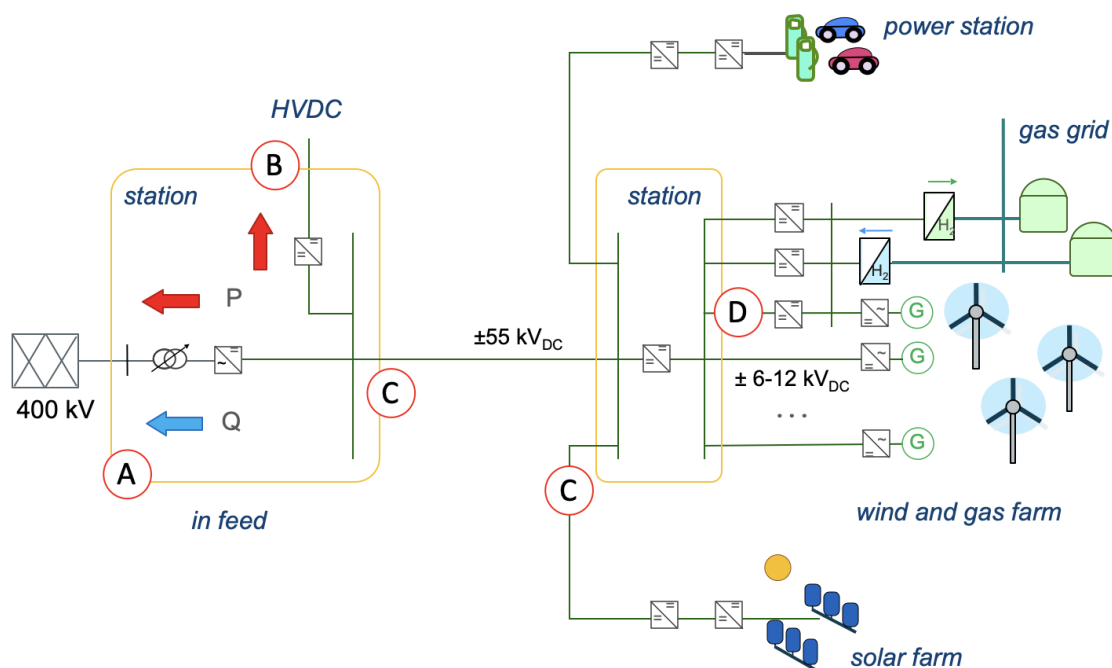


Figure 3.23 A multi-terminal MVDC grid scenario.

Concerning operation under fault conditions, the sample grid contains the following scenarios for

interconnection:

- **Case A: AC interconnection as POC.** This case is well described and common practice in current grid codes with one open issue: future grids will most likely demand a higher level of grid supporting functions beyond P(f). As now emerging in the case of HVDC links, systems connecting at this point most likely will need to be grid forming, at least under fault conditions. Such scenarios are under discussion in corresponding grid initiatives.
- **Case B: HVDC interconnection as POC.** This case is not well defined yet and will need more investigations and field trials. Support of fault conditions at the AC interconnection point of the HVDC system will need to be propagated to the systems at the HVDC interconnection in some way [ruling out P(f)].
- **Case C: DC interconnection at MV level as POC.** Unlike current HVDC systems and MVDC links, the DC interconnections need to be (1) open to any operator and supplier; and (2) supporting multi-terminal configurations. Corresponding DC grid codes need to be developed and put into practice in field trials. Existing AC grid codes may be used as a basis. However, concepts for grid supporting functions, fault ride through conditions, and grid forming functions need to be developed. In particular, grid supporting functions, grid forming functions, and fault conditions need to be propagated from the superior point of interconnection (Case A or Case B) to the Case C type of interconnection. The Case C type of interconnection either represents a boundary between grids or sections of a grid, or a boundary between the grid and DC systems.
- **Case D: DC interconnection at MV level as POC.** This point of interconnections replicates the properties of the Case C type of interconnection, but on a lower voltage level. Requirements of the Case C might be scaled down to the lower level of power of connected DC systems.

The scenario contains fault conditions both in the AC grid and in the DC grid.

### 3.4.2 Fault Conditions in AC and DC Grids

Depending on their origin, fault conditions have different implications. Depending on the role of grid components, handling fault conditions have different objectives: in an AC grid, generators are supposed to contribute to the short circuit currents to trigger grid protection. In an MVDC grid, fault conditions, fault effects and protection depend on the specific situation. **Fig. 3.24** shows different fault conditions in the grid scenario used in this section.

For AC faults (i.e. MV network related faults), the objective is to support grid protection in the case of near faults. For far faults, the objective is to maintain operation by supporting the grid. For a generator, this means to support the grid voltage. For DC faults (i.e. faults in the MVDC grid), the objective is to isolate the faulting part (by selective protection) and maintain operation of the rest in the same way as on AC grids. Reactions depend on the specific fault conditions.

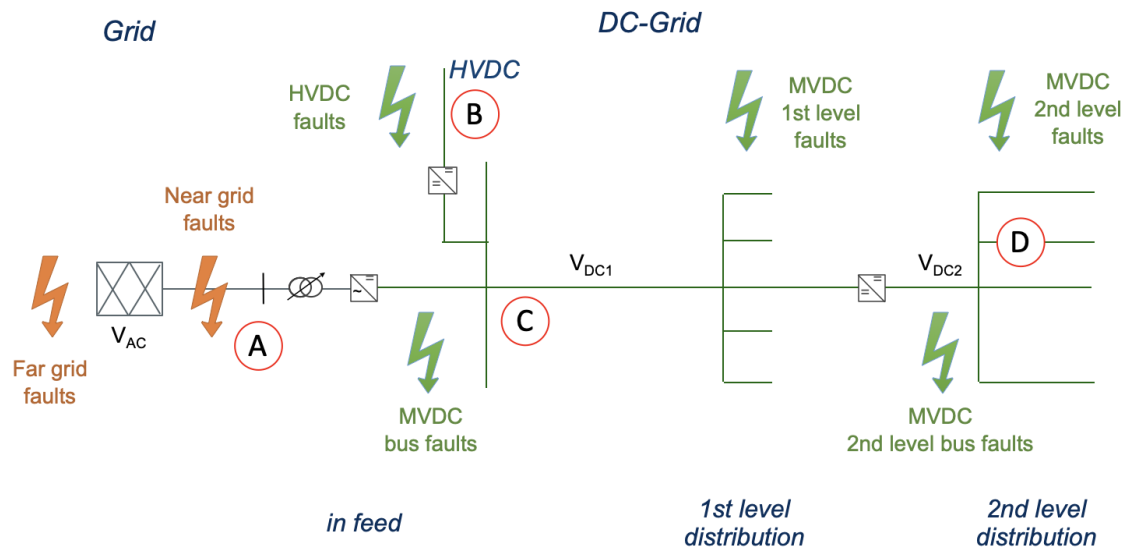


Figure 3.24 MVDC fault conditions.

Fault conditions may be classified into:

- Far grid faults:** Result in voltage drop and loss of short-circuit current in the grid. A power converter in power feeding mode will hence inject a current into a grid with increased grid impedance, which will aggravate the situation. Changing the operating mode of the converter from power feeding to grid forming might be considered, in case the MVDC grid represents a significant power source. In cases of smaller installations, fault ride through requirement from common practice according to grid codes apply.
- Near grid faults:** Faults close to the busbar or point of interconnection do not allow to maintain the regular operation. In this case, the objective is to trigger selective protection and to disconnect the faulting parts. For systems connecting at interconnection point A, this case is regulated in grid codes.
- HVDC faults:** Faults on an HVDC link should lead to a disabling of power transmission, often also resulting in blocking the power converters (see also CENELEC document CLC/TS 50654-1). In the case of a point-to-point transmission link (at interconnection point B), selectivity is limited to distance for single-ended fault detection. If double ended fault detection is used for the point-to-point link (with communication from the other end), then the fault detection is inherently selective and not limited by distance. Loss of voltage will cause power converters to trip. Concerning a converter connecting to point B, a grid code for the HVDC link needs to be defined [62]. There is a European connection regulation: Commission Regulation (EU) 2016/1447 of 26 August 2016 establishing a network code on requirements for grid connection of high voltage direct current systems and direct current-connected power park modules. An overview of protection for HVDC can be found at [63].
- MVDC bus faults:** MVDC bus faults should trigger breaks in all links which are feeding into the bus. On an AC busbar, this is achieved by circuit breakers. A circuit breaker allows to connect and disconnect systems to the busbar. For DC systems, connecting and disconnecting may be achieved by the converters. In some areas of application, such as ships, it is suggested to use power converters as circuit breakers in combination with isolating switches for protection [64]. Either way, the objective of handling faults at the busbar is to isolate all in-feeds on the bus. In the grid scenario shown above, this leads to the loss of the complete MVDC segment down from the first busbar. With busbar 1 entirely driven by power converters, short circuit power to trigger overcurrent protection may be limited. Alternatively, voltage based triggers may be used, as

suggested for converter based microgrids [65].

- **MVDC 1st level distribution faults:** Faults at feeder lines from the first level busbar (at interconnection point C) lead to a loss of voltage at the first level busbar. The objective of clearing faults in power distribution down from the first busbar is to isolate the defective parts by tripping circuit breakers. Short circuit power on the first level busbar should be sufficient to drive short circuit currents to trigger the protection in any of the feeders.
- **MVDC 2nd level bus faults:** Faults at the second level busbar are handled in the same way as faults on the first level busbar (see description above). At this point, depending on the number of first level feeders, short circuit power should be sufficient to drive overcurrent protection. This way, the second level busbar may be isolated in a selective way. Breaking DC currents needs special attention: For selective protection, the feeding converters may not be used to break currents, so DC circuit breakers may be required [2].
- **MVDC 2nd level distribution faults:** Faults at second level feeders (at interconnection points D) include faults in DER and DC loads. It may be expected that converter based terminals will trip in case of a voltage loss. Still, the defective feeder needs to be isolated by selective protection. As for first level distribution faults, it may be assumed that short circuit power at this level is sufficient to drive conventional overcurrent protection.

In summary, fault conditions correspond to fault conditions in AC distribution. Objectives of clearing faults are also the same. However, in a converter-based grid, short circuit power is limited in comparison to AC grids powered by synchronous machines. Power converters may be engaged in breaking and connecting circuits in a comparable way as circuit breakers. However, this method depends on the grid topology: in a hierarchy of feeders representing a tree structure, it cannot be selective (in comparison to linear or meshed topologies).

### 3.4.3 Effects on Fault and Protection of the MV Network

In the MVDC scenario, the MVDC grid represents a significant power source to the AC grid or MV network. Faults and protection of the MVDC grid will have impacts on the MV network. This holds in particular when the MVDC grid is providing grid forming features in case of faults in the AC grid. Some overlap with effects in HVDC links can be expected (see CENELEC document CLC/TS 50654-1 or CLC/TS 50645 Standard from June 2020 (HVDC Grid Systems and Connected Converter Stations – Guideline and Parameter Lists for Functional Specifications)). A discussion of impacts will need a closer look into the operation of the MVDC grid, which is driven by power converters. **Fig. 3.25** illustrates the case.

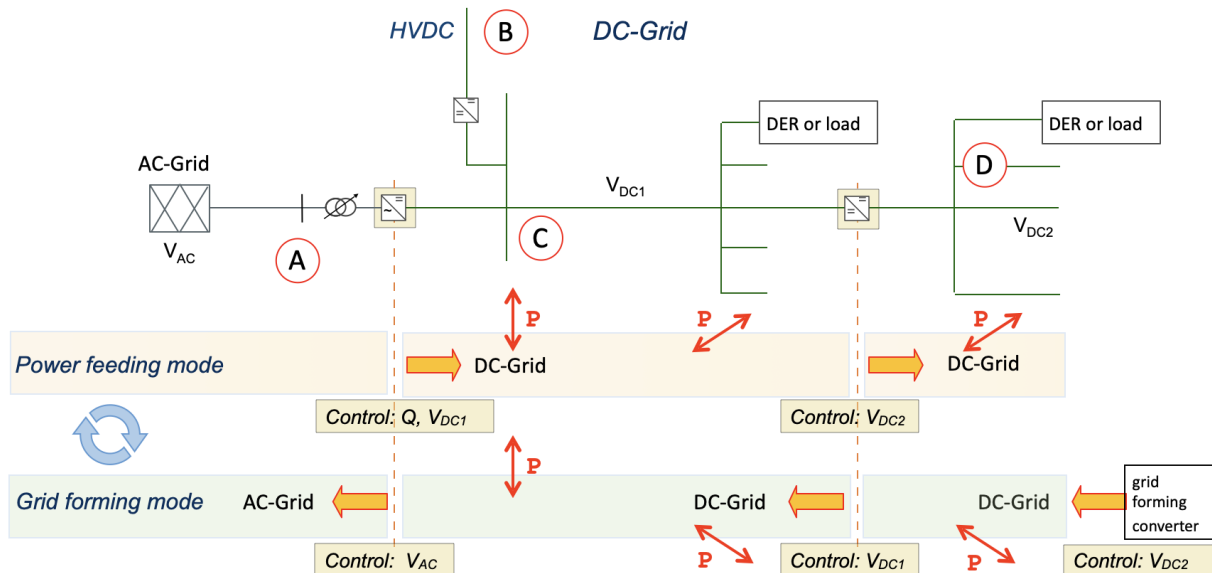


Figure 3.25 MVDC operating modes.

Separated by power transformers or power converters, the MVDC scenario contains the following power grids: (1) the AC grid at voltage level  $V_{ac}$ ; (2) the DC grid at voltage level  $V_{dc1}$ ; (3) the DC grid at voltage level  $V_{dc2}$ . Both DC grids are supplied by power converters. Power converters between two grids are coupled by active power transferred between the grids. Hence, either the voltage of the power converter on one end is defined by the coupling of power, or the current of the power converter on one end is defined by active power. In the first case, the power converter is operating in power feeding mode. In the second case, the power converter is operating in grid forming mode.

The implications of both operating modes on faults and protection in the MV network are different:

- Power feeding mode:** Objectives at interconnection points A or B are to provide sufficient fault currents in case of near grid failures to trigger over current protection. Grid codes specify the corresponding behaviour of the converter concerning fault ride through and dynamic stabilization on the grid. In case of far grid failures, including the loss of power generators, driving high currents into a high impedance grid does not represent a constructive way to support grid stability. In this case, the grid would benefit from switching to a different operating mode.
- Grid forming mode:** If there is a significant contribution of AC power by the power sources connected to the MVDC grid, the converter at interconnection point A may switch from power feeding operation into grid forming operation, i.e. helping to maintain the AC voltage  $V_{ac}$ . This will not necessarily affect the operating mode of the power converter at interconnection point B, which feeds into the HVDC link. The HVDC link may be engaged to transfer more power into the AC grid and thus support the power sources on the MVDC. However, the direction of power flow does not change the mode of operation of this power converter (which remains in the power feeding mode). At least one converter on the DC Grid 1 needs to be in grid forming mode. In **Fig. 3.25**, this is the AC/DC converter at reference A. The same holds for the converter at interconnection point B, depending on the operating mode of the HVDC-link. The scenario supports multiple grid forming converters.

A switch of operating modes between feeding power and grid forming represents a way to dynamically support and maintain the AC grid for HVDC transmission systems. In this case, power from one grid segment is transferred into the faulting grid segment in much the same way as a power plant or power generator would support and maintain the grid.

In an MVDC grid, the situation is different in the following respects: (1) There is no full grid at the opposite end of the MVDC grid, but a group of DER acting in much the same way as a power generator; (2) The subordinated grids at different voltage levels are maintained by power converters rather than by power transformers. Representing active devices, the latter case demands a closer look into operating the chain of subordinated power converters.

In an AC grid, such transitions between operating modes do not need to be considered: power transformers being passive devices just extend the reach of power sources connected to their respective terminals. In the grid forming mode shown above, power converter 2 (DC<sub>1</sub>/DC<sub>2</sub>) mirrors the operation of power converter 1 (AC/DC<sub>1</sub>): it changes from power feeding to grid forming operation and maintains DC grid 1 by keeping  $V_{DC1}$ . The implication is that converter 2 now cannot maintain DC grid 2. Some other converters further down the chain needs to pick up the role and mirror converter 2, as indicated on the right in **Fig. 3.25**.

**Fig. 3.26** illustrates the chain of power converters in power feeding mode. Power converter 1 is forming the first DC grid by maintaining  $V_{DC1}$ . This way, the current  $i_{AC1}$  feeding into the AC grid follows the power feeding into the DC grid 1: Maintaining  $V_{DC1}$  is achieved by maintaining a balance of power (see section 3.2.3). The settings for controlling converter 1 hence are  $V_{DC1}$ , with one degree of freedom left to administer reactive power  $Q$  to the AC grid.

With converter 1 forming DC grid 1, the subordinated power converter 2 mirrors the mode of operation of power converter 1: It maintains the subordinated DC grid by maintaining  $V_{DC2}$ . This implies balancing power in DC grid 2 in such a way that a surplus is feeding into DC grid 1 via  $i_{DC12}$ . This way (by accumulating the currents), all subordinated converters to power converter 1 feed power into the AC grid, including the DER.

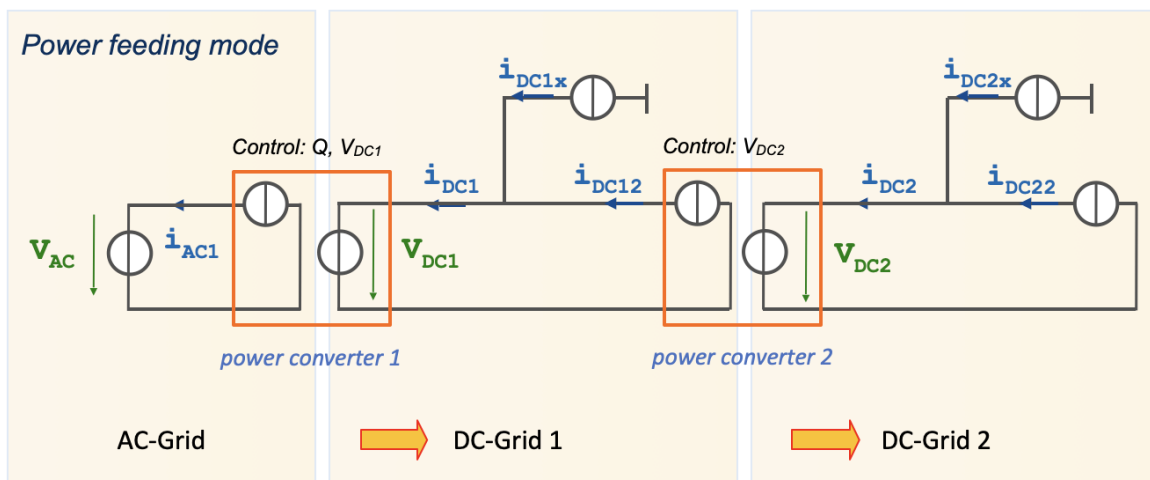


**Figure 3.26** Grid scenario in power feeding mode.

The direction of power flow does not matter. The power feeding mode also supports loads, so any mix of loads and DER may connect to the DC grids. If the accumulated power at interconnection point A represents a load rather than a power source, requirements during faults are different: a load is not expected to dynamically support the grid, nor to switch into a grid maintaining mode (which is impossible in this case).

In grid forming mode, the role of power converter 1 changes, and so do the roles of all subordinated power converters. **Fig. 3.27** illustrates the case.

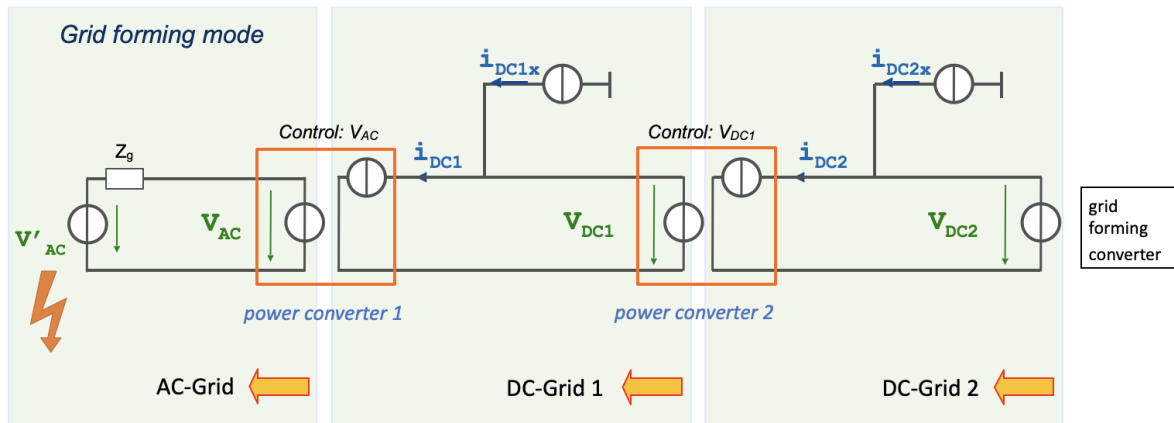


Figure 3.27 Grid scenario in grid forming mode.

Power converter 1 now assists in maintaining the AC voltage. This is achieved by taking as much power from the subordinated DC grid, as is needed. Power converter 1 cannot maintain the DC grid 1 at the same time. In comparison to the grid feeding mode shown in Fig. 3.25, the DC grid now needs to be maintained from another place, e.g. by the subordinated power converter 2.

Changing modes of operation in a chain of power converters raises a couple of questions to be addressed within the MVDC grid, which do not affect fault conditions at the MV network or AC grid, and hence are not considered in detail in this document. Among the questions are:

- How to communicate changing the mode of operation to selected subordinated power converters?
- How to implement dynamic support of the grid  $P(f)$ ? Grid support is defined at interconnection point A. Irrespective of its operating mode, the associated power converter 1 only feeds the power available from its cumulated sources. The corresponding power sources (DER) are located further down the chain in the subordinated DC grids 1 and 2. How to communicate the grid frequency  $f$  over the DC grid (unless using AC terminals for this purpose)?
- How to handle fault ride through conditions at interconnection point A? Options and limits for handling fault ride through depend on the implementation of power converters and on the type of power sources. In terms of wind farms, incoming power needs to be handled in some way, if it is not possible to feed it into the AC grid. Provision of energy storage devices, hydrogen generation and controllable loads provide means of channelling power flow.

It is expected that emerging MVDC grid codes will specify the corresponding measures and interfaces.

### 3.4.4 MVDC Protection Approaches, Fault Detection Algorithms and Settings

At present, the protection of MVDC systems is not mature. There are still no widely accepted standards. The improvement of protection strategies, the formulation of fault detection algorithms, and the development of equipment such as circuit breakers and IEDs are still of great importance. The strategy for DC fault isolation in DC distribution networks in the open literature can be categorised into:

- **AC circuit breaker:** the AC circuit breaker (ACCB) based DC fault protection method uses the converter AC side ACCBs to isolate the DC fault, which is simple and economical. However, this method will lead to the power outage of the whole DC network, and therefore is difficult to meet the requirement of protection selectivity. This method has been implemented in the  $\pm 20$  kV four-

terminal MVDC pilot project in Suzhou Industrial Park, China [17]. The ANGLE-DC MVDC link also uses the ACCB based protection to isolate DC faults.

- **Converters with fault blocking capability:** These converters can isolate the fault due to their converter topology. However, the converter is relatively more complicated with more investment and, therefore, high capital cost and power losses. The  $\pm 10$  kV Zhangbei AC/DC pilot Distribution Project adopts such a converter topology: a double clamp modular multilevel converter [66].
- **DC circuit breaker:** DC circuit breakers (DCCBs) can achieve fast fault isolation and, therefore, can be applied in DC grids. However, the cost and reliability of DCCBs should be further improved for their wide application. The  $\pm 10$  kV three-terminal Tangjia Bay MVDC distribution pilot project uses DCCBs to achieve the MVDC system protection [67].

The above approaches are the technologies in place for future MVDC networks. However, these protection strategies are project based. The development of MVDC protection standards is needed and urgent. Differing from the HVDC transmission grids, the MVDC system contains a large number of distributed energy resources and directly supplies the users. When a fault occurs, the tripping of the entire network without selectivity will impact the system adversely. Hence, the use of DCCBs is desirable in MVDC networks. In addition, even though the MVDC grid usually benefits from converters with fault blocking capability, this kind of converter, to a greater or lesser extent, challenges the speed and the sensitivity of DC protection. Therefore, the possible conflict between the fault blocking converters and the DCCB based protection scheme needs to be further studied.

Many fault detection algorithms have been proposed for MVDC systems [68]. Notably, many of these fault detection algorithms correspond to those suggested for HVDC systems [69]. The choice of a specific fault detection algorithm depends on the MVDC grid topology and - to some degree - the chosen protection strategy. Compared to AC systems, the fault detection algorithms in MVDC systems have to consider the active behaviour of sources and loads, the DC nature of the system to be protected, and, in particular, the requirement for high speed to avoid large currents.

Protection settings in the MV network (AC grid) at interconnection point A essentially correspond to the protection settings for an HVDC station. Both represent converter powered interconnections, including the option of running in a grid forming mode in case of far MV grid faults. The protection settings additionally also depend on the chosen strategy (ACCBs, DCCBs, converter fault blocking) as well as the chosen fault detection algorithm and additional information (local measurements versus communication based fault detection, converter status).

Protection settings in the MVDC grid correspond to conventional settings as in AC grids, minus the limited short circuit power in case of bus faults, and minus the use of DC circuit breakers (depending on grid topology, see fault conditions in section 3.4.2). With different power levels, power converters in DC grids take the principal role of power transformers in AC grids with one major difference: power converters represent active devices in comparison to power transformers (passive devices).

In terms of protection settings, DC grids lead to the following new aspects in comparison to AC grids:

- Setting the mode of control of power converters: power converters in subordinated grids need to mirror the operating mode of the top level power converter. If the top level converter transitions from power feeding mode into grid forming mode (and back), subordinate power converters need to follow suit. The mode of operation needs to propagate through the converter chain.
- The need for galvanic isolation between DC grids: protection with clear fault indications demands galvanic isolation between DC grids. For HVDC links and at the interconnection point A to the AC

grid, conventional transformers are used to provide galvanic isolation. On a DC grid, this is not feasible. Galvanic isolation needs to be implemented by using an appropriate type of power converter.

- Use of power converters to connect and to break circuits: Where the topology allows it (i.e. at busbars, in linear or meshed configurations) the power converter can take the role of a circuit breaker. Voltage separation is provided by isolating switches. Selective protection on feeders needs DC circuit breakers. In converter powered grids, protection on faults may be triggered by voltage rather than overcurrent.

Representing active devices, power converters offer a much higher level of measurement and control, plus extremely short reaction times. Rather than translating established concepts from AC to DC, this enables new ways and new concepts for protection.

## 4 Interconnections of MVDC to HV and LV Systems

While HVAC and HVDC are already standard options for electric power grids, MV and LV DC with a relevant proliferation in the field are yet to emerge. So currently HVDC is mainly restricted to point-to-point connections between HVAC grid nodes. Very few HV grids with multi-terminal topology are in operation, not having left the prototype stage yet. Aside from a seamless DC-power grid, the advantages of DC technology could also help to address challenges in hybrid grid situations. The benefits of the MVDC technologies discussed in previous sections allow for interconnection between AC/DC grid segments at the HV and LV level (horizontal vs. vertical coupling). Power levelling between adjacent transmission and distribution grid areas becomes possible with the key enabling MVDC technology.

Just introducing an additional MVDC component in the electric power grid would not only include one more voltage conversion step but also two more DC/DC or AC/DC conversion steps between the HV and MV level and the MV and LV level. This is undesirable, both from investment and operating cost, as well as from complexity, reliability and efficiency perspectives. DC direct voltage level conversion is highly desirable.

This chapter will explore the need for the interconnection of MVDC to HV and LV systems to form a cross connected hybrid and multi-voltage system. The key power conversion equipment and the requirements for their operation and control will be discussed, along with the presentations of some practical applications.

### 4.1 Interconnection of MV and HV to Form Larger Grids

A direct HVDC/MVDC substation, at the same time, would convert an HVDC line practically into a multi-terminal grid, since the total power capacity of an HVDC line may safely be considered to be much higher than that of a single HVDC/MVDC substation. Thus, a reasonable configuration would stipulate many such substations along an HVDC line, which necessarily would be of the VSC type. Assuming such a scenario, several converter topologies can be considered.

Advantages of DC grid technology may be easily offset by cost and losses in efficiency in power converters. It should be therefore an objective to keep the number of power conversion blocks in series to as few as possible. In particular, conversion between AC and DC could appear several times and should be avoided. A direct connection of the MVDC domain to the HVDC transmission grid could save in each string two AC/DC conversion steps and hence cost and power losses and complexity.

AC substations may require to be interconnected for several reasons including but not limited to the following:

- Improve the voltage profile and the dynamic control of the reactive power.
- Control the power flow to optimize its dispatch and reduce network losses.
- Improve the stability, the reliability and the flexibility of the network.
- Solve network congestions, overcoming capacity limits in certain parts of the grid and providing capacity enhancement.
- Improve the integration of renewable energy sources in the grid.

Apart from these needs, several issues may not allow the interconnection of AC substations by means of AC links:

- There can be a phase difference among the voltages at the substations.
- The systems at which the substations are connected can be asynchronous.
- The poor power quality, in terms of harmonics and flicker, of a network can affect the other network too.
- The equipment cannot withstand an increase in the short-circuit current.
- The neutral earthing configuration of the grids can differ.

MVDC networks represent an excellent candidate technology to overcome these hindrances and enhance benefits to the AC grids at the same time. A back-to-back and point-to-point link can be used for two substations; meanwhile, a multi-terminal configuration is suitable to control the power flows between several substations. These configurations are shown in **Fig. 4.1**.

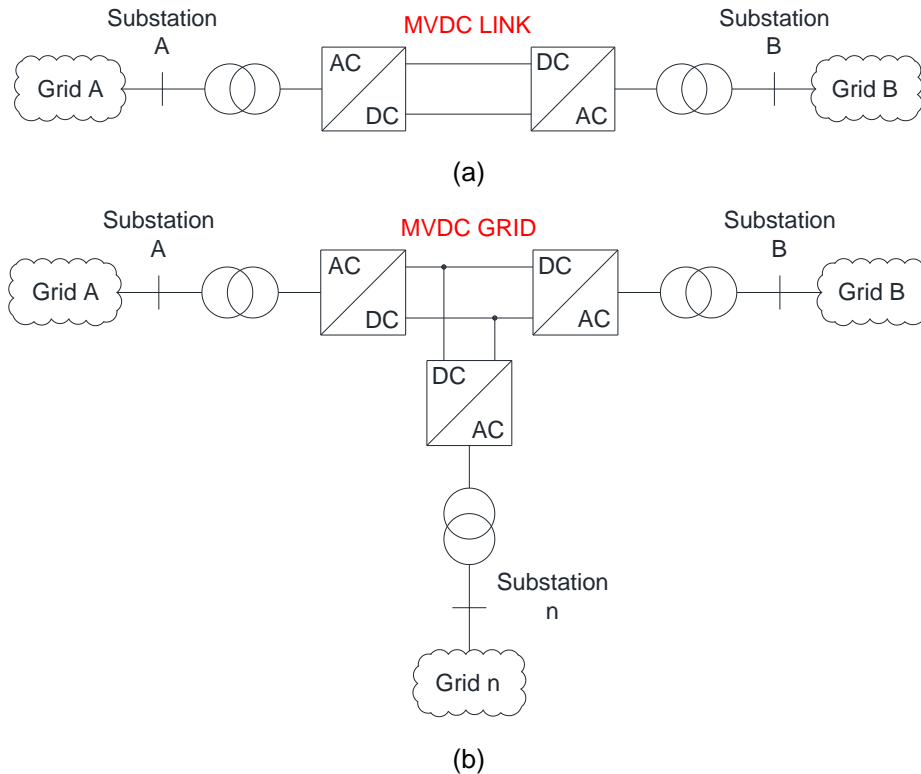


**Figure 4.1 Schematic of AC substation connections: (a) point-to-point, (b) multi-terminal.**

The control and operation modes of HVDC links can be adapted to the MVDC grids of **Fig. 4.1**. A different task is assigned to the converters from what concerns the management of the power flow in the MVDC grid. Generally, only one converter station oversees the control of the DC voltage whereas the others manage the absorbed/injected power in the MVDC grid. These tasks can be swapped among the converter stations. Moreover, the droop control mentioned in Section 3.3.2 can be used. Considering the reactive power exchanges with the AC grids, each converter can be independently controlled from the others. Furthermore, it is worth noting that each converter can be operated standalone as a STATCOM, when disconnected from the MVDC grid.

Typically, dedicated inter-station telecommunication systems are installed for both control and protection purposes. If they are out-of-service, system operators will be in charge to coordinate with each other for managing the DC system. When the inter-station telecommunications are in service, a joint control can be implemented to achieve coordinated operations and sequences. This control strategy presumes the definition of a master station, whereas the other/s must be slaves. The input of orders and automatic sequences can be done at the master station only, and the slave converter station(s) follow. The commands at the master station, in terms of active and reactive power setpoints and ramp rates, AC voltage setpoint (if any), etc., can be inserted by a local operator or by

a remote dispatching centre. The latter control location is only suitable if remote telecommunications are available.

The development of MVDC systems will require an interface with HVDC systems, via a DC-DC converter. CIGRE WG B4.76 in TB 827 [70] has studied DC-DC converters in HVDC grids and for connections to HVDC systems. TB 827 focuses mainly on DC-DC converters to interface two HVDC systems. A study of DC-DC converters for connecting HVDC to MVDC has been also presented, with such converters characterised by a high stepping ratio [71]. These DC-DC converters can be classified according to two main requirements, as shown in **Fig. 4.2**:

- power flow directionality:
  - bidirectional power flow (HVDC ↔ MVDC),
  - unidirectional power flow:
    - stepping down HVDC → MVDC,
    - stepping up MVDC → HVDC,
- galvanic isolation:
  - isolated,
  - non-isolated.

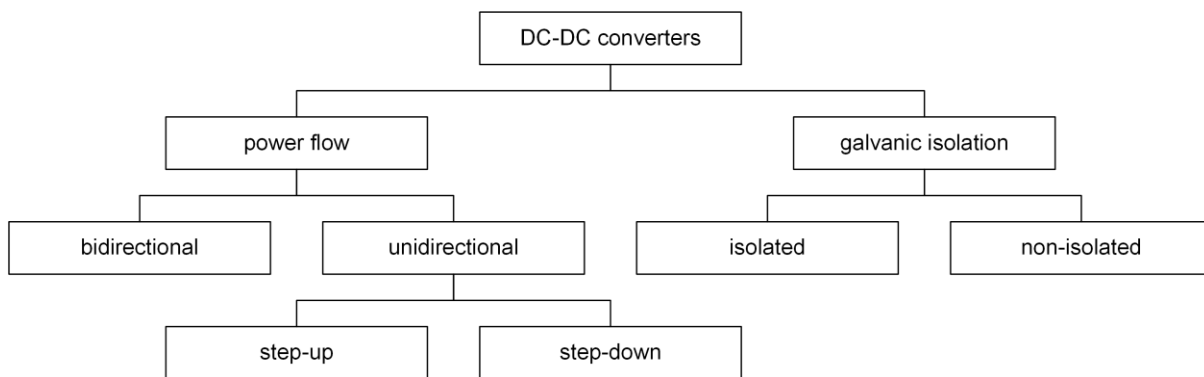


**Figure 4.2 Classification of DC-DC converter topologies.**

The power flow directionality and galvanic isolation are considered here as the requirements. Although the power flow directionality is clearly defined by the application requirements, the galvanic isolation can be considered as a requirement or a converter property. Bidirectional power flow converters can be used in unidirectional power flow applications but the opposite is not possible. The general diagrams of isolated DC-DC converters are presented in **Fig. 4.3**.

The review of DC-DC converters suitable in HVDC applications is presented in [72]-[73]. CIGRE WG B4.76 in TB 827 proposed one isolated DC-DC converter and one non-isolated DC-DC converter. Both provide bidirectional power flow. They are presented in **Fig. 4.4**.

Some examples of converter topologies suitable in HVDC connection to MVDC grid are presented in:

- [74] for the isolated bidirectional DC-DC converter,
- [75] for the isolated unidirectional step-up DC-DC converter,
- [76]-[77] for the non-isolated bidirectional DC-DC converter.

The isolated DC-DC converters include DC-AC-DC conversion with galvanic isolation provided by the magnetic coupling in the AC circuit. These converters adopt the same methodology as a dual active bridge (DAB) [78]. The main benefits of isolated topologies include their ability to easily interconnect

two DC grids with different grounding schemes. They are more suitable where a high stepping ratio is required. They have also an inherent fault blocking capability.

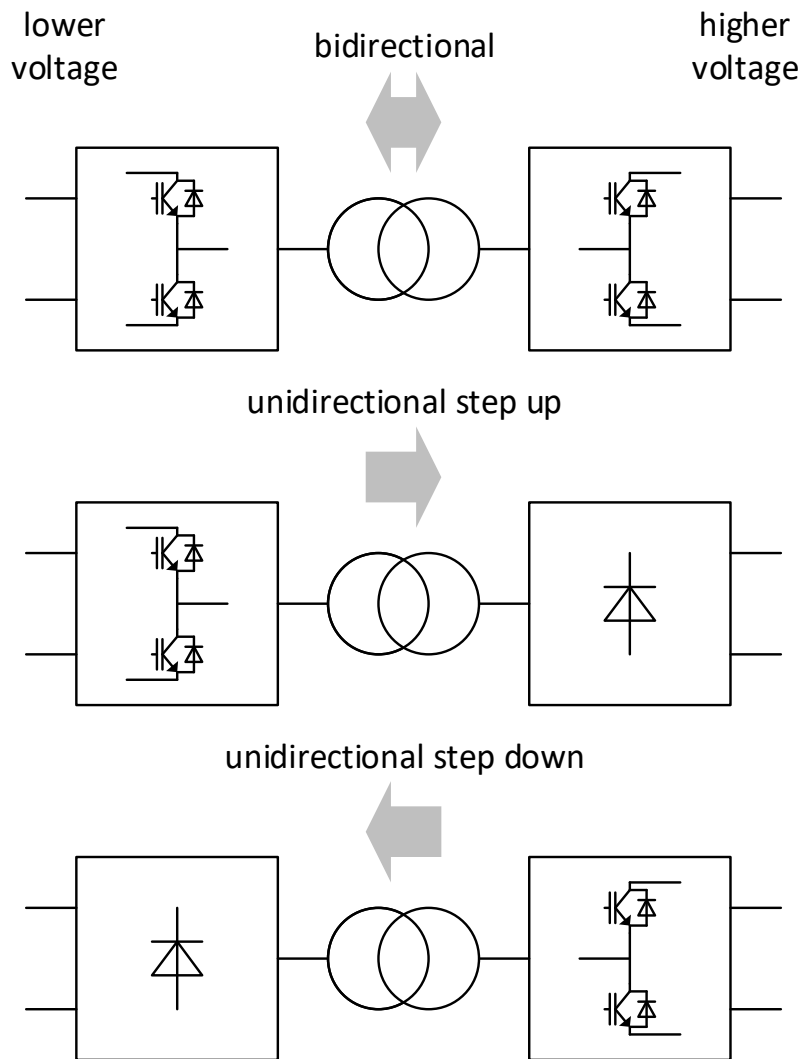


Figure 4.3 General diagrams of isolated DC-DC converter topologies: bidirectional, unidirectional step-up and unidirectional step-down.

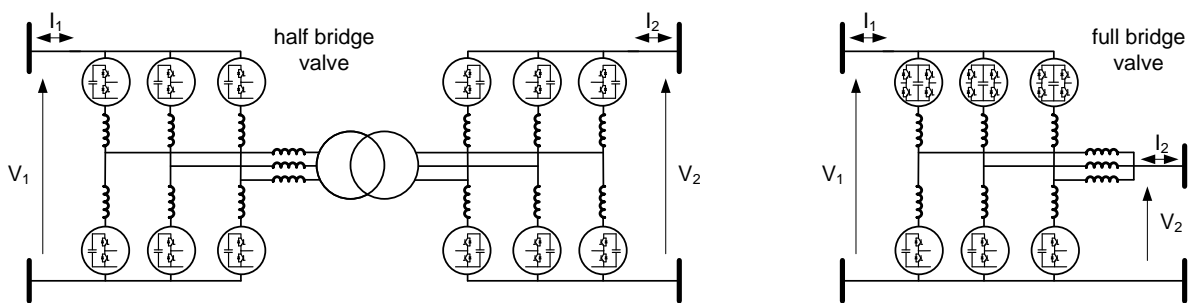


Figure 4.4 HVDC DC-DC converters proposed in CIGRE TB 827: isolated DC-DC converter (left) and non-isolated DC-DC converter (right) [70].

The non-isolated DC-DC converters are often derived from buck/boost while adapting them to the HV environment. The main benefits of non-isolated topologies include their low cost because, usually, they require fewer power semiconductor devices. They do not require a transformer or at least the transformer is not rated for the full power of the DC-DC converter.

For MVDC-HVDC power conversion where the voltage step-up ratio is high, galvanic isolation is

preferred not only for safety but also to reduce power-semiconductor total device ratings and losses.

An isolated soft-switching converter proposed in [74] is a promising solution for this application. It combines parallel-connected two-level converters (TLCs) on the MV side and a modular multilevel converter (MMC) on the HV side as depicted in Fig. 4.5, and it is named the TLC-MMC converter. A dedicated operation method of the TLC-MMC converter is developed correspondingly in [74], whereby a certain reactive current is injected into the MV side by the MMC to realize soft-switching operation and low total device ratings of power-semiconductor devices (PSDs) in the TLCs on the MV side.

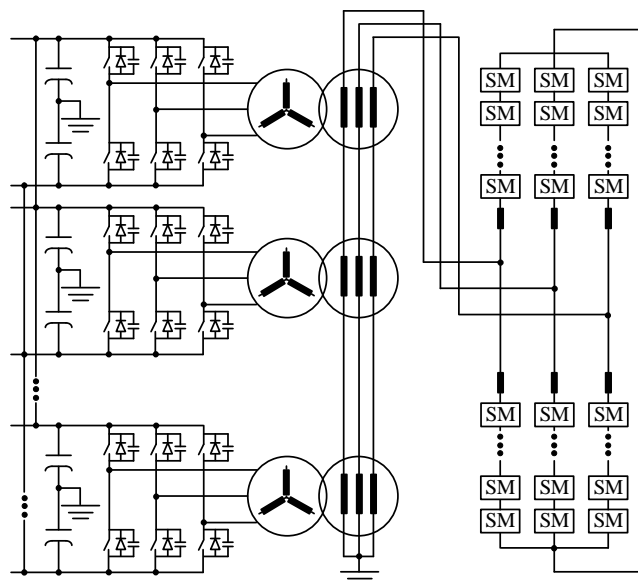


Figure 4.5 Configuration of the TLC-MMC converter dedicated to MVDC-HVDC power conversion [74].

A detailed comparison of the TLC-MMC converter compared to the state-of-the-art converter topology dedicated to this application, which is based on the front-to-front configuration of MMCs (FTF-MMC) [79], is carried out based on an application scenario of a 50 kV / 400 kV, 400 MW DC-DC converter system. The TLC-MMC converter presents the following advantages. The number of employed medium-voltage devices can be reduced by 44%, and the total volume of employed power capacitors can be reduced by 46%. Moreover, the device losses can be reduced by 30–40% over the entire operation power range as presented in [74]. Additionally, with normal low-speed AC mechanical disconnectors, the fault-tolerant operation can be enabled in case of multiple device failures on either the MV or HV sides, and the availability of the converter can be enhanced [80]. Due to the isolated nature of both sides, fault-ride through (FRT) with fault current clearance is inherently capable in case of a DC short-circuit fault on one side [81].

It should be mentioned that although there have been many topologies of DC-DC converters for HVDC-MVDC interconnection proposed in the academic literature, there is still no commercial product available. The reliability, capital cost, and fault handling capability are still the bottleneck of their development. Moreover, the use of MVDC for a customer installation (e.g. production plant or power generating plant), connected to the transmission grid by means of larger inverters, offers the advantage that grid code compliance only needs to be fulfilled at the interface to the transmission grid. In other words, assuming that a universal MVDC grid code is in place, the many loads or generating units connected to the MVDC grid do not need to be configured and tested individually to account for regional or national differences in grid codes; instead, only the larger inverters to the transmission grid need to be customized. This can be of special importance for following new grid code requirements expected to be formulated in the future.

## 4.2 Interconnection of MVDC Networks to LVDC

Connection of an MVDC network to LVDC inevitably requires a DC-DC converter. The DC-DC converters interfacing MVDC and LVDC are characterised by a high stepping ratio [82] (for example 20 kV/ 1 kV). These DC-DC converters can be classified according to power flow directionality and galvanic isolation.

This classification is the same as for the DC-DC converters interfacing HVDC and MVDC but the power converter topologies and technologies are different.

The DC-DC converters with a high voltage ratio are likely to be isolated. These DC-DC converters include a DC-AC-DC conversion with galvanic isolation provided by the magnetic coupling in the AC circuit. There are at least two arguments for using isolated DC-DC converters in high ratio applications:

- insulation coordination in LVDC network,
- power electronics constraints.

The galvanic isolation between MVDC and LVDC allows for independent design of the MVDC network and LVDC network [IEC 61800-5-1]. If there were no galvanic isolation, then the LVDC network would have to respect the overvoltage constraints of the MVDC network resulting in more bulky and costly equipment. The same approach applies to AC networks where the non-isolated AC-AC conversion - the autotransformer is used in low ratio applications only.

The power electronics constraints in DC-DC converters with a high stepping ratio are clearly visible when analysing a basic bidirectional non-isolated converter as presented in **Fig. 4.6**. In this circuit, the power electronic switches have to withstand the MVDC voltage (high voltage) and the LVDC current (high current). This results in a design which is far from the optimum.

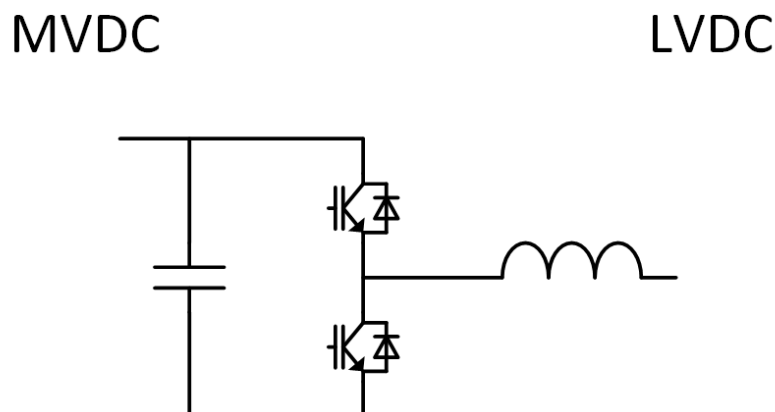


**Figure 4.6 Basic bidirectional non-isolated DC-DC converter.**

The isolated DC-DC converters allow to decouple the MVDC constraints and the LVDC constraints in a similar way as it is done in transformers. The transformers have a high number of turns of thin wire in the high voltage winding and a low number of turns of thick wire in the low voltage winding. Finally, a comparable quantity of copper in both high voltage and low voltage windings is used. In isolated DC-DC converters based on a conversion chain of DC-AC/transformer/AC-DC, each item of equipment can be designed optimally. The general diagrams of isolated DC-DC converters are presented in **Fig. 4.3**.

The isolated DC-DC converter topologies can be further classified according to their main structural properties:

- modularity,
- number of phases (single-phase, three-phase or multi-phase),
- including a resonant circuit or not.

The major constraint in the design of MVDC power converters is the availability of power electronic switches with a high blocking voltage. The commonly used IGBTs include: 1.7 kV, 3.3 kV, 4.5 kV and 6.5 kV. This is well below the required MVDC voltage levels. Individual IGBTs can be connected in series but it is a significant technical challenge. The modular approach allows to use standard IGBTs by arranging several power converters in series or in parallel.

The number of phases within the DC-DC converter allows to optimise the design according to power requirement and current constraint of the available power electronic switches. The vector group of the transformer can be freely chosen. The multi-phase circuits allow the operation in case of a fault in one phase.

The resonant topologies are usually more energy efficient but the design of the resonant circuit may be challenging.

Some examples of bulk, single-phase and 2-level VSC-based DC-DC converter topologies are detailed hereafter:

- series resonant converter (SRC),
- LLC DC-DC resonant converter (LLC),
- phase-shifted full bridge (PSFB),
- dual active bridge (DAB).

The SRC is composed of a VSC, LC resonant circuit ( $L_{ac}$ ,  $C_{ac}$ ), transformer and diode bridge with capacitor filter as presented in **Fig. 4.7**. It was proposed in [83] using thyristors, where the LC circuit ensures device commutation and energy transfer. However, the topology can be implemented with any power semiconductor device (MOSFET in the presented diagram). Natively, the topology offers unidirectional power flow. If the diode bridge is replaced with a VSC than it can offer bidirectional power flow.

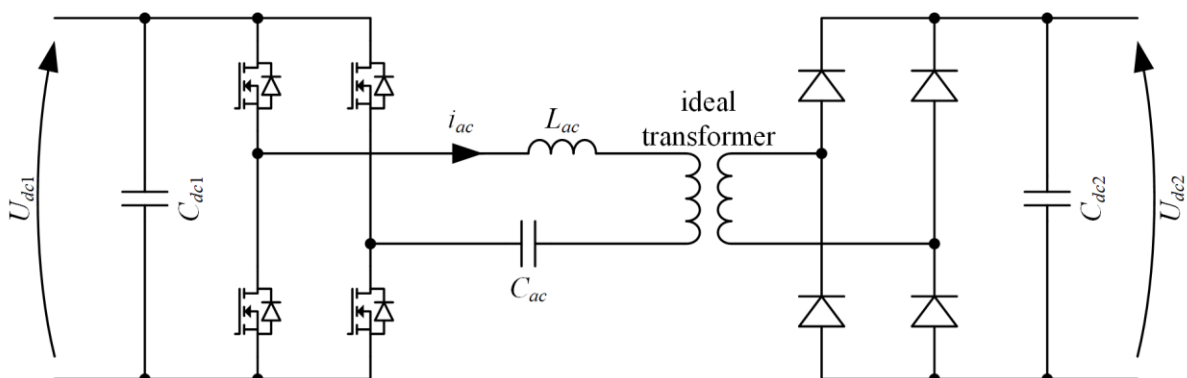


**Figure 4.7 Series resonant converter (SRC).**

The LLC converter is composed of a VSC, LLC resonant circuit ( $L_{ac}$ ,  $L_m$ ,  $C_{ac}$ ), transformer and diode bridge with capacitor filter as presented in **Fig. 4.8**. The LLC circuit may be physically realised with the leakage  $L_{ac}$  and magnetizing  $L_m$  inductance of the transformer. The analysis of the circuit is presented in [84]. The circuit offers buck and boost operation with zero-voltage switching (ZVS) in the entire power range. Natively, the topology offers unidirectional power flow. If the diode bridge is

replaced with a VSC than it can offer bidirectional power flow.

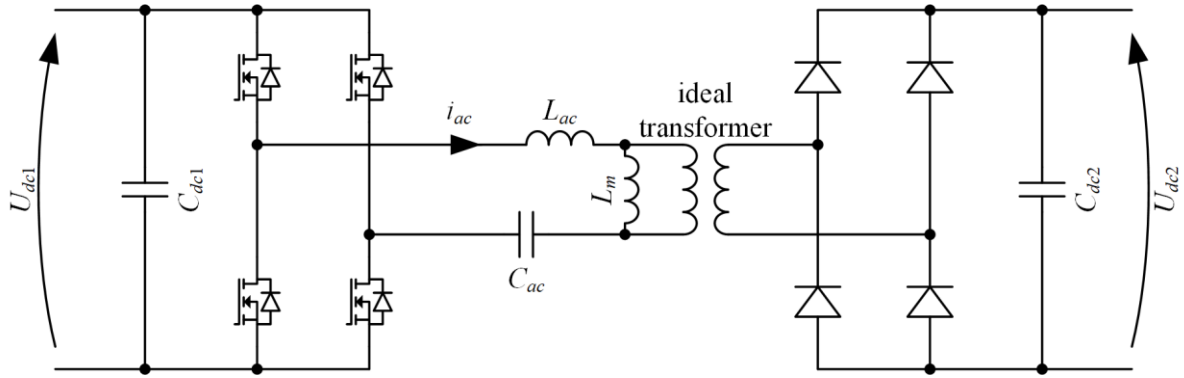


Figure 4.8 LLC DC-DC resonant converter (LLC).

The PSFB is composed of a VSC, transformer and diode bridge with LC filter ( $L_{dc}$ ,  $C_{dc2}$ ) as presented in Fig. 4.9. It was proposed in [85]. The topology offers the possibility of avoiding the LC resonant circuit which may cause technological challenges in high power applications. In principle, the topology offers unidirectional power flow only.

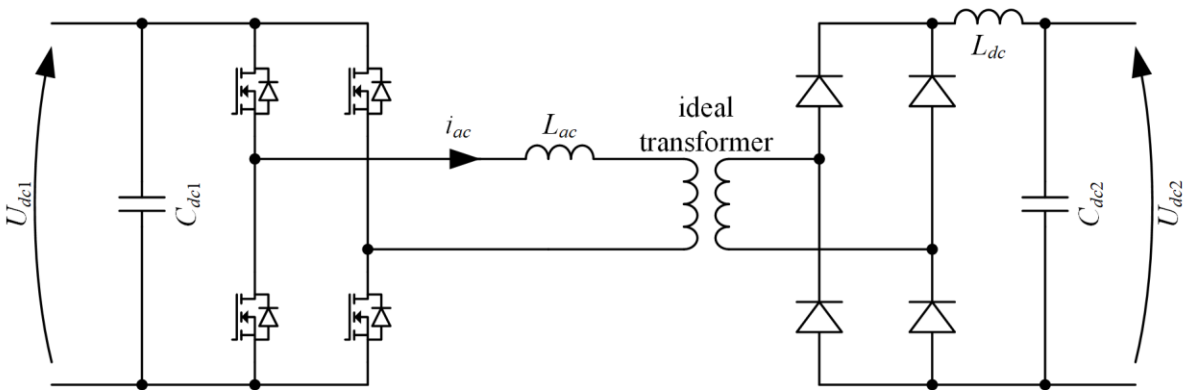


Figure 4.9 Phase-shifted full bridge (PSFB).

The DAB is composed of two VSCs connected with a transformer. It offers bidirectional power flow, but it requires the use of two VSCs [86]. The DAB circuit diagram is presented in Fig. 4.10. The operation of the DAB is based on the phase shift between the two VSCs.

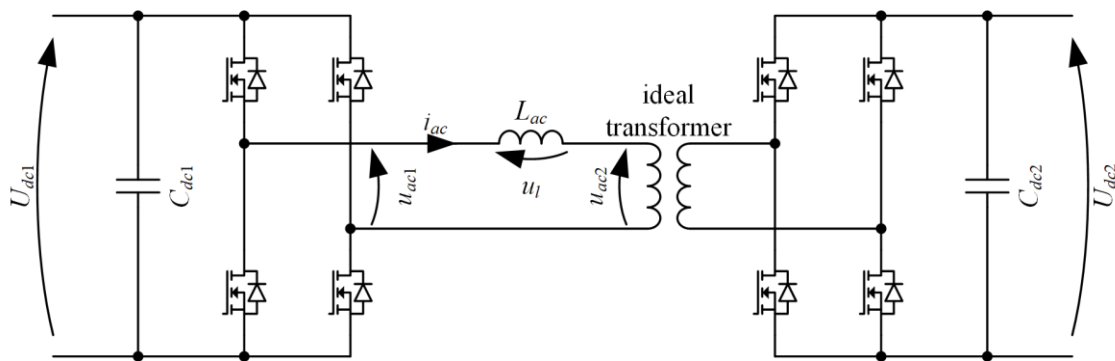


Figure 4.10 Dual active bridge (DAB).

The qualitative comparison of the aforementioned isolated DC-DC converter topologies is presented in Table 4.1. This should be considered as a preliminary comparison because each topology offers a number of variants in terms of topology and control.

Table 4.1 Qualitative comparison of selected isolated DC-DC converter topologies highlighting the main differences (\* - bidirectional power flow is possible).

	<b>SRC</b>	<b>LLC</b>	<b>PSFB</b>	<b>DAB</b>
Power flow	Unidirectional *	Unidirectional *	Unidirectional	Bidirectional
Voltage ratio	Buck in narrow range	Buck/boost in narrow range	Buck	Buck/boost
Control (basic method)	Frequency	Frequency	Phase shift between two legs	Phase shift between two bridges
DC fault blocking	At both terminals	At both terminals	At both terminals with limited overcurrent in diode bridge	At both terminals
Semiconductor components	Input active bridge Output diode bridge	Input active bridge Output diode bridge	Input active bridge Output diode bridge	Input active bridge Output active bridge
Transformer	Quasi-sinusoidal current; Variable frequency design; Turns ratio must be higher than the converter voltage ratio	Quasi-sinusoidal current; Variable frequency design; Constraint on magnetizing inductance	Constraint on leakage inductance; Turns ratio must be higher than the converter voltage ratio	Quasi-sinusoidal current in 3 phase or resonant configuration
Extra passive components	Resonant capacitor	Resonant capacitor	DC inductor	-
Efficiency	High efficiency at sweet spot	High efficiency at sweet spot	High efficiency in wide range of voltage ratio	High efficiency in wide power range

### 4.3 LV DER Integration

Reference [87] shows that the distributed renewable energy resources (wind, solar, etc.) in **Fig. 4.11** can be integrated into the power grid, and energy storage devices can be used as buffering pools to reduce and mitigate the fluctuation of power transmission and distribution. Thus, integrating distributed energy resources and storage devices to effectively transmit and distribute electric power is essential to meet users' energy demand in the smart grid.

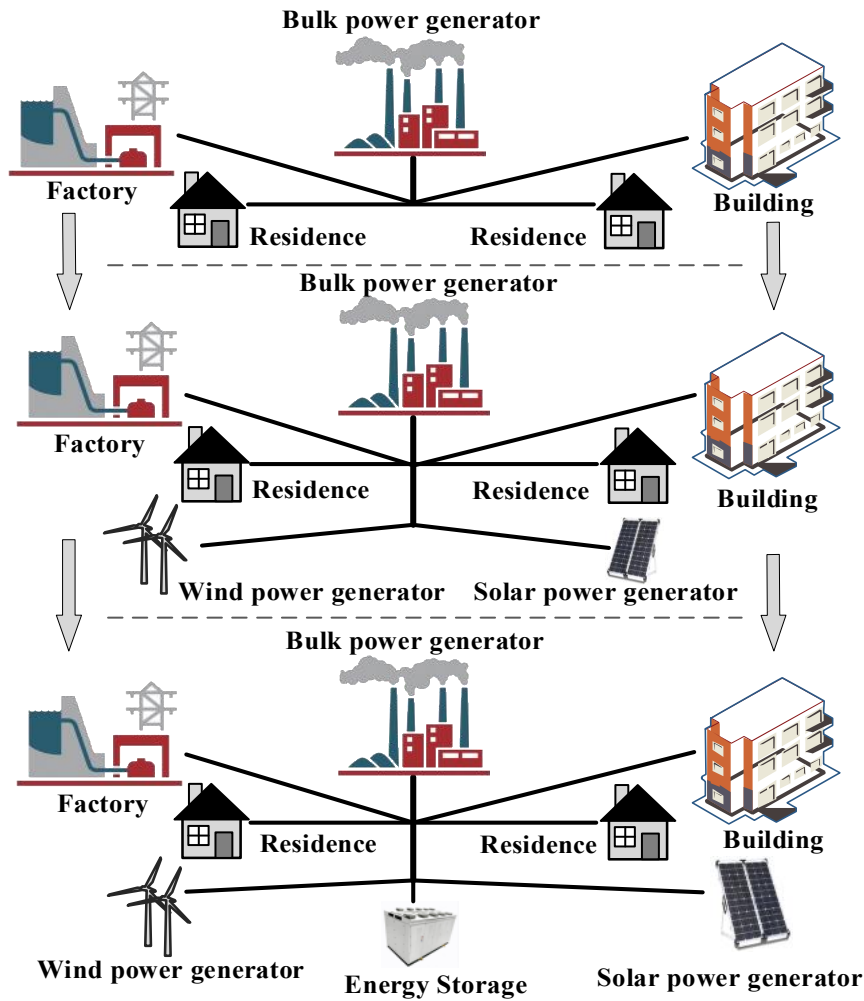


Figure 4.11 Example of power grid modernization [87].

Reference [88] outlines all DC system architectures and proposes the MVDC system reference network based on the knowledge of existing HVDC and LVDC system networks. An MVDC system showed in Fig. 4.12 is a new conceptual platform for coupling renewable power generation systems (wind and solar plants, fuel cells, etc.), energy storage systems (batteries, capacitors, etc.), loads (industrial facilities, data centres, electric vehicle charging stations, power electronic-based load, etc.) and AC utilities. They are expected to improve AC system efficiency between transmission and distribution by reducing the source and load conversion stages. However, unexplored challenges related to system behaviour under various operating conditions (fault protection and control, power flow study, etc.) must be resolved to ensure their feasibility and reliability. To do this, an MVDC system benchmark network must be defined beforehand.

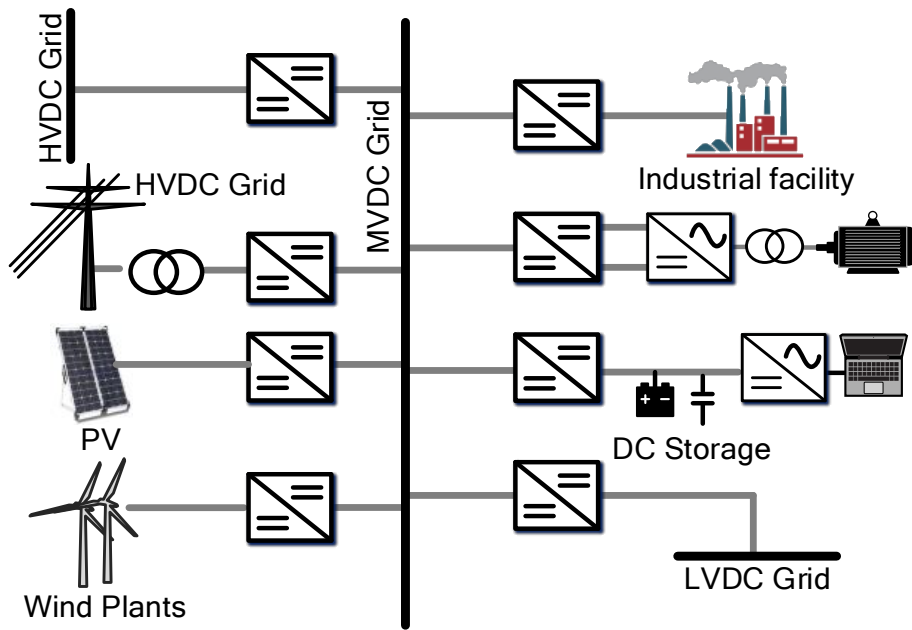


Figure 4.12 Example of an MVDC system [88].

The LVDC system in Fig. 4.13 is a microgrid generally consisting of ring networks working in open (as radial networks) or closed loops. They are used for coupling distributed generation systems (small wind power plants, photovoltaic arrays, etc.), energy storage devices (batteries, capacitors, etc.), local electric vehicle charging stations and loads (customers with power electronic-based loads, industrial facilities, etc.). LVDC systems can also be supplied from AC networks using AC/DC converters and MVDC networks. They are well suited for local distribution systems (office buildings, rural power systems, electric vehicle charging stations, etc.) and allow the use of simpler and more efficient power electronic interfaces.

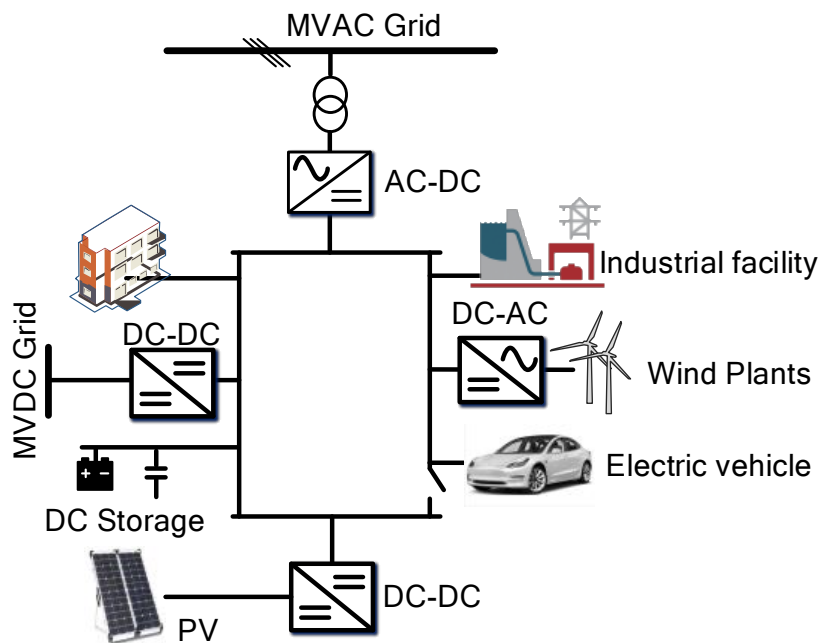


Figure 4.13 Example of an LVDC system [88].

#### 4.4 Connection of AC and DC Loads

The implementation of DER into the MVDC grid inevitably requires DC-AC and DC-DC interfaces. DC loads may be connected directly, through an appropriate protection device. The DC-DC interface

is required if the DC load voltage is different than the MVDC voltage or if additional interface or control requirements are present. For example, in case of a different grounding scheme between the MVDC grid and the DC load, an isolated DC-DC converter may be required. A typical application would be a DC railway catenary (asymmetric monopole) supplied from a symmetric monopole MVDC grid.

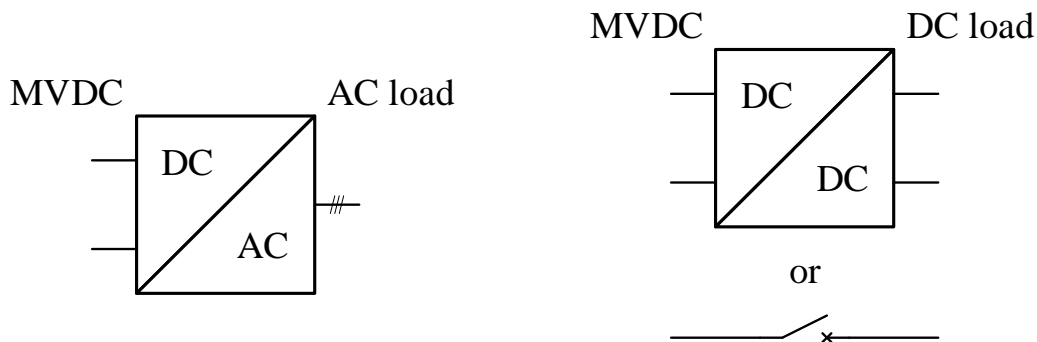


Figure 4.14 Implementation of AC and DC loads in the MVDC grid.

The most straightforward DC-AC interface is a voltage source converter (VSC) with a transformer (Fig. 4.15). The DC load protection may be ensured by the VSC or an AC circuit breaker. The voltage level and the grounding scheme can be freely adjusted due to the transformer. A transformerless interface is possible if the AC voltage level is equivalent to the MVDC voltage and if there are no specific grounding requirements.

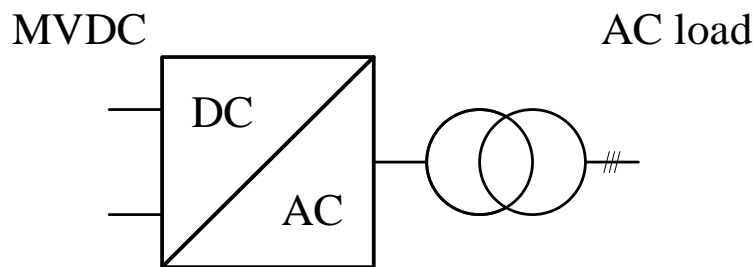


Figure 4.15 DC-AC interface with a VSC and a transformer.

The DC-AC interface can be also realised with a solid-state transformer (SST). It is a technologically sophisticated solution which may offer a smaller size when compared to a low-frequency transformer connected to a standard inverter. The integration of SST technology in distribution networks is studied in the ongoing CIGRE WG B4.91. It is expected that the benefits of SST in medium voltage applications will be highlighted. The optional energy storage can be integrated within the converter.

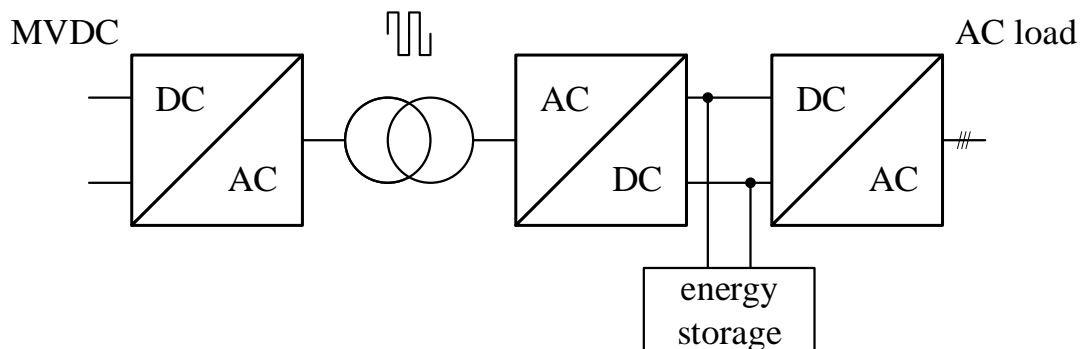


Figure 4.16 DC-AC interface with a solid-state transformer and an optional energy storage.

If the DC load cannot be connected directly to the MVDC grid, then a DC-DC converter is required. An isolated DC-DC converter, providing galvanic isolation, facilitates the grounding scheme and may

be more suitable if a high voltage ratio is required. A non-isolated DC-DC converter is usually smaller and simpler than an isolated DC-DC converter.

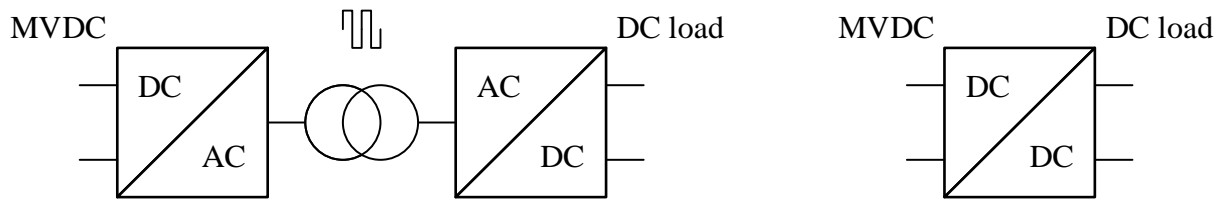


Figure 4.17 DC-DC interface with isolated and non-isolated DC-DC converter.

Some detailed interface technologies are introduced as follows:

[89] illustrates a new energy storage system (ESS) management strategy for a bipolar-type LVDC distribution system. The structure is shown in Fig. 4.18. The DC distribution system is considered as an alternative to the existing AC system for the increase of DC loads and DC output type DER such as photovoltaic (PV) systems and ESSs. The DC distribution system has several advantages such as conversion losses reduction, easy connection scheme for DC-based DER, simple energy management strategies (no reactive power issues). In a bipolar-type as shown in Fig. 4.18, the converters in the upper- and lower-sides can operate individually or collectively.

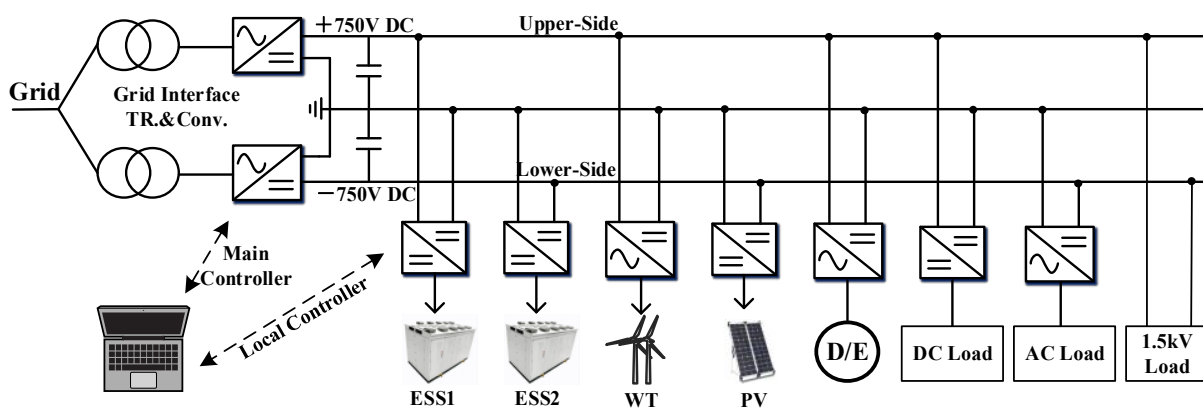


Figure 4.18 Configuration of bipolar-type DC distribution system with the EV stations [89].

Reference [90] proposes a system which can operate in islanded (grid isolated), passive grid interaction (both utility grid and battery operative), and active grid interaction (battery isolated) modes, as shown in Fig. 4.19. The battery uses a bidirectional DC-DC converter for buck and boost operation during charging and discharging modes. In the case of islanded operating mode, the battery bank maintains power balance within the configured system, further regulating the MVDC bus voltage. In grid-connected mode, the bidirectional DC-AC interlinking converter (ILC) operates in current-controlled mode. In islanded mode, the ILC operates in voltage control mode, regulating the AC bus parameters. Moreover, the ILC controls the MVDC voltage while operating in grid-connected mode. The MVDC loads are fed directly from the bus stabilized through the ILC and battery unit. For LVDC loads a closed-loop buck voltage controller is used for providing a stiff voltage supply. Efficient and economic operation of the hybrid DER lying within the household premises is the need of current time. Hybrid DER provide flexibility in terms of planning and economic scenarios. Combining the grid-connected micro-grid system with energy storage makes the overall system much more reliable, affordable and efficient.

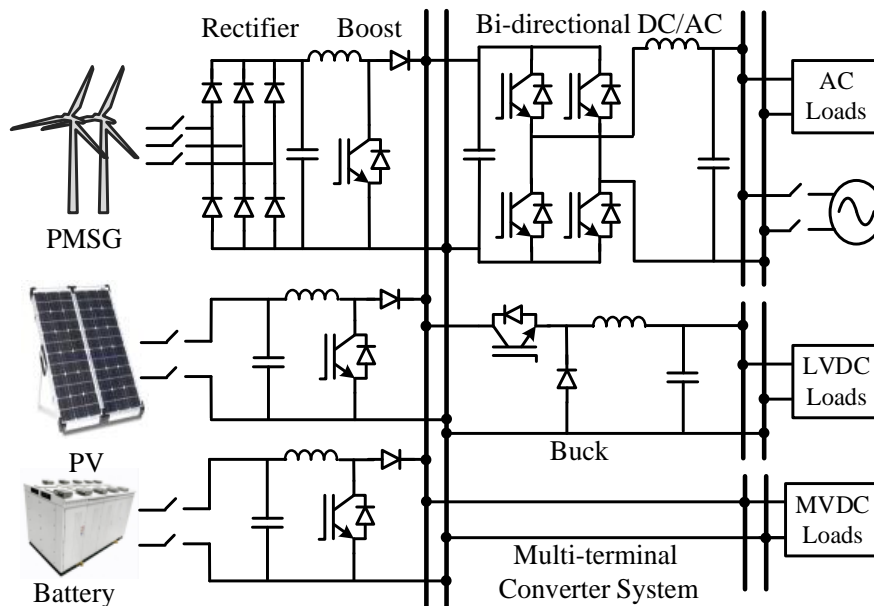
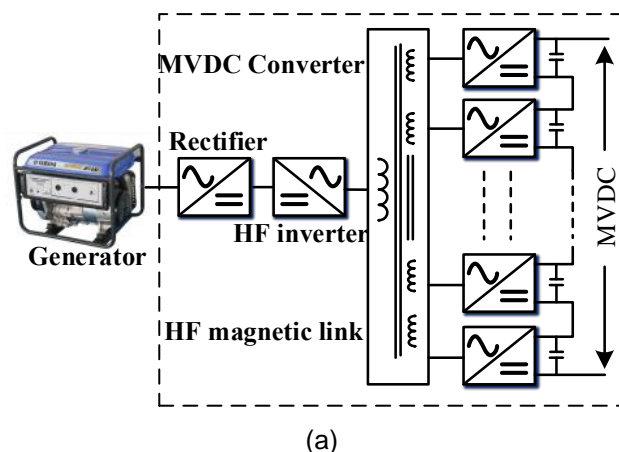


Figure 4.19 System layout with solar PV, wind DER; LVDC, MVDC, AC buses [90].

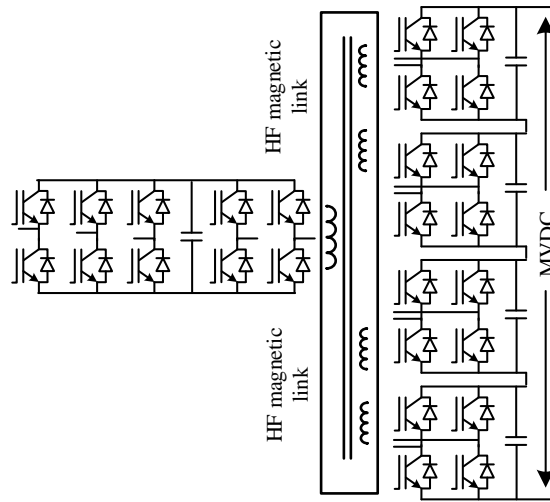
Over the last few years, several converter topologies have been proposed for offshore wind farm applications [91]. In particular, a modular DC converter:

- using multiple DAB DC-DC converters, as discussed in [92],
- with a multi-segmented stator-based special generator to eliminate the requirement of the step-up transformer in the wind turbine, and
- a magnetic linked MVDC converter for high-temperature superconducting (HTS) cable-based DC transmission systems to eliminate the requirement of large and heavy low-frequency step-up transformers and line filters.

Reference [91] proposes a new MVDC converter which can convert the generator's low voltage AC output to MVDC directly, as shown in **Fig. 4.20**. In addition, this new technology not only eliminates the requirement of large and heavy low-frequency step-up transformer and line filters but can also eliminate the voltage conversion stages to allow the entire power transmission networks to use MVDC HTS cables. Besides, the compact, lightweight, and efficient high-frequency common magnetic link are used in the proposed converter located in **Fig. 4.20**. The magnetic link can inherently solve the isolation problem.



(a)

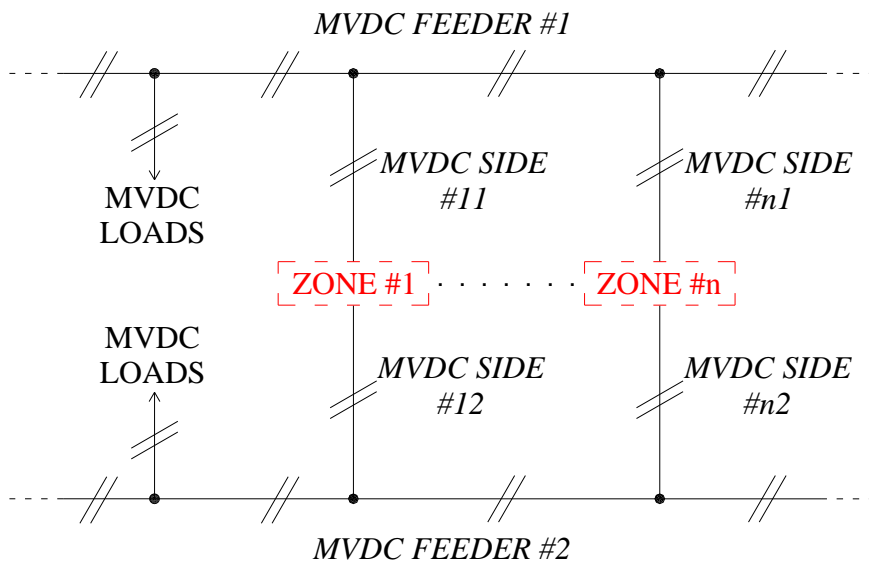


(b)

Figure 4.20 (a) Magnetic linked MVDC converter-based wind power conversion system; (b) Magnetic linked MV converter for HTS cable-based DC transmission systems [91].

Considering shipboard distribution systems, the Zonal Electrical Distribution System (ZEDS) topology can be built-up, in order to improve the quality of service of the LVDC loads. Many different DC-DC converter topologies for MVDC to LVDC interconnection have been presented in the literature. In IEEE Std 1826-2020, a ZEDS is defined as an agglomeration of elements, of which the aim is the supply of a group of loads. These elements are power electronics converters (PECs), controls, switchgear, cabling, and, if required, energy storage systems and generation. A ZEDS plus the loads it serves constitute a zone [94]. Thanks to this configuration, modularity is also achieved.

Each zone can be interconnected to several DC feeders for reducing the out-of-service time of its loads. Spatially separated cabinets, especially for navy ships, should drive these feeders. In this way, if a part of the ship is destroyed during a battle, at least one feeder will supply the zone. Fig. 4.21(a) shows an example of a ZEDS; while, Fig. 4.21(b) depicts how the zone can internally be configured [95].



(a)

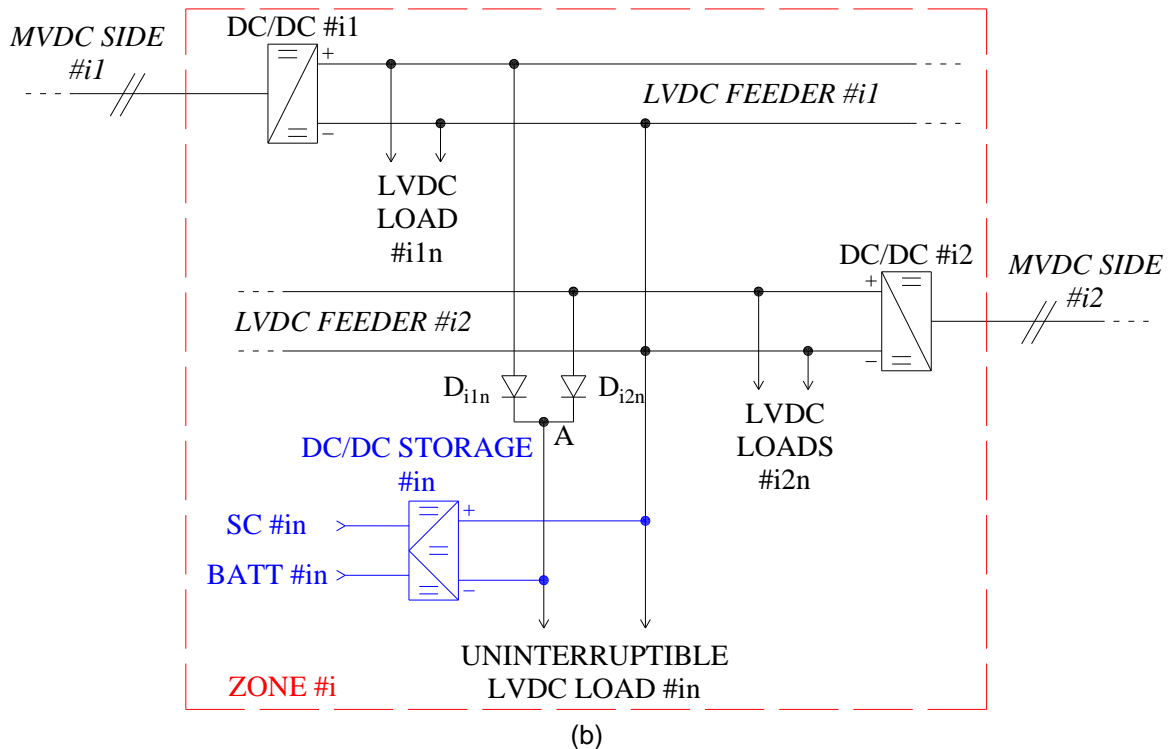


Figure 4.21 Schematic of a ZEDS and a generic  $i$ -th zone.

As can be seen from Fig. 4.21, the  $i$ -th zone can supply several kind of loads with different quality of service requirements. A generic  $i$ -th uninterruptible load is connected to redundant feeders and two auctioneering diodes  $D_{i1n}$  and  $D_{i2n}$ . The latter play a crucial role in decoupling the LVDC feeders during both normal working and fault conditions. Practically, they must be installed as close as possible to the uninterruptible loads. In addition to their advantages, these diodes also lead to an increase in losses, since they carry the total current withdrawn by the uninterruptible loads. In order to improve the continuity and quality of service, storage systems, along with a dedicated converter, can be installed, as shown in Fig. 4.21 (with blue addition).

DC-DC converters are used to transform MVDC to LVDC. A DAB is suitable for this purpose. For what concerns the converter control, a different voltage set point among the feeders is generally imposed. In this way, only the feeder at the highest voltage supplies the uninterruptible loads. Only if this feeder is lost will the supply be automatically switched to the other one by the auctioneering diodes. Many different DC-DC converter topologies for MVDC to LVDC interconnection have been presented in the literature [96]-[99], such as the modular multilevel DC-DC converters and the DAB based DC-DC converters. The DAB based DC-DC converters have been deployed in the  $\pm 10$  kV three-terminal Tangjia Bay MVDC distribution pilot project [67].

## 4.5 MVDC Power Conversion Topologies

### 4.5.1 Modular Multilevel DC-DC Converters

Reference [96] presents a novel galvanic isolated bidirectional DC-DC converter based on MMCs with energy storage and DC active power filter function, as shown in Fig. 4.22. In this circuit, one three-phase MMC and one cascaded converter (both employing full-bridge cells) are connected through a high-frequency AC transformer. This topology features the smoothing of load current on the MVDC bus. It can achieve both energy storage and active filter functions.

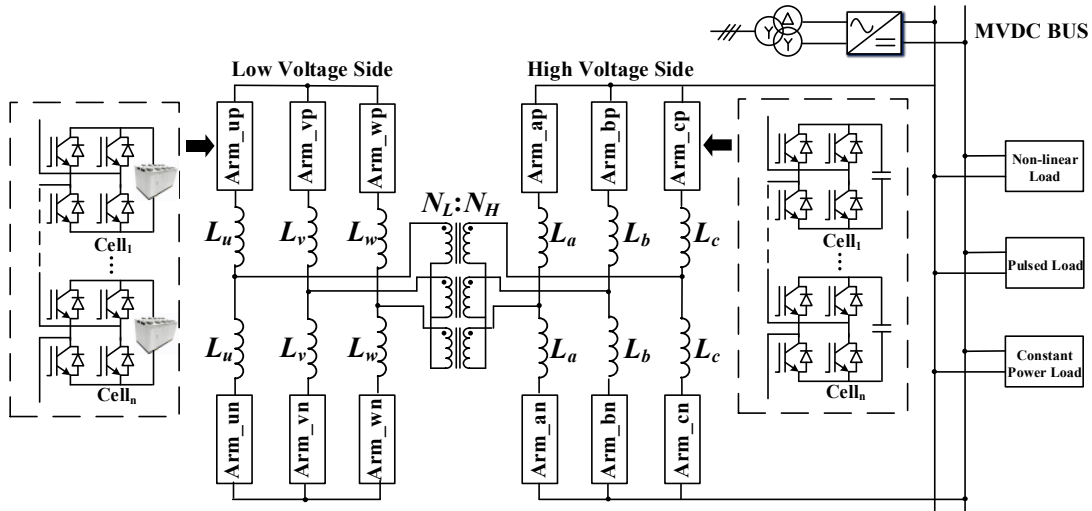


Figure 4.22 Isolated modular multilevel DC-DC converter [96].

Reference [97] proposes an isolated resonant mode modular converter (RMMC) with flexible modulation and assorted configurations to satisfy a wide variety of interface requirements for MVDC networks, as shown in Fig. 4.23. The high-voltage side contains a stack of half-bridge SMs connected to the primary winding  $N_1$  of the transformer  $T$ . The leakage inductance of the transformer can serve as the resonant inductance  $L_r$ , and the magnetizing inductor  $L_m$  appears in parallel and provides the return path for the DC current component. This RMMC approach inherits from the transformer-less RMMC the beneficial features of inherent SM voltage-balancing and soft-switching, and provides galvanic isolation and bidirectional power flow between the high-voltage link and low-voltage sides.

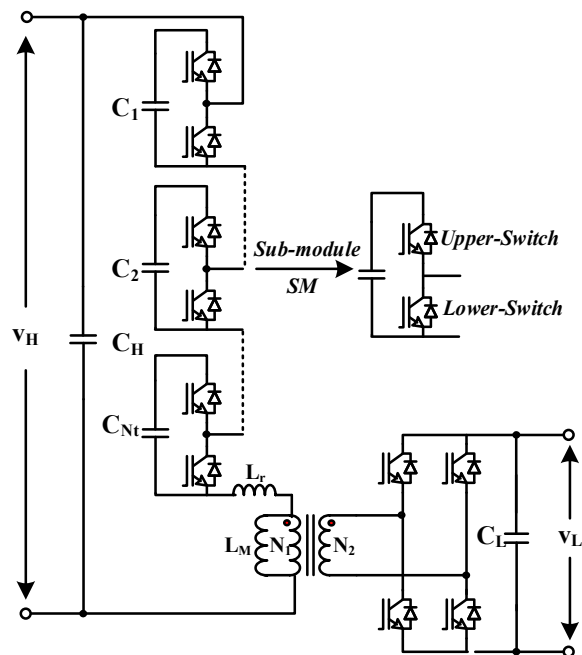


Figure 4.23 Isolated resonant mode modular DC-DC converter [97].

Reference [100] proposes a phase-shifted square wave modulation strategy for MMCs as well as DC transformers for MVDC applications, as shown in Fig. 4.24. The operational principle of the proposed method is based on an isolated modular multilevel DC-DC converter, which consists of an MMC stage and a medium frequency AC transformer. This topology can achieve low passive component size without increasing the total device rating and degrading the DC current control capability.

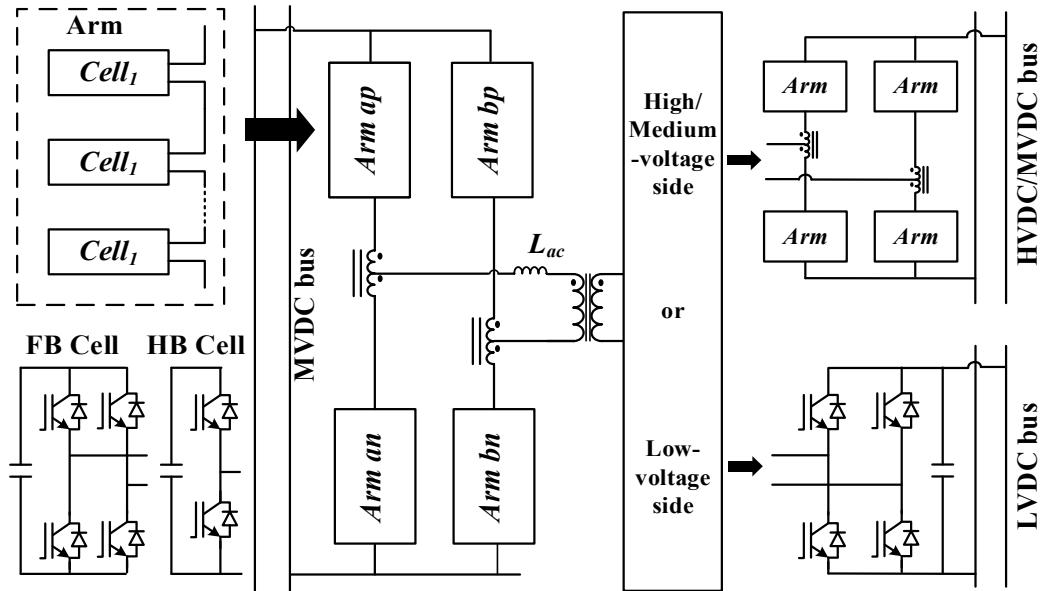


Figure 4.24 Isolated modular multilevel DC-DC converter consisting of an MMC stage at medium-voltage side connected to an MVDC bus [100].

Reference [101] proposes a modular multilevel DC-DC converter with a high step-ratio for medium-voltage and high-voltage applications, as shown in Fig. 4.25. It features low power throughput but high voltage ratio (LPHR). The high-voltage side contains two stacks of half-bridge SMs,  $SM_T$  and  $SM_B$  in the top and bottom arm, forming a single-phase MMC configuration with arm inductors  $L_T$  and  $L_B$ . There are  $N$  SMs in total, divided equally between top and bottom stacks. The primary winding of the transformer ( $r_T = N_1/N_2$ ) is connected between the phase midpoint and a neutral point created by two DC-link capacitors  $C_T$  and  $C_B$ . The topology on the high-voltage side is the half-bridge single-phase inverter with stacks of SMs in each of the switch positions to withstand the high-side voltage stress. The high voltage side processes all the power by only two SM stacks, so the total volume required by stack isolation can be kept low.

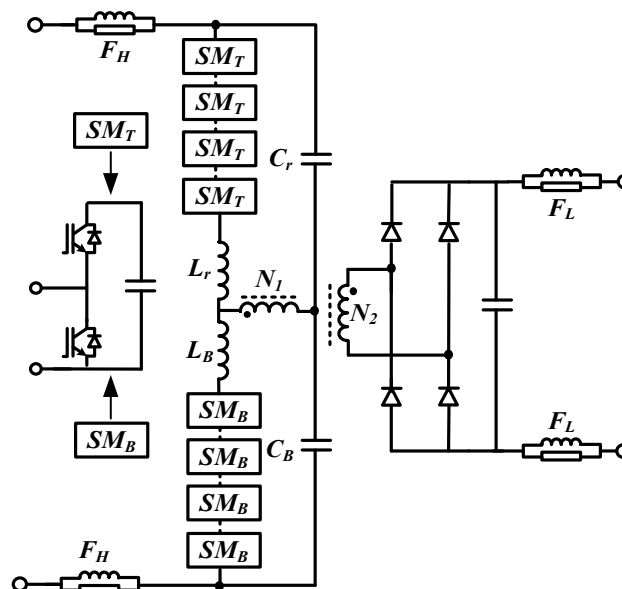


Figure 4.25 LPHR modular multilevel DC-DC converter [101].

#### 4.5.2 Dual Active Bridge Based DC-DC Converters

Reference [98] proposes a practical solution of a high frequency-link DC transformer based on switched capacitors (SCDCT) for MVDC power distribution application, as shown in Fig. 4.26. The

SCDCT is mainly composed of a series of switched capacitor interfaces (SSCI) and high-frequency link interfaces (HFLI). Compared to the traditional DC transformer scheme, the proposed SCDCT can disconnect from the MVDC distribution grid effectively as a DC breaker when a short fault occurs in the distribution network, can enhance power transfer capacity, and always ensures high-frequency-link voltage match to improve current impact and efficiency performances, and the redundancy in the design can improve the reliability if some submodules fail.

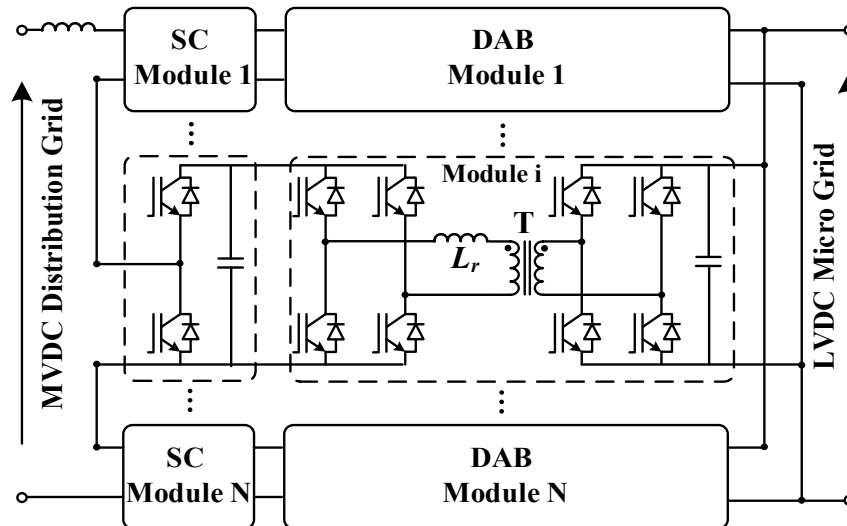


Figure 4.26 High frequency-link DC transformer based on switched capacitor [98].

Reference [99] proposes a current-fed modular multilevel dual active bridge (CF-MDAB) DC-DC converter for MVDC applications, as shown in Fig. 4.27. The CF-MDAB converter can be treated as two current-fed quasi-three-level converters (CF-Q3LCs) in front-to-front connection through a medium or high-frequency transformer  $T$ . The CF-MDAB combines the advantages of both DAB-based and MMC-based DC-DC converters, i.e., the soft-switching operation, small passive components, and DC fault-ride-through capability. The CF-MDAB converter not only can be utilized as a battery energy storage system (BESS) but also a DC transformer for MVDC applications when a DC fault current control capability of the converter is required or preferred.

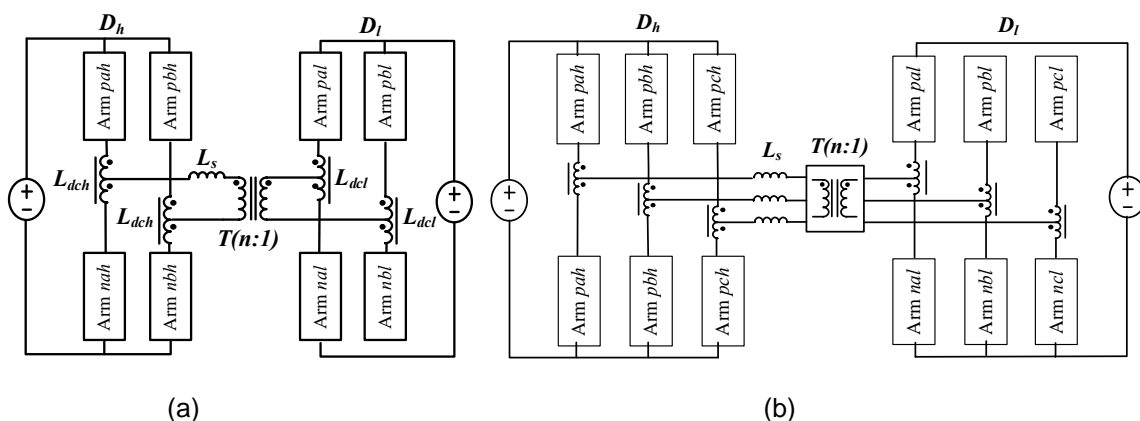


Figure 4.27 CF-MDAB converters: (a) Single-phase, and (b) three-phase [99].

Reference [102] presents a comprehensive comparison of a multilevel high-frequency-link (HFL) DC transformer (abbreviated MDCT) based on the MMC and a multilevel-DC-link DC transformer (abbreviated ADCT) based on a dual active bridge (DAB) for MVDC application. The topologies of MDCT and ADCT are shown in Fig. 4.28. MDCT employs an MMC structure to increase the voltage level. Each bridge arm is composed of  $N$  SMs and an HF inductor. The HFL is composed of  $m$  HF isolated transformers, which are connected in series on the primary side. The LVDC interface of the

MDCT is composed of M full bridges, which are connected in parallel on the DC side to increase the current level. The ADCT still employs a DAB structure as a basic cell. The system is composed of N DAB modules, but the series multilevel DC-link (MDCL), based on a half-bridge SM, is used as the interface for MVDC. By using the SM, no concentrated capacitor is required on the MVDC side for both MDCT and ADCT. A redundant module can be added easily in both DCTs, and then the DCTs can operate well when some SMs fail. Moreover, when a short-circuit fault is produced in the MVDC grid, the DCTs can work as a DC breaker to cut off the connection between the MVDC and LVDC buses.

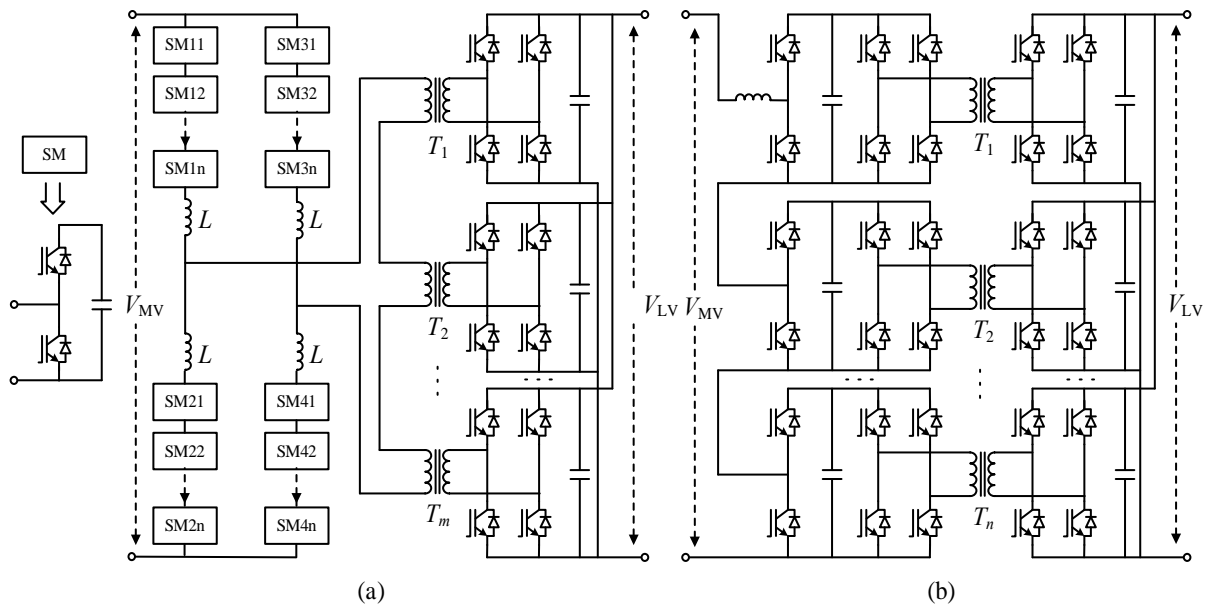


Figure 4.28 Comparison of (a) MDCT, and (b) ADCT [102].

Reference [103] proposes a 5-level DAB DC-DC converter with three degrees of freedom, which improves its ability to regulate power flow, as shown in Fig. 4.29. On the primary side of the high-frequency transformer, an H-bridge consisting of four power switches (S2, S3, S4, S5) is connected with one auxiliary switch S1. Auxiliary switch S1 is responsible for half voltage stage at the primary side. On the secondary side, the H-bridge is connected consisting of four switches (S6, S7, S8, S9). A square wave voltage ( $V_s$ ) is obtained on the secondary side of the high-frequency transformer. Moreover, due to an increase in voltage levels,  $dv/dt$  across switches reduces significantly and it also reduces the circulating power which improves the efficiency of the system.

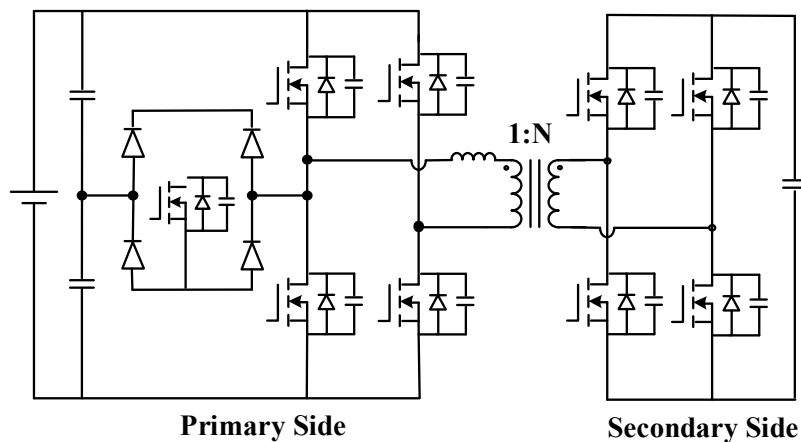


Figure 4.29 5-level DAB DC-DC converter [103].

A double step-down DAB DC-DC converter with high voltage gain and high efficiency is proposed in reference [104], as shown in Fig. 4.30. The proposed converter achieves double step-down

functionality by adding only one capacitor on the primary side of the transformer. The transformer voltage and the voltage across the three switches on the primary side of the proposed converter is equal to half of the input voltage. In addition, the proposed converter naturally solves the transformer saturation problem by the addition of the extra capacitor.

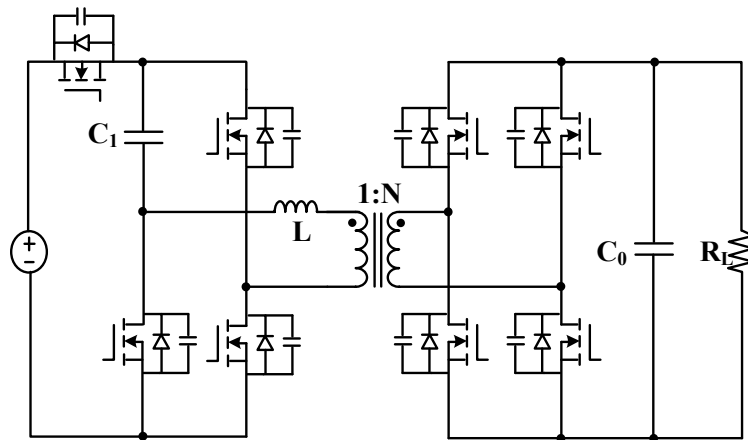


Figure 4.30 Isolated double step-down converter [104].

## 5 MVDC Drive Systems

The development of medium voltage (MV) drive systems started from the mid-1980s when 4.5 kV switching devices (GTOs) became commercially available. Since then, the IGBT and IGCT based converters have shown their superior switching characteristics, reduced power losses, and better control capability.

The high-power MV drives have been widely installed in the industry, such as the pipeline pumps in the petrochemical industry, fans in the cement industry, pumps in water pumping stations, traction applications in transportation systems, propulsion systems for electric ships, etc. The ratings of MV drives range from 0.4 to 40 MW at the MV level of 2.3-13.8 kV and the majority of the installed MV drives are in the 1-4 MW range with voltage ratings from 3.3 to 6.6 kV.

In this Chapter, converter topologies, stability and fault protection of MV drive systems will be discussed with the consideration of their applications. The learnings for this field will be presented as well.

### 5.1 MV Drive Power Conversion

Voltage source converters (VSCs) are used to convert a DC voltage to a three-phase AC voltage with variable magnitude and frequency to feed electrical machines. The topologies of power converters in MV drive systems mainly include two-level VSC (2L-VSC), three-level VSC (3L-VSC), cascaded H-bridge (CHB) converters, and modular multilevel converters (MMCs), etc. Their characteristics for MV drive systems are summarized as follows.

2L-VSC is mainly used for low-power applications. **Fig. 5.1** shows the inverter based on two-level topology interconnecting the DC link with the three-phase load, generating variable voltage and frequency. In fact, in MV applications, the 2L-VSC has been superseded by other topologies such as the 3L-VSCs due to their better harmonics performance and lower power losses.

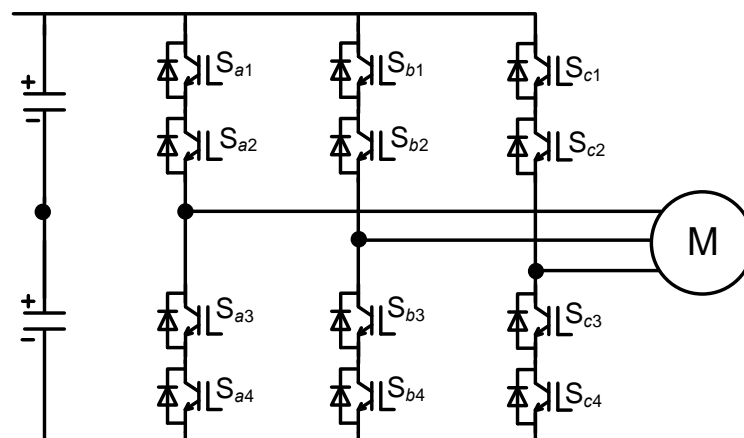


**Figure 5.1** Two-level converter topology.

The three-level neutral point clamped (NPC) converter has been used in high-power MV drive systems. **Fig 5.2** shows the three-level NPC converter topology. Compared to the two-level converter topology, it benefits from lower losses and better harmonic performance. As with the two-level converter, the inverter interconnects the DC link with the three-phase motor, generating variable voltage and frequency. The topology has found practical application in high-power medium voltage drives.

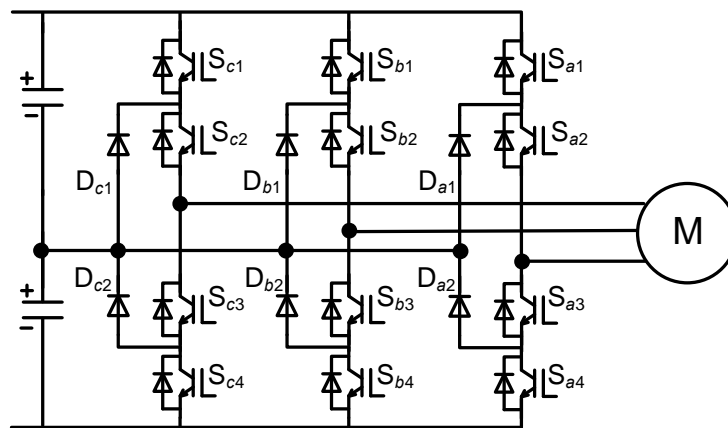


Figure 5.2 Three-level NPC converter.

Some manufacturers have developed their products with such topologies. The power ranges from 0.3 to 36 MVA. The maximum power can reach to 36 MVA when adopting IGBT devices in some products. Compared to 2L-VSC, the 3L-NPC converter has shown its advantages in increasing power capacity, power quality, and efficiency of MV drive systems. However, this popular inverter topology has an issue with unequal power losses among the switching devices, which leads to an uneven semiconductor-junction temperature distribution. This causes unequal utilization of the switching devices in the inverter. For a given power rating of the inverter, the switching devices that have lower junction temperatures are not fully utilized. Furthermore, in order to enhance the capability of such topology, a three-level ANPC inverter has been proposed, as shown in **Fig. 5.3**. This inverter topology is derived from the 3L-NPC where the clamping diodes are replaced by active clamping switches.

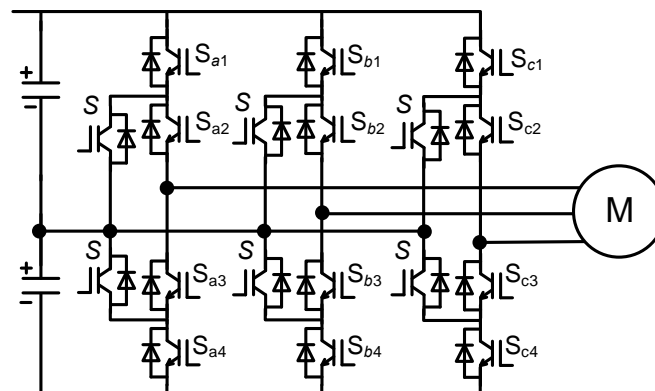


Figure 5.3 Three-level ANPC converter.

Multi-level CHB converters and MMCs have also been considered as promising topologies in MV drive areas with better harmonic performance, lower power losses and larger power rating. The multi-level CHB inverter uses multiple units of H-bridge power cells connected in a series chain to produce high AC voltages. A typical configuration of a five-level CHB inverter is shown in **Fig. 5.4**. It should also be noted that, for such configurations, each of the H-bridge cells needs to be connected with a transformer and a diode rectifier to provide separated DC links. This will complicate the structure and design of the system. Due to not including a common DC link, such a topology may not be applicable to MVDC application. Manufacturers have already adopted CHB in building their converters. The power ratings are from 0.2 to 60 MVA.

Similar to the cascaded H-bridge topology, the MMC topology consists of a high number of sub-modules (SMs) as shown in **Fig. 5.5**. Each of these SMs consists of a half-bridge or a full-bridge topology with a DC capacitor. The power rating of the MV drive using the MMC topology with half-

bridge SMs can reach to 16 MVA with the output voltage up to 7.2 kV [105].

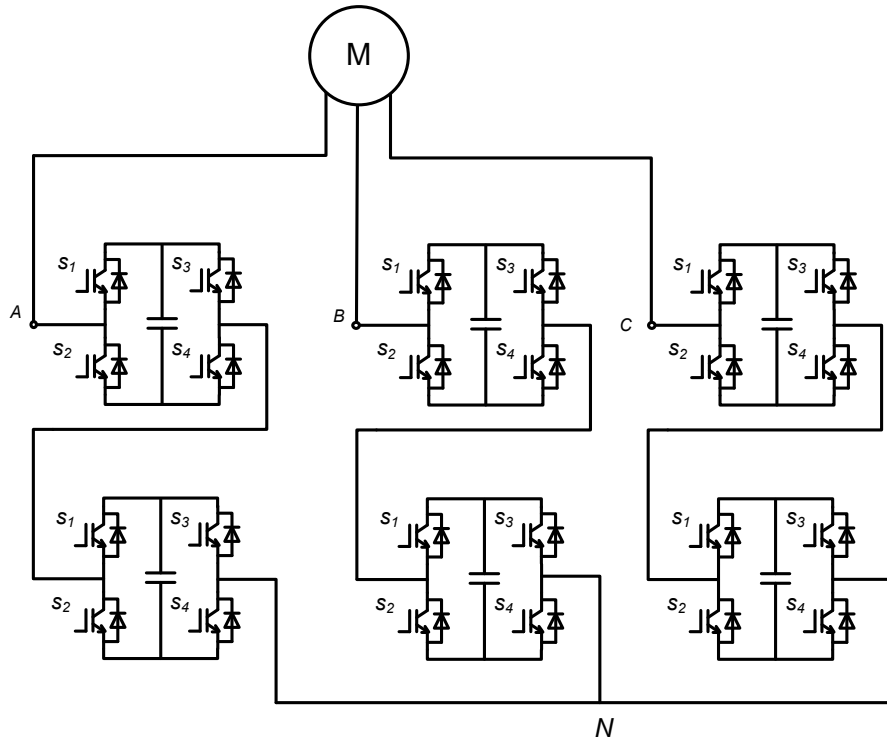


Figure 5.4 Five-level cascaded H-bridge converter [105].

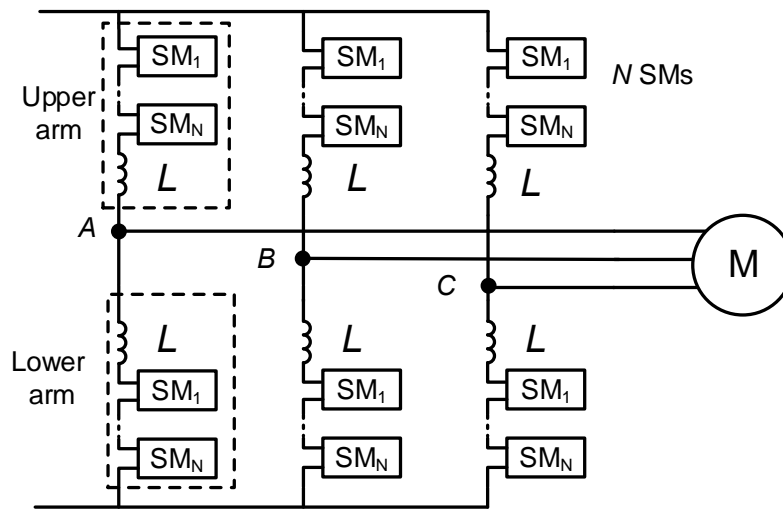


Figure 5.5 Modular multilevel converter for MV drives [105].

## 5.2 Stability Issues of MV Drive Systems

Stability is an important aspect that needs to be considered before the deployment of MV drive systems. A small-signal analysis method to define the impedance specifications of the power converters has been proposed in [106]. The studies show that the interactions between individually designed subsystems/power converters may cause instability of the whole DC system, as shown in Fig. 5.6.

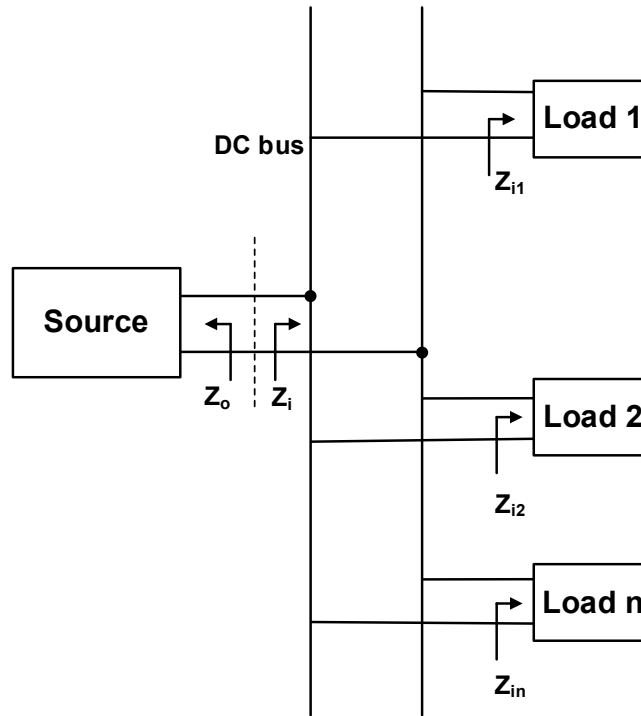


Figure 5.6 DC distributed power system [106].

A method for the sizing of filter parameters considering stability and power quality criteria based on an MV drive system with DC filter has been proposed in [107], as shown in Fig. 5.7. To ensure the whole system stability, this filter has to prevent converter harmonic pollution from being re-injected by the DC network. Furthermore, [107] proposes to minimize the energy storage in the filter. The analytical linearized model of the system is automatically built from a circuit description. System stability conditions are firstly assessed in this model with the Routh-Hurwitz criterion. Then, filtering and damping conditions are introduced. To complete the sizing, optimization algorithms are introduced to minimize the energy stored in inductive and capacitive components.

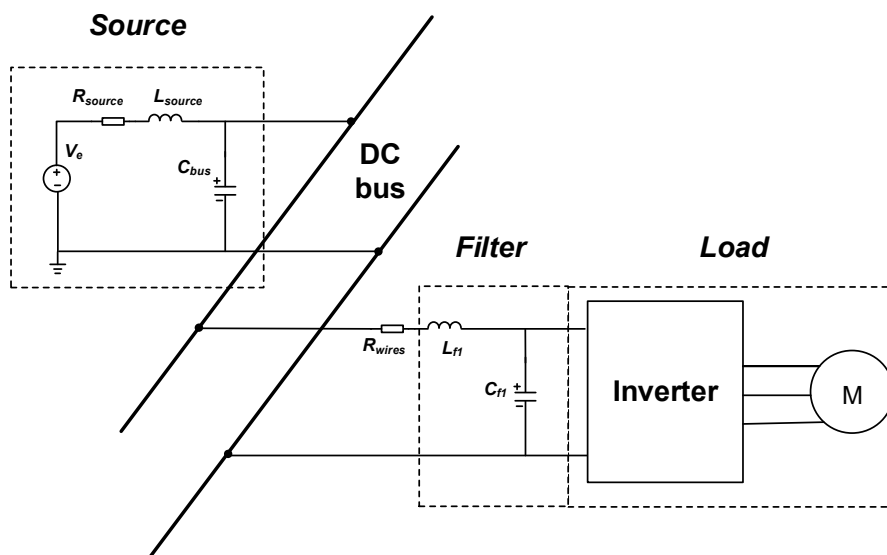


Figure 5.7 A typical MV drive system with DC filters [107].

In more electric aircraft, the optimization of passive elements, such as DC bus capacitance and filtering inductance, is an important issue. However, the reduction of DC bus capacitance may lead to instability of an MVDC network. So, if no stabilizer is used, the risk of instability must be considered

when designing the passive elements in the system.

A method for implementing a global stabilization block for a DC power network is presented in [108]. The small-signal stability of the MVDC network with three loads (an inverter supplying a permanent magnet synchronous motor, a DC-DC converter feeding a resistive load, and a supercapacitor controlled by a bidirectional DC-DC converter) has been investigated. Loads are modelled as constant power loads, which allows a simple representation. Then, a large-signal-stabilizing system to ensure global stability by generating proper stabilizing power references for the whole system has been proposed.

### 5.3 Standards Used for Drive Systems

There have been some standards for drive systems:

- IEC 61800-3: Adjustable speed electrical power drive systems - Part 3: EMC requirements and specific test methods
- IEC 61800-2: Adjustable speed electrical power drive systems - Part 4: General requirements - Rating specifications for ac power drive systems above 1 000 V ac and not exceeding 35 kV
- IEC 61800-5-1: Adjustable speed electrical power drive systems - Part 5-1: Safety requirements - Electrical, thermal and energy
- IEC 61800-5-2: Adjustable speed electrical power drive systems - Part 5-2: Safety requirements - Functional
- IEC 61800-7 series: Adjustable speed electrical power drive systems - Part 7-x: Generic interface and use of profiles for power drive systems
- IEC 62477-1: Safety requirements for power electronic converter systems and equipment - Part 1: General
- IEC 62477-2: Safety requirements for power electronic converter systems and equipment - Part 2: Power electronic converters from 1 000 V AC or 1 500 V DC up to 36 kV AC or 54 kV DC
- UL 347A: Standard for Medium Voltage Power Conversion Equipment
- IEEE Std. 1709-2018 - Recommended Practice for 1 kV to 35 kV Medium-Voltage DC Power Systems on Ships.
- IEEE Std. 1662-2008 - Guide for the Design and Application of Power Electronics in Electrical Power Systems on Ships.

The requirements for loads and power sources to connect and disconnect from the MVDC bus on ship power systems has been illustrated in IEEE Std 1709-2018.

### 5.4 Learnings from Drive Systems

MV drive systems normally create a common DC bus. This can de-couple tight connections between different sources and loads. The power electronic converters in an MV drive system provide three-phase AC voltages with variable magnitudes and frequencies to feed AC motors. By transferring electric power between the AC and DC sides, many advantages can be achieved.

A DC shipboard distribution system envisioned by the U.S. Navy is presented in [109]. The system configuration is shown in **Fig.5.8**. The generated energy is transferred from AC to DC through power electronic converters to form a common DC bus. The whole system is divided into different zones by DC-DC converters which isolate the loads in the local zone from the other part of the system. In this way, any fault and disturbances are limited within that zone. Another advantage is that the converter can eliminate the tight frequency regulation and synchronization requirements, which will increase

the stability of the whole system. Meanwhile, DC cables can transfer more power than AC. This is also one of the main reasons for the Navy to employ the DC distribution system.

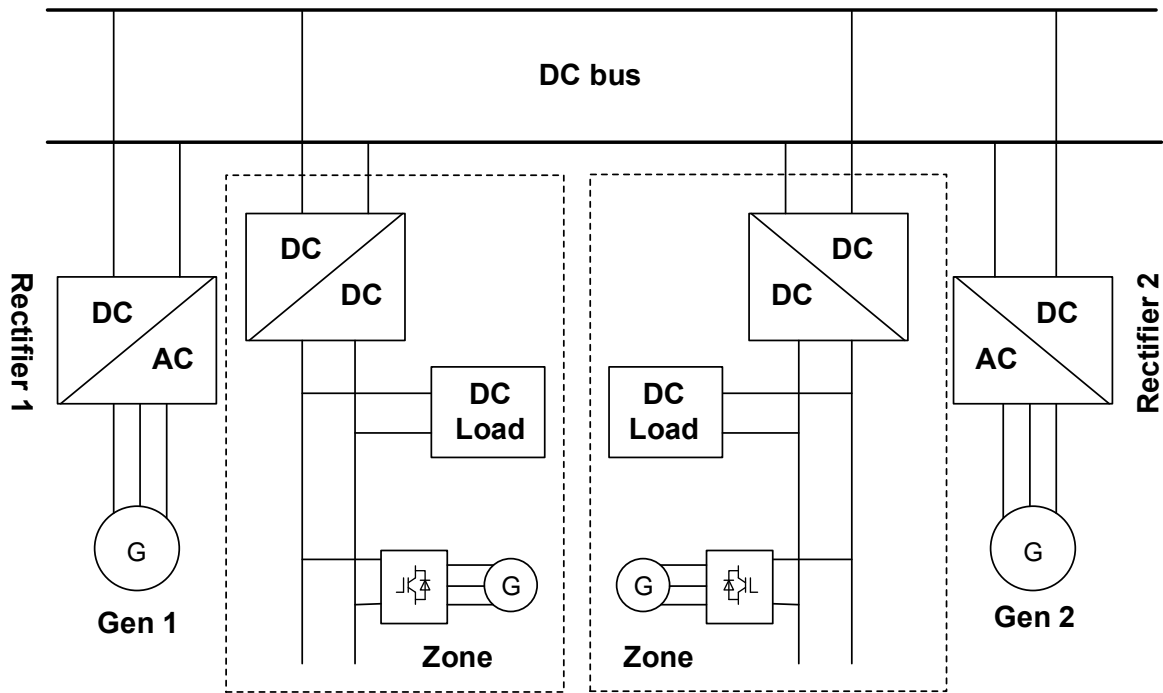


Figure 5.8 DC shipboard distribution system [109].

Traction power systems are important areas where MV drive systems are widely used. An MVDC based traction power supply system (TPSS) is presented [110], as shown in Fig. 5.9.

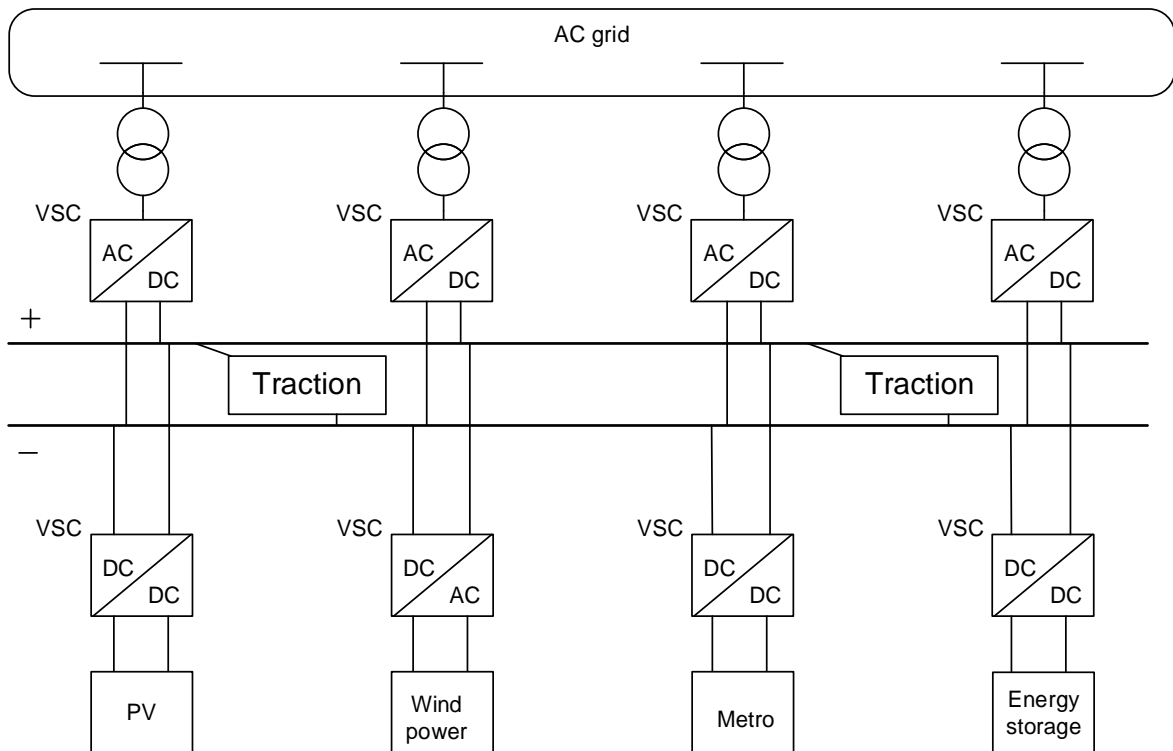


Figure 5.9 Structure of VSC-based MVDC TPSS [110].

The system consists of the following units: 1) Traction substations equipped with VSCs connected to high-voltage three-phase utility grid through step-down transformers. 2) Renewable energy sources (RESs), such as wind and photovoltaic, connected with DC grids through DC/DC or AC/DC

converters. 3) Energy storage systems (ESSs), such as batteries, ultracapacitors and flywheels, which are connected with power converters to smooth power flow. 4) Lower voltage level DC systems, which are mainly adopted for urban rail traffic and connected with DC grids with DC/DC converters. By employing such a structure, advantages can be achieved compared with the conventional 25 kV pure AC system: Improvement of power quality; Easy integration of distributed RESs and ESSs; Increase of power supply distance and simplification of catenary networks; Connectivity among other heterogeneous railway systems [110].

A concept for power distribution is presented in [111], which utilizes the well proven AC generators and motors, and opens new opportunities for efficiency improvements and space savings. The new freedom of controlling each power consumer totally independently opens numerous ways of optimizing the fuel consumption. Since the main switchboard is omitted, including its generator and feeder circuit breakers, a new design of the protection system is proposed. As discussed in [111], there are several ways of configuring the onboard DC grid from a multidrive approach to a fully distributed system, as shown in **Fig.5.10**.

For many MV drive cases, the power is transmitted from the three-phase power grid to motors. Four-quadrant operation is not required. Therefore, in these cases, a relatively simple passive diode rectifier can be used as the front converter, very often in a 12-pulse, 18-pulse or even 24-pulse configuration, depending on the power rating of the drive and the requirements related to harmonics at the supply point. However, for MVDC applications, the four-quadrant operation is needed due to the requirement of bidirectional power transmissions. Among the above-discussed topologies, 2L-VSC, 3L-VSC and MMC are suitable for MVDC applications. The 2L-VSC and 3L-VSC are more suitable for systems with lower power rating while MMCs are preferable for systems with higher power ratings.

As discussed in Chapter 4, the drive system for vessels is an important application. For the system level configurations, in the multidrive approach, all converter modules are located in one or multiple line-ups and occupy the same space as today's main AC switchboard. For the distributed system, each converter component may be placed more freely around the vessel, normally close to the respective power source or load, and the rectifier can be integrated in the synchronous generator. All generated electric power is fed directly or via a rectifier into a common DC bus that distributes the electrical energy to the consumers as shown in **Fig.5.10**.

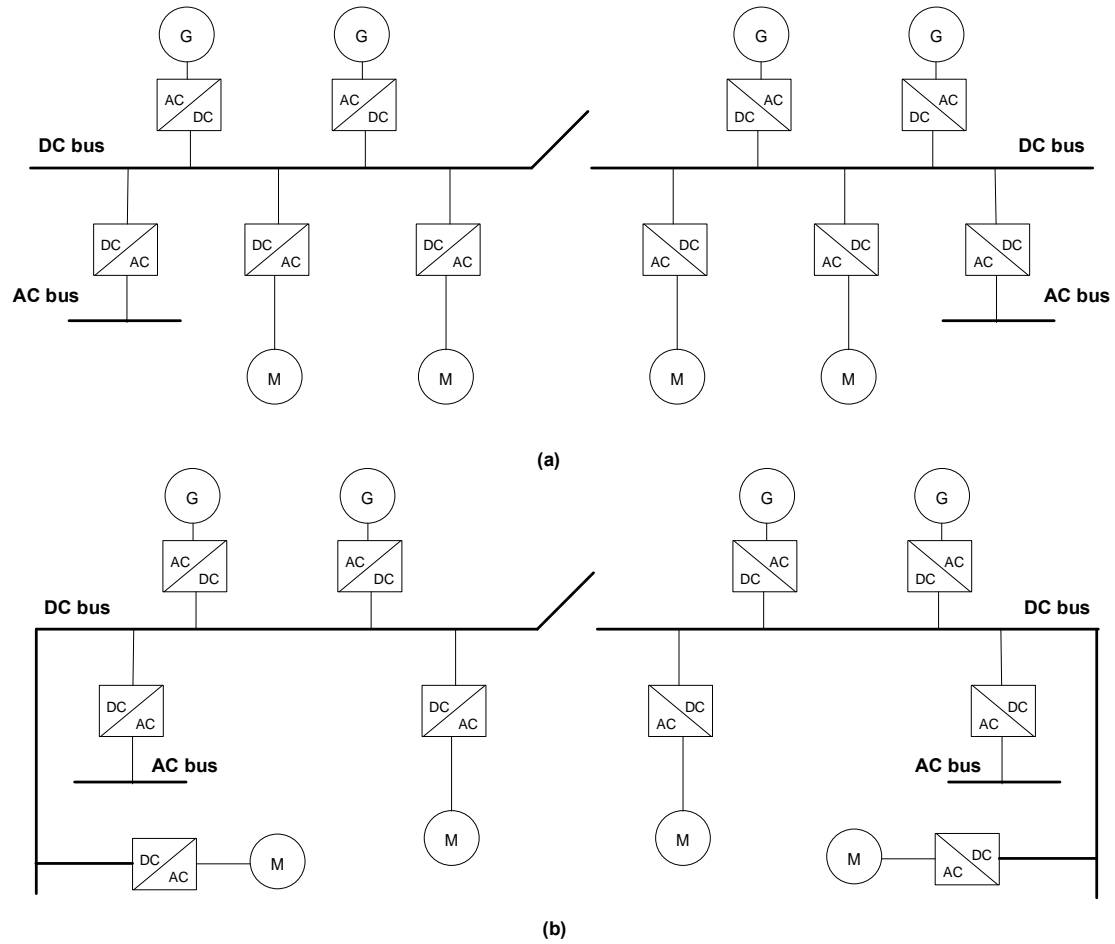


Figure 5.10 Various DC grid configurations and interface: (a) multidrive approach and (b) distributed approach [111].

A general scheme of the next-generation MVDC shipboard power systems has been proposed in [112], as shown in Fig. 5.11. The scheme is composed of a main diesel generator set, an auxiliary generator set, on-board battery bank, solid oxide fuel cell, conversion devices, main switchboard, two drive systems, propellers and ship-service loads. Power electronic converters are important interfaces between MVDC networks and loads.

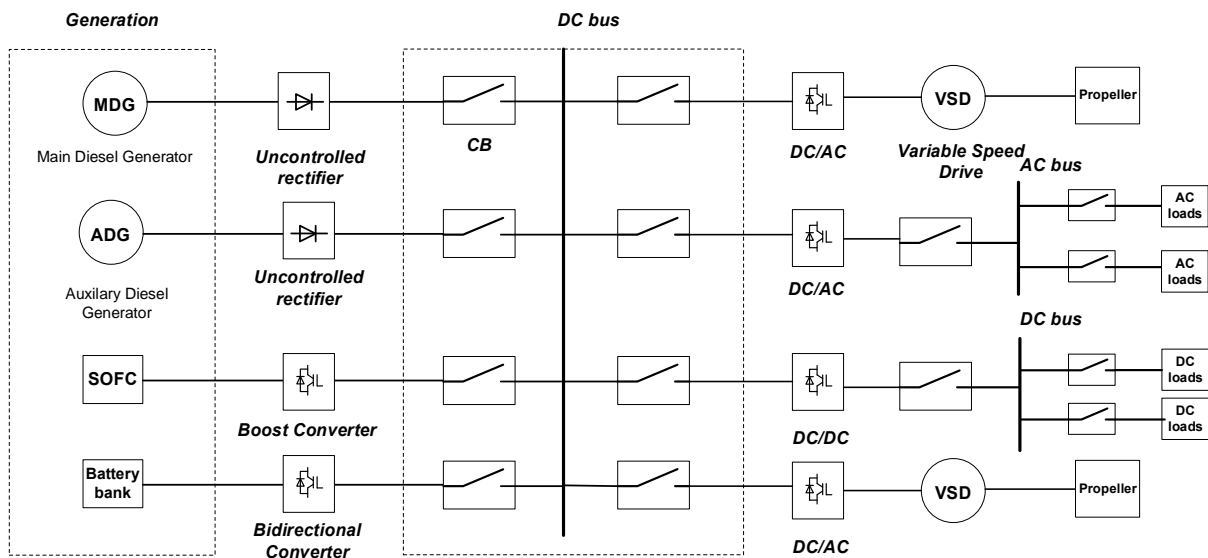


Figure 5.11 The structure of the next-generation MVDC shipboard power system [112].

## 6 MVDC Applications

MVDC covers a wide area of applications, from well-known 1.5 kV and 3 kV DC railway networks to DC distribution networks within vehicles/vessels or cities, to DC collection grids to even MVDC transmission. [93] presents a survey of MVDC applications, technical solutions, required key components, the state-of-the-art solutions and those expected to be available soon.

### 6.1 Offshore Wind Power MVDC Collection Systems

For renewable power parks (offshore and onshore wind parks, solar parks), MVDC collection systems have been proposed in [113]-[114]. The mentioned main arguments to establish DC in these applications are:

- Renewables, especially PV solar, are in fact DC power generators.
- DC collection is expected to be more efficient as there are no other losses related to AC (losses due to reactive current, additional losses due to skin effect).
- Potentially less conversion stages involved.
- DC collection grid potentially less costly because of fewer cables.

The use of a local MVDC system at the 5 kV to 20 kV level (or even higher depending on the park power rating) within the wind turbine cluster would improve the power collection efficiency and the overall cost. **Fig. 6.1** shows a possible MVDC cluster for a wind park [93].

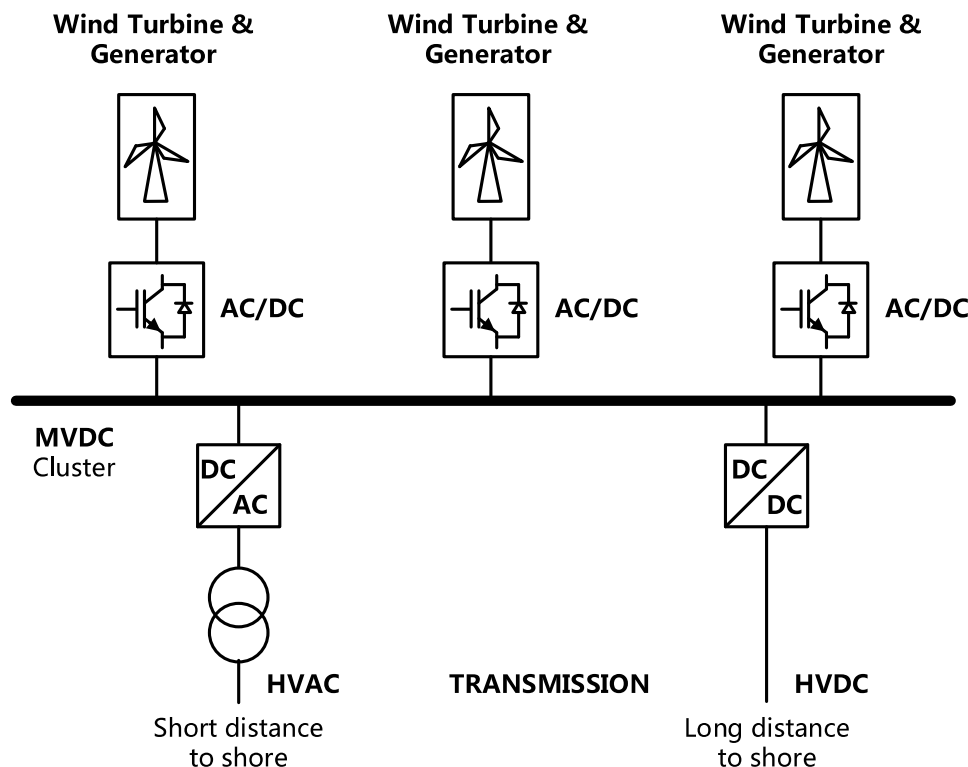


**Figure 6.1** MVDC cluster for a wind park [93].

Compared to state-of-the-art solutions the following components are needed:

- For each renewable generator: converters from LVDC or LVAC to MVDC
- MVDC breakers (depending on the selected protection concept)
- MVDC/AC inverter

- MVDC/HVDC converter (in case of coupling into an HVDC link)

Also, for solar power parks, MVDC has been considered as beneficial for collector grids [115], but also postponed because of a very competitive state-of-the-art market situation [116].

The utilization of wind energy is steadily growing worldwide. The collection system in offshore wind parks is normally based on AC and connects each wind turbine (WT) to an offshore substation platform. However, DC collector systems within offshore wind parks offer substantial benefits in efficiency and investment costs.

Reference [117] discusses a variety of DC collection models for offshore wind farms. **Fig. 6.2** shows a few illustrations of conventional AC and DC collection system arrangements for an offshore wind farm [118]. DC-DC boost technology allows turbine generators to output their power directly into a DC array.

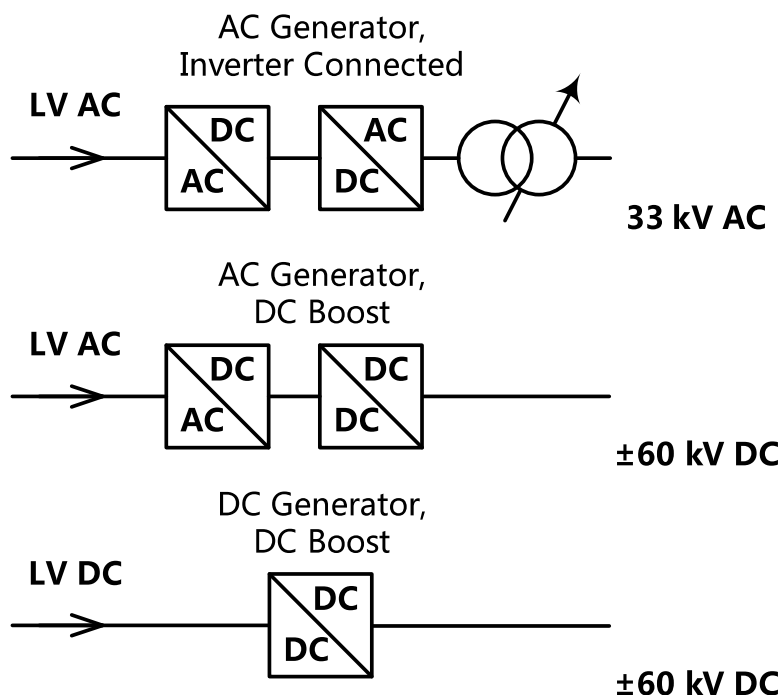


**Figure 6.2** MVDC cluster for a wind park [118].

In the past, many government-sponsored projects in the United States have been focusing on various means of integrating renewable generation resources, specifically wind and solar, into the grid [119] to provide an environmentally responsible, economical, and potentially optimal method of transmitting renewable energy.

Previous studies and research mentioned that the collocation of offshore drilling platforms and wind generation can utilize MVDC collection systems and transmit power to the offshore oil platforms drives. Offshore oil-drilling operations [119], such as those shown in **Fig. 6.3**, which are heavy industrial environments, rely primarily on variable-frequency AC drives for applications such as propulsion, station keeping, drilling, and pumping product to the surface. In drilling rigs, drill ships, and offshore production platforms, the nonlinear variable-speed drive load makes up 85% of the installed kW. The system in **Fig. 6.3** provides a system-level interconnection of a local wind power generation with an offshore oil-drilling platform.

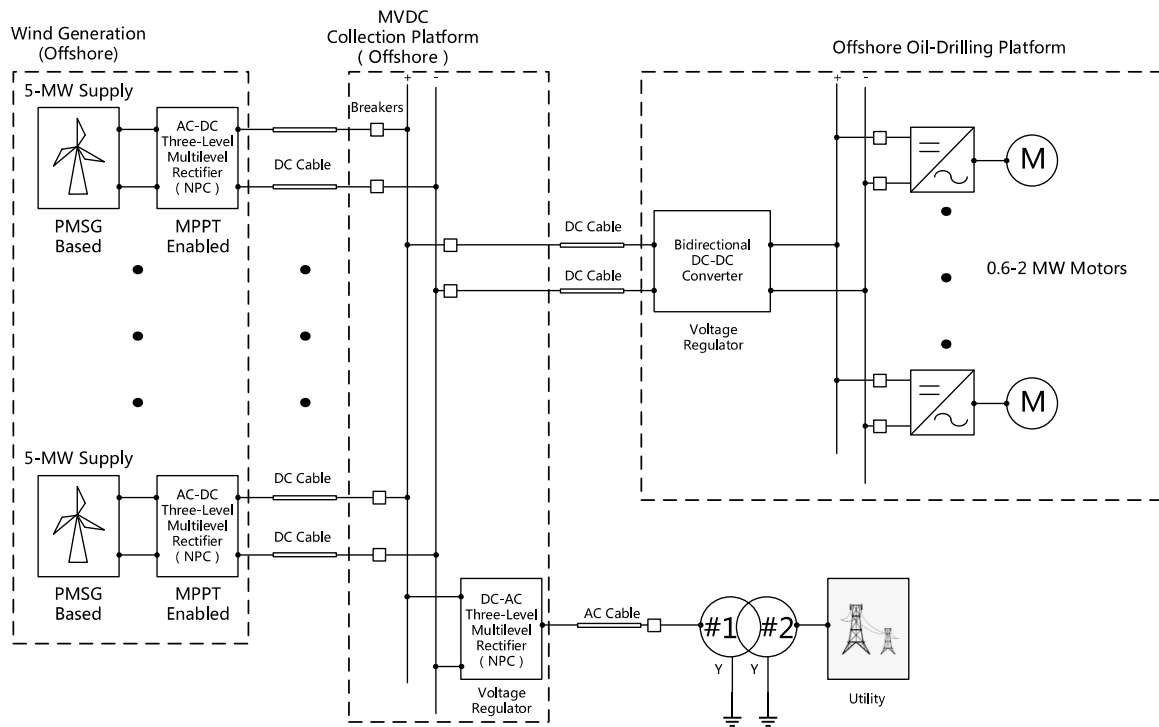


Figure 6.3 MVDC architecture in an offshore oil-drilling application with a co-located wind farm [119].

## 6.2 Marine Vessels

In marine electrical systems, the application of MVDC distribution has been in growing popularity over the MVAC for ship on-board power systems. The MVDC power system in the core of marine vessels or ships, can generate, store, and deliver electrical power of the proper quality and maintain continuity to the served loads with minimal risks [120].

Generators, loads and energy storage devices are normally connected to the DC bus via controllable power electronic converters, DC/AC, DC/DC, or AC/DC. This topology requires a smaller footprint and allows limiting of fault currents and relative ease of connection of different ratings of speed generators, storage devices, and loads as described in [121]. Fig. 6.4 represents a functional MVDC block diagram [121] of an MVDC power system for ships or marine vessels. The functional blocks consist of shore power interface, power generation, energy storage, pulsed load, propulsion, ship service, dedicated high-power load, and MVDC Bus. There are several independent functions, such as interruption, isolation, and configuration, to be performed by one or more devices, e.g., circuit breakers, fuses, loads switches, and power electronics on output generators. This functional breakdown provides key design purposes of any kind of MVDC ship power system. The number of blocks and modules is not limited to any marine vessels or ships.

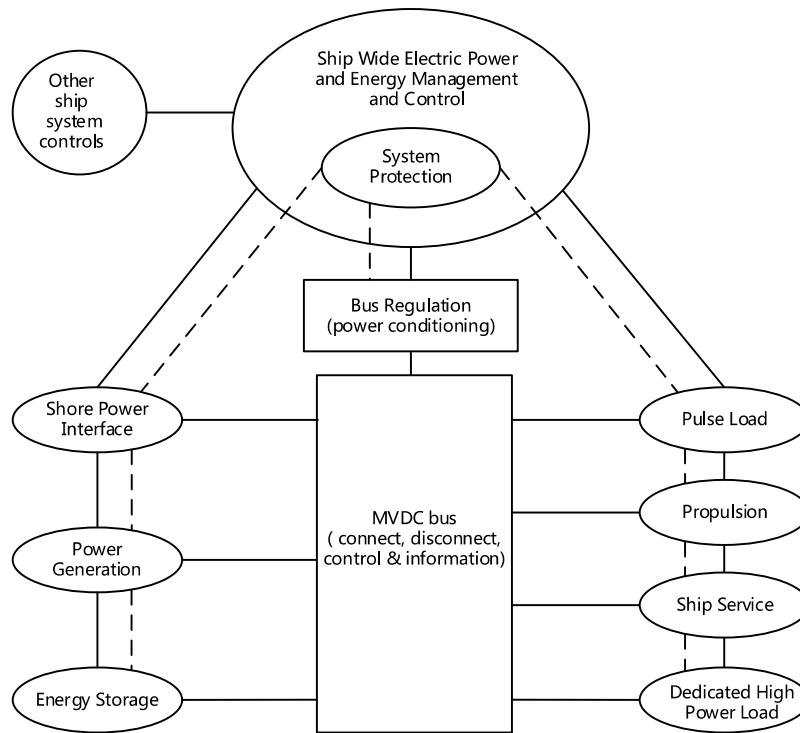


Figure 6.4 Functional MVDC block diagram [121].

A specific example of a high-performance ship system has been presented in [121]. This architecture maximizes operational capability even under extremely adverse conditions. Ship service loads are distributed in four zones from bow to stern along the ship and fed MVDC power from both port and starboard DC buses, which run longitudinally along the ship. Zone 5 represents the deckhouse and the only significant electrical equipment is high power radar. Bow and stern cross-hull links are provided between the port and starboard DC buses to provide the capability of configuring a ring-bus, from which the power generation and load subsystems operate. One main and one auxiliary gas turbine generator set is connected to each longitudinal bus. Therefore, opening the bow can enhance power system survivability and stern cross-hull disconnect switches to create a "split-plant" configuration.

The essential loads including primary mission system radar (as described in 2018[121]) are continuously supplied power from either port or starboard buses through automatic bus transfer switches. MVDC power from the port and starboard longitudinal buses is stepped down in the zonal load centres to LVDC (e.g., 800 V) by DC/DC converters. Some loads operate directly off of this LVDC bus. Other AC loads are supplied low-voltage, three-phase AC power (e.g., at 450 V) by a DC/AC converter operating off of the LVDC bus.

MVDC distribution for marine vessels mainly leads to the following benefits [122]:

- No need of phase angle synchronization when the ship's network has to be interconnected with the harbour grid.
- No need of large low-frequency transformers.
- Enabling reconfiguration after faults.
- Reduction of power system volume/weight by using high speed generators.
- Improvement of the power flow control, especially during transient and emergency conditions.
- Fuel saving, thanks to variable speed prime mover operation.

### 6.3 Transportation

Electrification of railways started with DC due to the availability of DC motors and their easy speed control [123]. For historical reasons, many railway lines, such as tramways, metro but also long-distance rail in some countries, stayed at DC until today. The voltage ranges up to a nominal value of 3 kV. DC railway lines are mostly supplied from AC through diode rectifiers, specified according to EN standards, [124], [125]. This classical approach is depicted in Fig. 6.5 a). Research activities explore possibilities to increase the DC voltage for railways and their advantages compared to the classical approach [93], see Fig. 6.5 b).

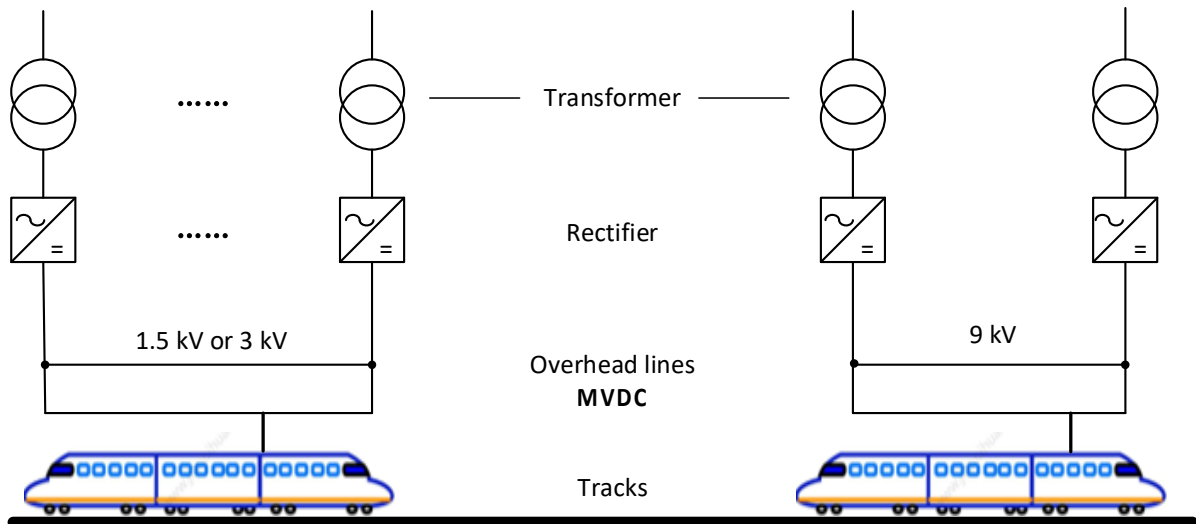


Figure 6.5 MVDC used in railway systems, a) classical approach; b) possible future approach [93].

Fig. 6.6 presents a proposed VSC-based MVDC traction power supply system (TPSS) for electric traction as an alternative supply solution for high-speed railways (HSRs) [126]. Compared to the existing 25-kV AC railway electrification system in Europe, the power quality problems, such as unbalance and harmonic distortion, will be substantially reduced by utilizing a VSC-based MVDC traction system. The DC system is fed from the bulk AC power system with VSC-based self-commutated power electronic devices (e.g., IGBTs or IGCTs). The railway infrastructure truly becomes a multi-terminal MVDC super-grid, which is a geographically distributed DC bus feeding multiple mobile loads. This proposed arrangement offers several benefits ranging from simpler rolling stock layouts, cost-effective railway infrastructure, higher reliability and modularity, more friendly addition to the AC grid and new business opportunities for the railway system operator [126]. Modern traction systems are based on induction motors, which are fed through IGBT based VSCs sharing a common DC bus.

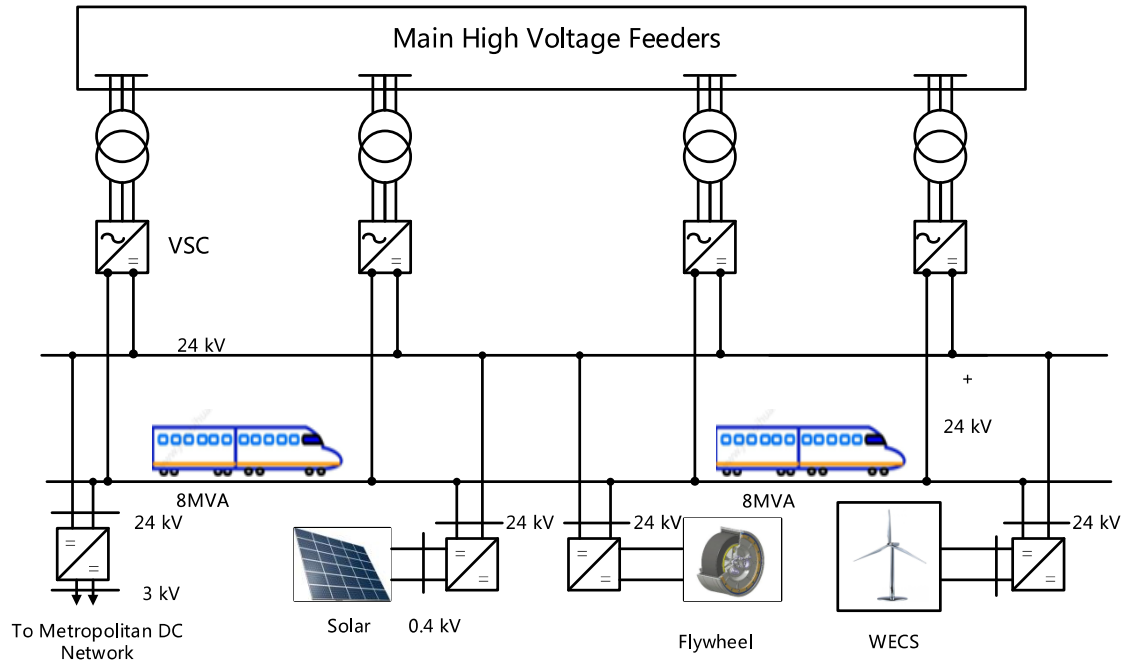


Figure 6.6 A VSC-based MVDC traction power supply system [126].

The rated DC voltage of this trunk network could lie between 15 kV and 25 kV (as shown in Fig. 6.7), considering the power flows limit. This single catenary is fed from the AC transmission grid through a number of equally spaced substations, designed in such a way that voltage drops are acceptable in case of single contingency. Each substation will be equipped with multi-level VSCs. On the AC side, the VSC can inject or absorb reactive power, while it is also capable of controlling either the exchanged active power or the DC voltage.

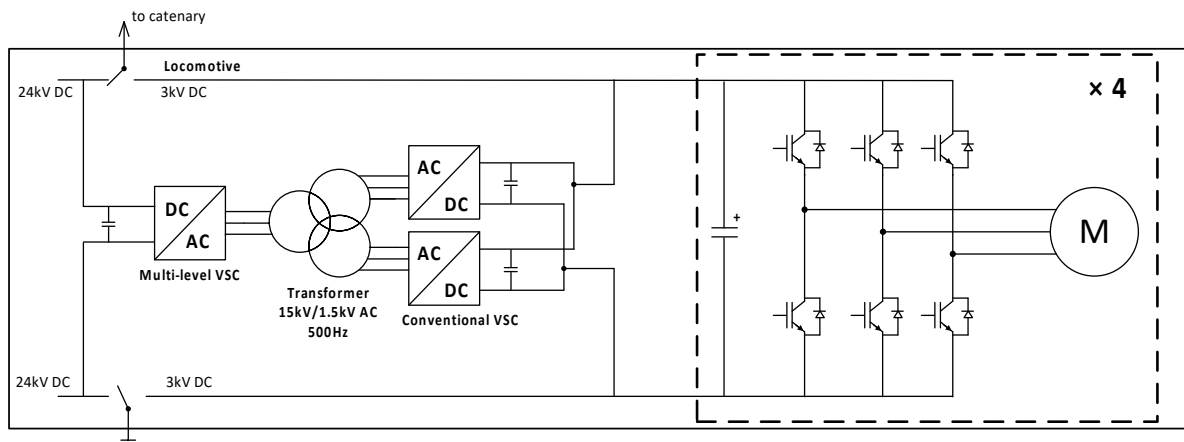


Figure 6.7 Dual-voltage locomotive for 24 kV and 3 kV DC catenary voltages [126].

Inside or around large cities, where short-distance trains and trams coexist, a lower DC voltage (e.g., 3 kV DC) catenary will be preferable, which can be connected through bidirectional DC DC links to the higher voltage trunk catenary. Furthermore, the full DC railway system provides a physically distributed bus to which scattered renewable generation can be more easily connected than in the AC traction power supply system [126]. There is no actual or demonstration project exist. However, the concept of MVDC TPSS, considering the number of DC components (PV, BESS, EV, etc.), may be possible in the near future.

## 6.4 Microgrids at Mine Sites

Mine sites are often located far away from populated areas, where mineral resources are abundant,

but seldom is there a large and well-established grid infrastructure. A recent study [127] proposes a secure and reliable power supply for operating sensitive mining loads and equipment efficiently and reliably through an MVDC microgrid. In the proposed microgrid, various local DER are considered, including photovoltaic arrays, wind turbines, a fuel-cell stack, an energy storage system, and mobile diesel generators. Fig. 6.8 shows a simplified schematic of an islanded MVDC microgrid at the mine site.

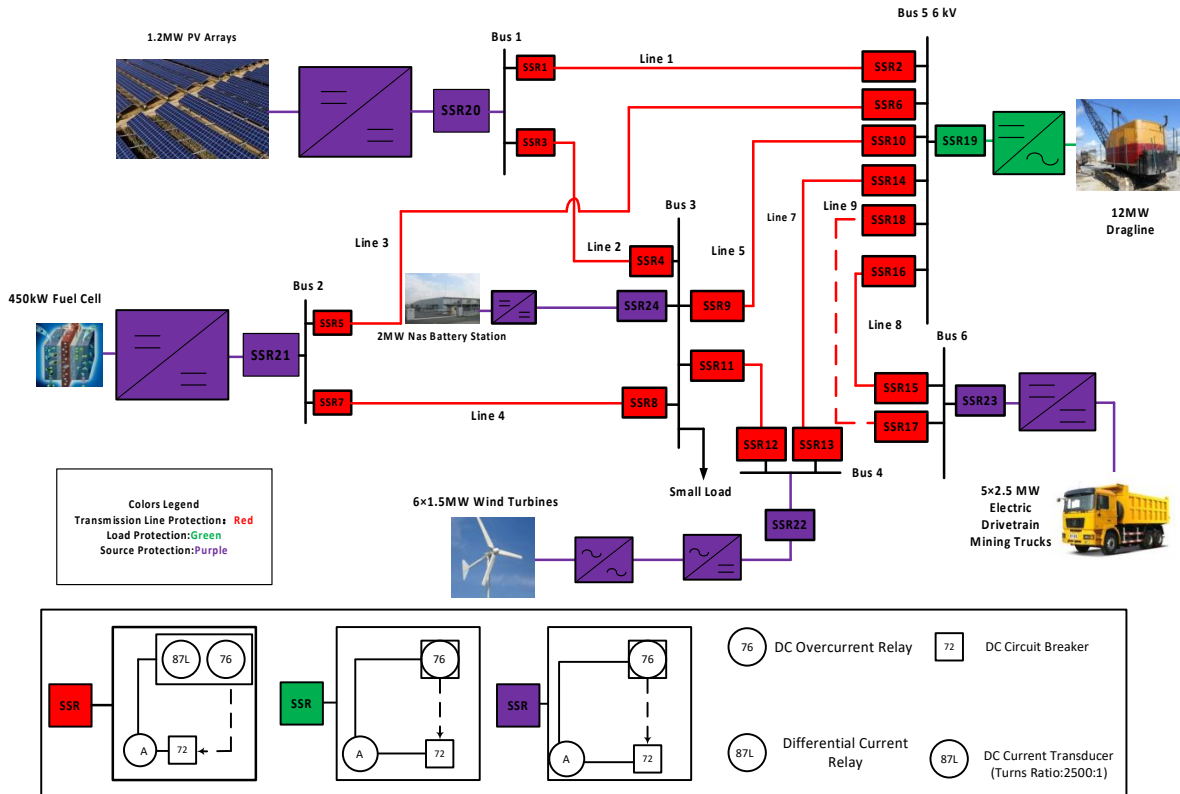


Figure 6.8 The schematic of an islanded MVDC microgrid at the mine site [127].

The proposed MVDC microgrid comprises a diverse set of distributed energy and storage resources such as PV arrays, wind turbines, a fuel-cell stack, a battery energy storage system, and mobile diesel generators. The microgrid makes the use of DC-bus signalling to control the power drawn from the fuel-cell stack, the energy storage system, and diesel generators for maintaining a constant DC-bus voltage (cf. Fig. 6.9). The NaS battery energy storage exploits a voltage hysteresis control scheme, whereas the fuel stack uses a state trajectory approximation strategy known as the hybrid control algorithm. The backup power sources of mobile diesel generators in the mining machinery are also included.

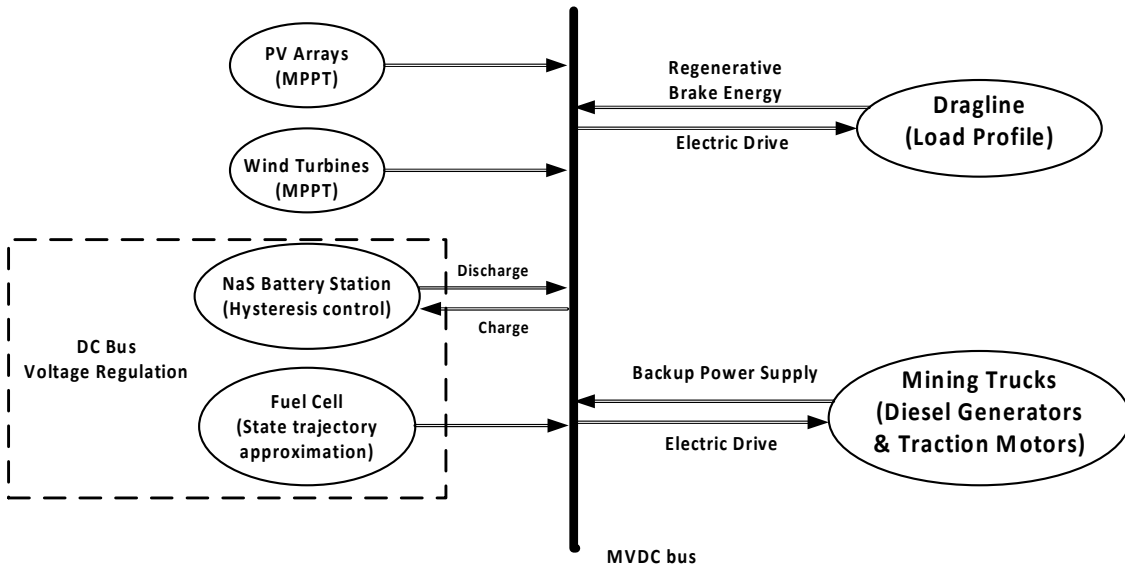


Figure 6.9 Block diagram of the control strategy and the power flow [127].

## 7 Summary and Outlook

Power electronics will play a key role in the energy systems of the future with multiple functionalities. An important area has been identified in the distribution networks for an increasing uptake of low carbon technologies. With the intermittent nature associated with renewable resources (such as solar and wind), the evolving network topologies and the changing role of an active distribution system operator, enhanced co-ordination and management are required. The engineering challenges associated with integrating the unprecedented level of distributed renewable generations can include but are not limited to: (i) the unpredictable power flow from the embedded generation; (ii) imbalance of energy demand between the 3-phases of AC supply; (iii) wide voltage angle deviation and/or different grounding concepts can prevent the connection between key circuits; (iv) voltage control at both transmission and distribution level; and power quality.

MVDC distribution systems will be important to applications of the power electronics devices. They will be deployed at the renewable sector to fulfil the requirements set out in the grid code or connection codes, such as the reactive power control (and the voltage control) on the connected busbar. With the help of MVDC distribution networks, power flow can be controlled in a wide range of conditions and made possible to implement widely. The requirement to maintain a secure, reliable and economical MVDC distribution network has seen increasing activities in both engineering developments, such as hardware design (e.g. new topology of the converter; solid-state transformer); and commercial innovation, such as the planning and design of MVDC networks and the integrated function of a synchronous condenser and STATCOM to provide frequency support. Therefore, it is very likely that MVDC distribution systems will be an integral section of power systems in the near future.

In addition to the ongoing engineering and commercial innovation in MVDC distribution systems, there are still challenges prevailing over their widespread application in the power systems domain. The challenges associated with the proliferation of power electronic devices in distribution grids can include but are not limited to: (i) converter topology suitable for different voltage levels in the distribution grids; (ii) the selection of passive (inductors, capacitors and resistors) and power electronic components, with respect to size and power density; selection of suitable converters based on application and voltage level; (iii) reliability of the power electronic and its associated components; (iv) capital cost, associated protection and control systems and the efficiency and power losses related to MVDC networks. However, the ongoing efforts from the industry and academia will accelerate the deployment of MVDC distribution systems in the future.

## Acknowledgements

Thanks to all members and corresponding members for their participation and contributions. Special thanks to Stephan Rupp, Philippe Maibach, Tapan Manna, Xiaohui Wang, Piotr Dworakowski, Ritwik Majumder, Staffan Norrga, Chuang Liu, Peter Lürkens and Matteo Corti for their hard work and valuable contributions. Thanks to Wei Liu and Gayan Abeynayake for the strong support for the technical chapters. Thanks to David Corbet and Zhao Ma, for the participation and valuable comments to the technical brochure. Thanks to Samuel Jupe for proofreading the final draft of the technical brochure. Thanks to Gen Li and Tibin Joseph for the coordination and organisation of the activities of this working group. Thanks to Gen Li for finishing the editing and proofreading of the technical brochure.

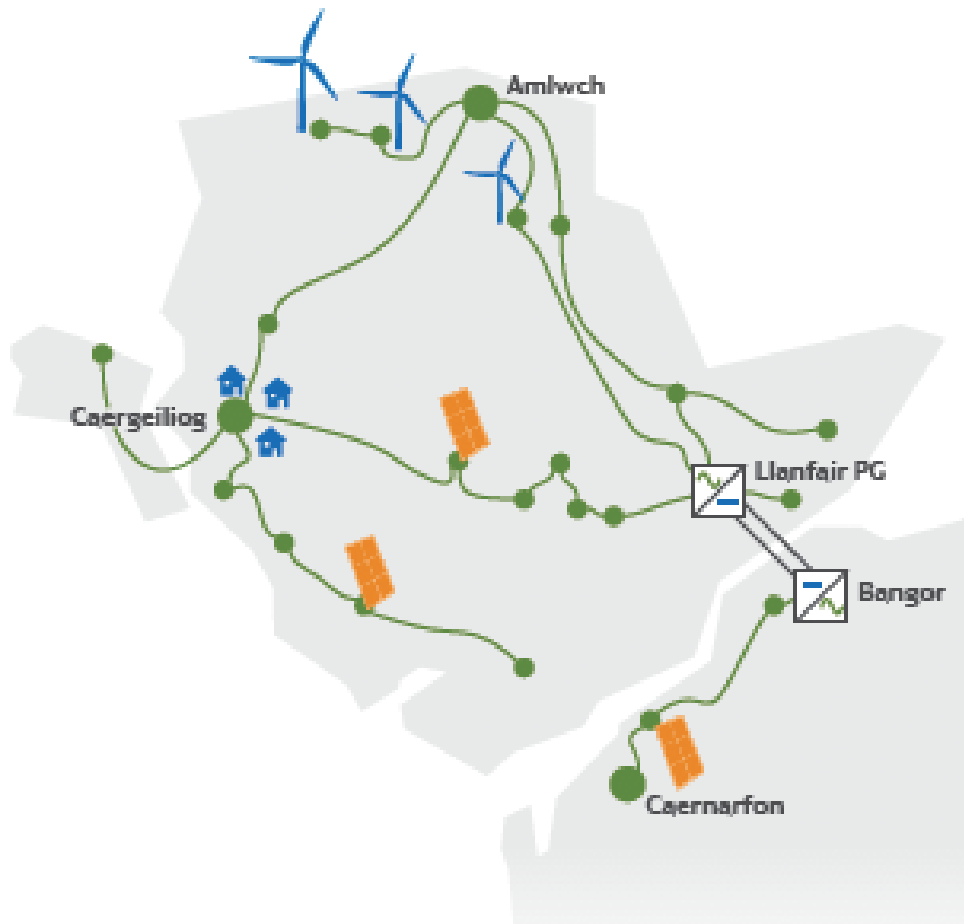
## Appendix A List of Abbreviations

BtB	Back-to-back
DAB	Dual active bridge
DER	Distributed energy resources
DG	Distributed generation
DCCB	DC circuit breaker
DNO	Distribution Network Operator
HVDC	High voltage direct current
IGBT	insulated-gate bipolar transistor.
LCC	Line commuted converter
LVDC	Low voltage direct current
MMC	Modular multilevel converter
MVAC	Medium voltage alternating current
MVDC	Medium voltage direct current
NPC	Neutral point clamped
PtP	Point-to-point
PV	Photovoltaic
SM	Sub-module
TB	Technical brochure
TCO	Total cost of ownership
VSC	Voltage source converter
XLPE	Cross-linked polyethylene

## Appendix B Case Studies

### ANGLE DC MVDC link

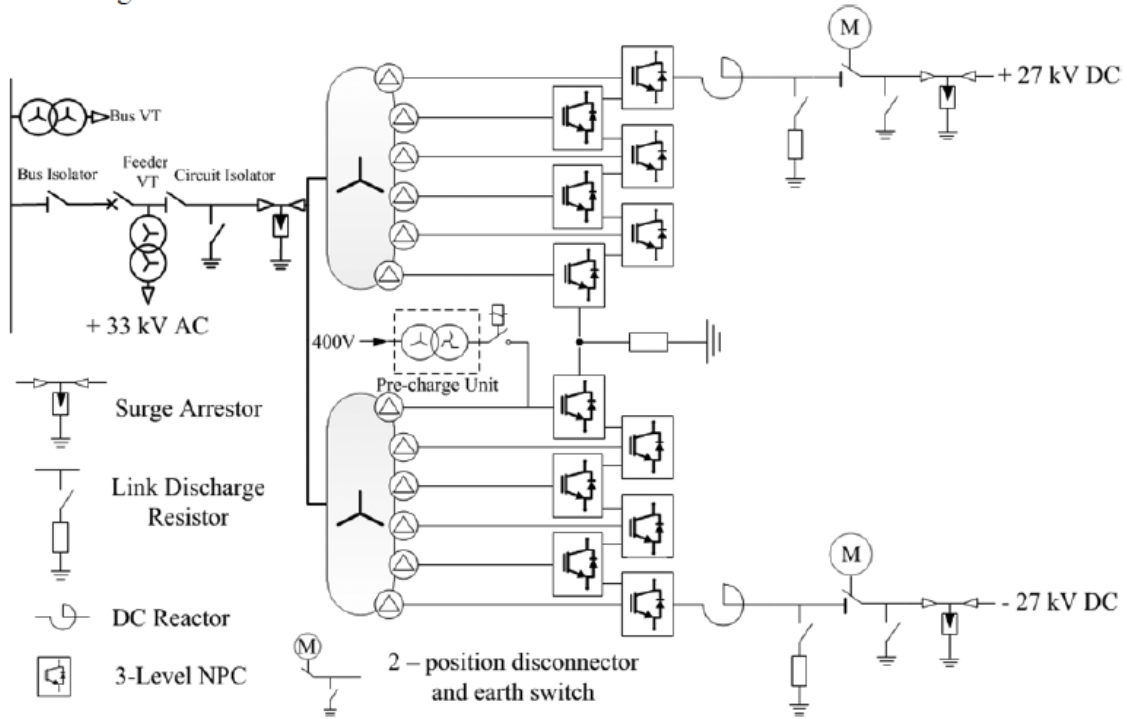
ANGLE DC is an innovative project which converts two existing 33 kV AC lines between the island of Anglesey (Llanfair Station) and the Welsh mainland (Bangor Station) into DC operation as shown in **Fig. D.1**. The project was constructed by SP Energy Networks under the 2015 UK Network Innovation Competition framework. The project is the first of its kind in the UK in converting existing AC lines to DC operation, aiming to increase the power capacity of the lines. Through the conversion to DC operation, the power capacity of the existing lines will be increased by 23%. In this section, configurations and simulations of the ANGLE DC project will be given.



App Figure D.1 - Angle DC project.

### System configurations

The configuration of the MVDC link is shown in **Fig. D.2**. It is configured as a symmetrical monopole system. Each pole is built up of 6 three-level neutral point clamped (NPC) converters, which are connected in series. The rated DC link voltage is  $\pm 27$  kV. The MVDC link is connected to each 33 kV AC network via two 33/2.1 kV interface transformers. Each transformer is rated at 17 MVA and at the LV side, each three-phase winding is rated at 2.85 MVA. The total rated power rating of the ANGLE DC project is 34 MVA.

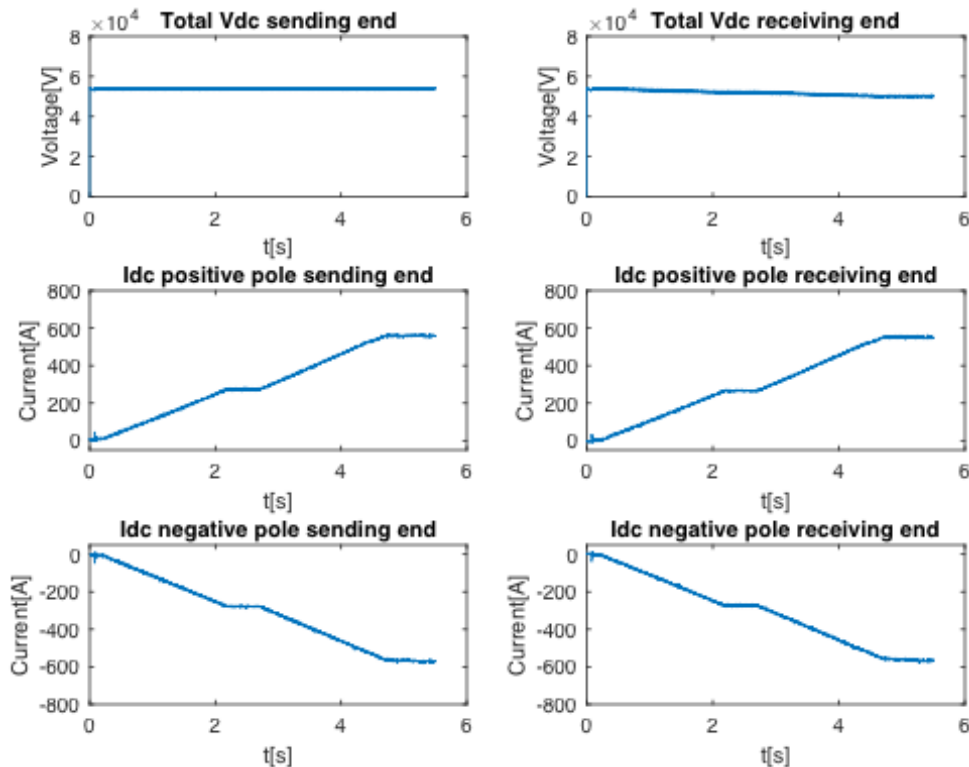


App Figure D.2 - System configuration of the ANGLE-DC project with three-level NPC converters.

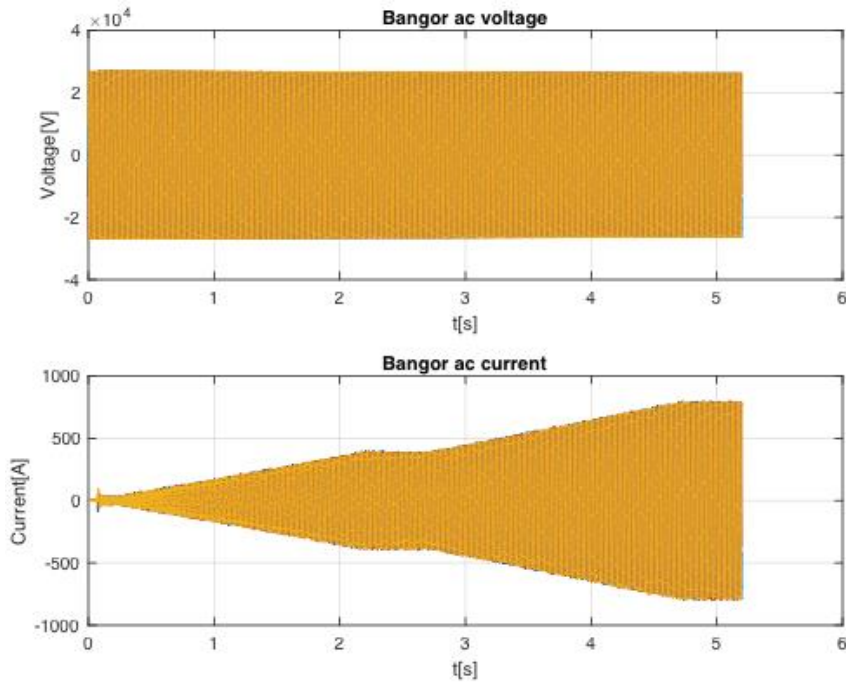
### Simulation results

(1) Power increase from 0 to 100%

Fig. D.3 shows the DC voltages and currents under normal operation. As shown in the figure, the total DC link voltage is 54 kV (i.e.  $\pm 27$  kV). The DC link current increase from 0 to the full power rating (i.e. 564 A). Therefore, the total power transferred is around 30.5 MW when full power rating is achieved. Fig. D.4 shows the AC voltages and currents at the Bangor station. From the figure, it can be seen that with the power increasing, the AC side currents are also increasing at the same time. Normal operation is illustrated in this case study.



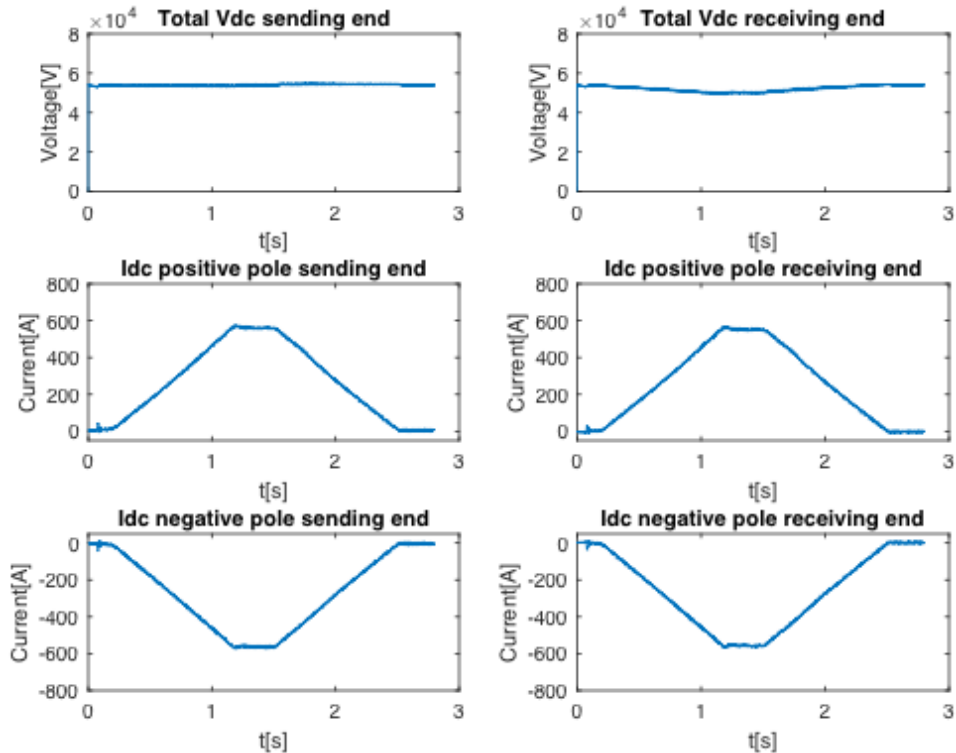
App Figure D.3 - DC voltages and currents with power flow increasing from 0 to 100%.



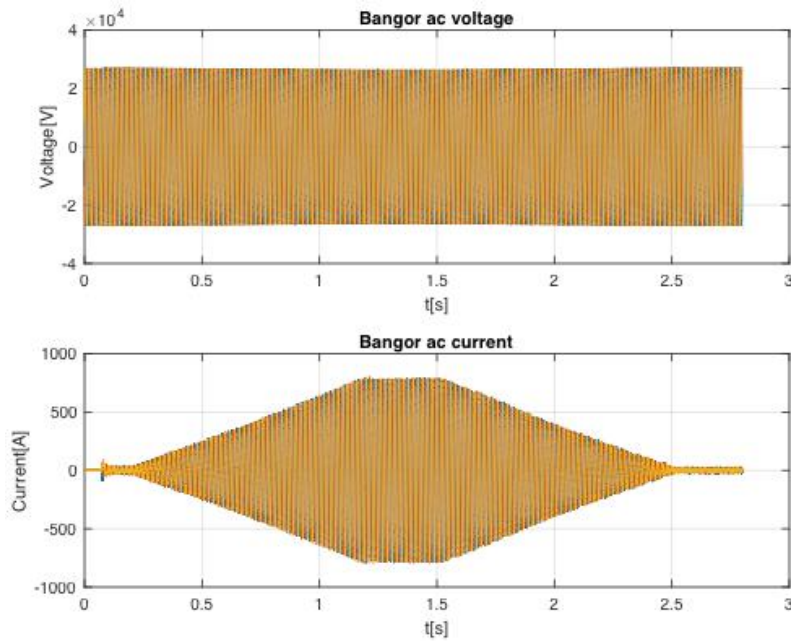
App Figure D.4 - AC voltages and currents with power flow increasing from 0 to 100%.

(2) Ramp change of power from 0 to 100% to 0

Fig. D.5 shows the DC voltages and currents when the power flow is under a ramp change. As shown in the figure, the power flow increases from 0 to 100% within 1 second and the DC link voltage stays constant, which can ensure a stable power transformation. Fig. D.6 shows the AC voltages and currents at the Bangor station. From the figure, it can be seen that with the power increasing, the AC side current is also changing. At the same time the AC side voltages are within its normal operating range. These simulation results show the capability of the MVDC link in regulating power flow rapidly. In real application conditions, the regulating of power flow will follow the dispatching information received.



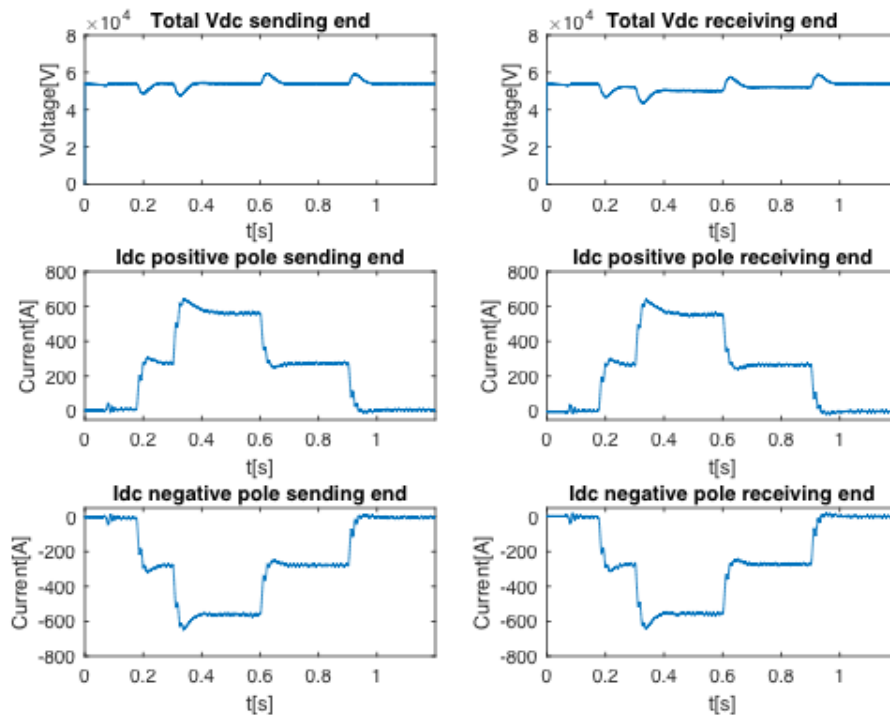
App Figure D.5 - DC voltages and currents with ramp change of power from 0 to 100% to 0.



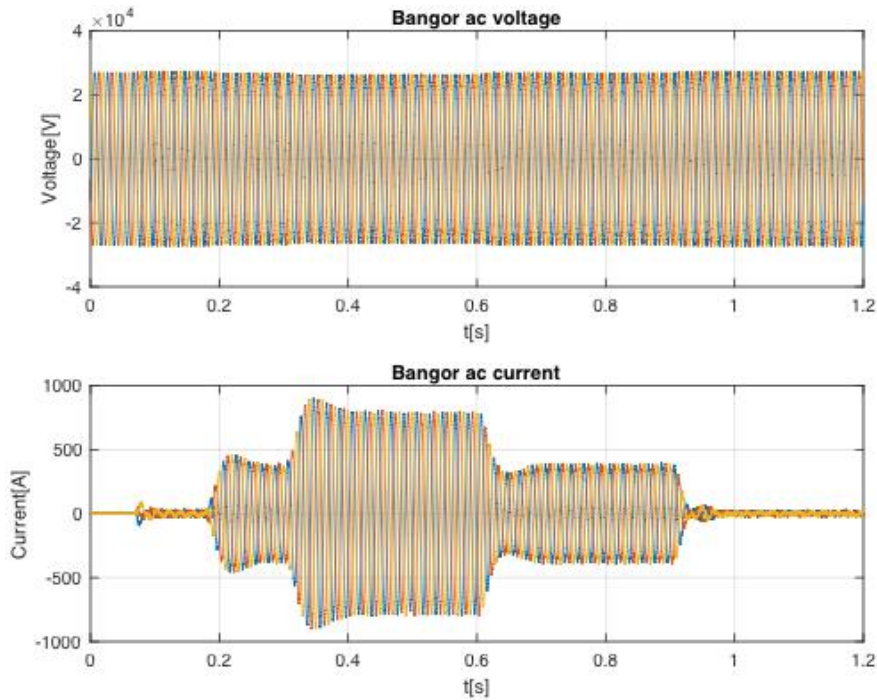
App Figure D.6 - AC voltages and currents with ramp change of power from 0 to 100% to 0.

(3) Step change of power

**Fig. D.7** shows the DC voltages and currents when the power undergoes a step change. As shown in the figure, the power experiences a 50% positive step change at around  $t = 0.2$  s and  $0.3$  s and a negative 50% step change at  $t = 0.6$  s and  $0.9$  s. The DC link voltages experience transient processes when the step change of power flow occurs. One of the reasons is that the inductance in the DC link will generate voltage drop or overshoot when experiencing  $di/dt$ . The transient processes will end when the  $di/dt$  become stable. **Fig. D.8** shows the AC voltages and currents at the Bangor station. From the figure, it can be seen that when a step change of power flow occurs, the AC side current also changes. At the same time the AC side voltages are within its normal operating range. This simulation results shows the capability of the MVDC link in regulating power flow even under step change conditions. In the real application conditions, the regulating of power flow will follow the dispatching information received.



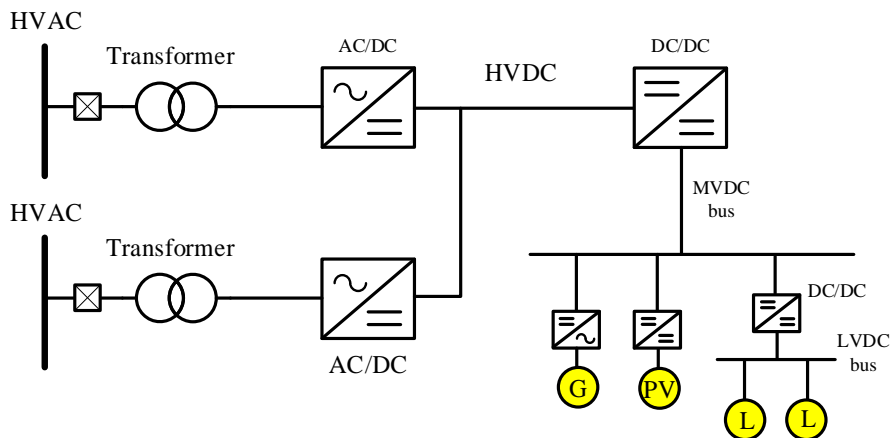
App Figure D.7 - DC voltages and currents with step change of power flow.



App Figure D.8 - AC voltages and currents with step changes of power flow.

### Interconnections of MVDC to HV and LV systems

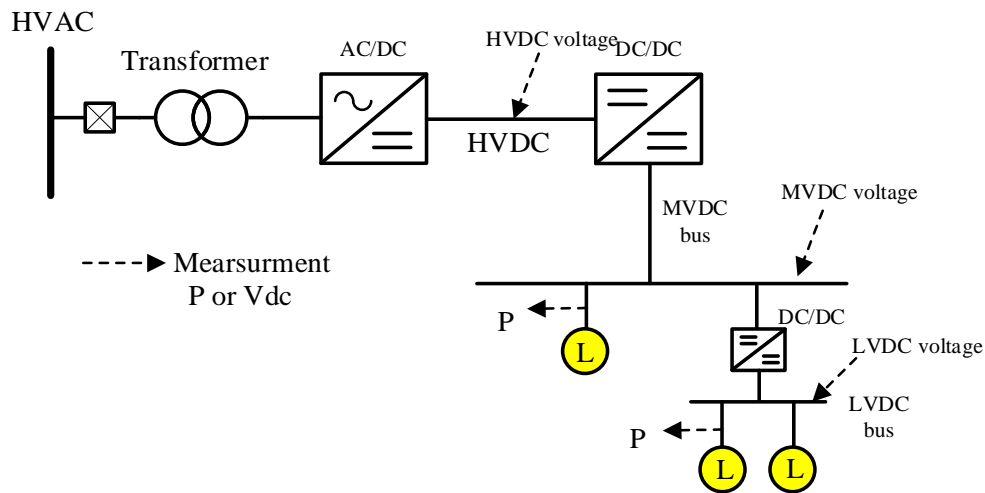
HVAC and HVDC systems are already standard options for power grids. With the development of power electronics technology, distributed power generation and consumption, MVDC technologies are attracting more and more attention. MVDC grids allow for interconnection between AC and DC grids and to both HV and LV segments. Therefore, with MVDC technologies, power levelling between adjacent transmission and distribution grid areas becomes possible. Fig. D.9 shows one example of interconnections of MVDC to HV and LV system. A DC-DC converter is connected to the HVDC link, which aims to step-down the level of DC voltage to form a MVDC bus. By such a conversion, MV loads or MV generation can be connected to the MVDC bus. By adding a DC-DC converter, the voltage can be further stepped-down to the LV level, which supplies the LV loads directly.



App Figure D.9 - Interconnections of MVDC to HV and LV systems.

### System configurations

Cases studies will be given in this section to show the feasibility of interconnections of MVDC to HV and LV systems. To simplify the system and focus on the power conversion, MVDC and LVDC loads are added to their buses directly. The configuration of the simulated system is given in Fig. D.10. An MMC based HVDC converter is used to form a HVDC link. By adding a solid-state DC-DC converter, the HVDC link is stepped-down to the MV level. The MVDC bus supplies an MV load. Furthermore, an LV system is connected to the MVDC bus through a DC-DC converter.

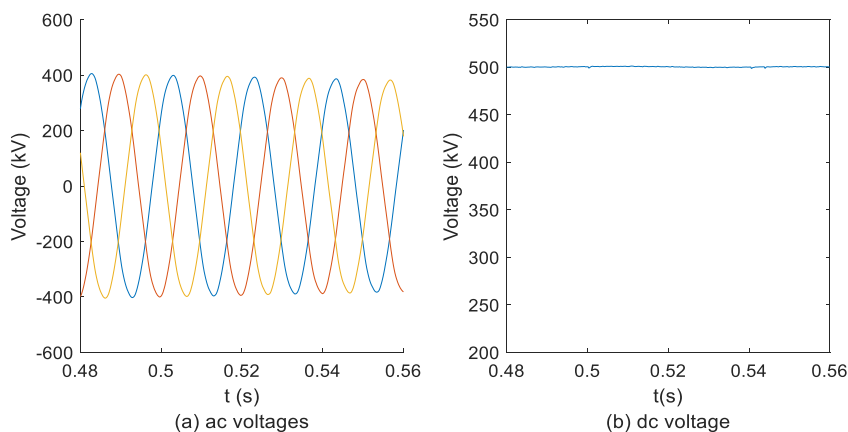


App Figure D.10 - Configurations of the DC system.

### Simulation results

#### (1) Connections of HVAC to HVDC

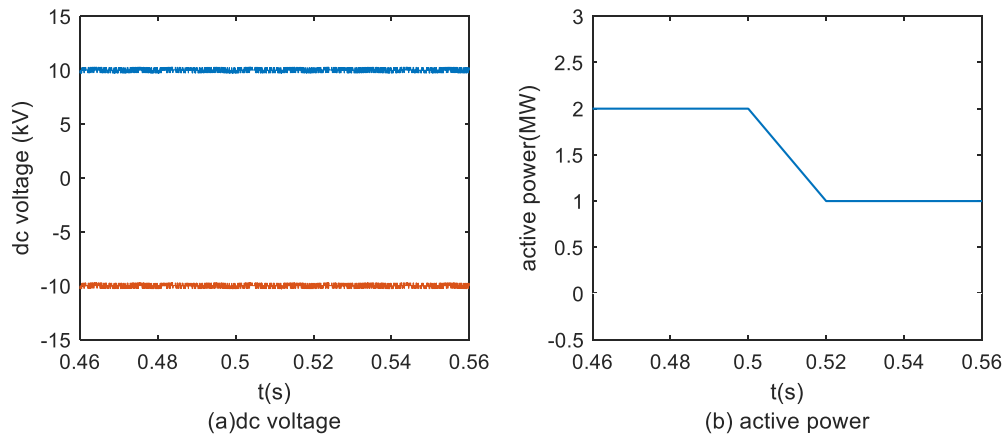
Fig. D.11 shows the AC voltages of the HVAC system and DC voltage of the HVDC system. AC voltages is shown in Fig. D.11(a). The MMC converter is connected to a 500 kV AC grid. In this case study, the MMC converter is regulating the dc link voltage. The DC link voltage is  $\pm 250$  kV. The total DC link voltage is 500 kV as shown in Fig. D.11(b).



App Figure D.11 - Waveforms of AC voltages and DC.

#### (2) Conversion of HVDC to MVDC

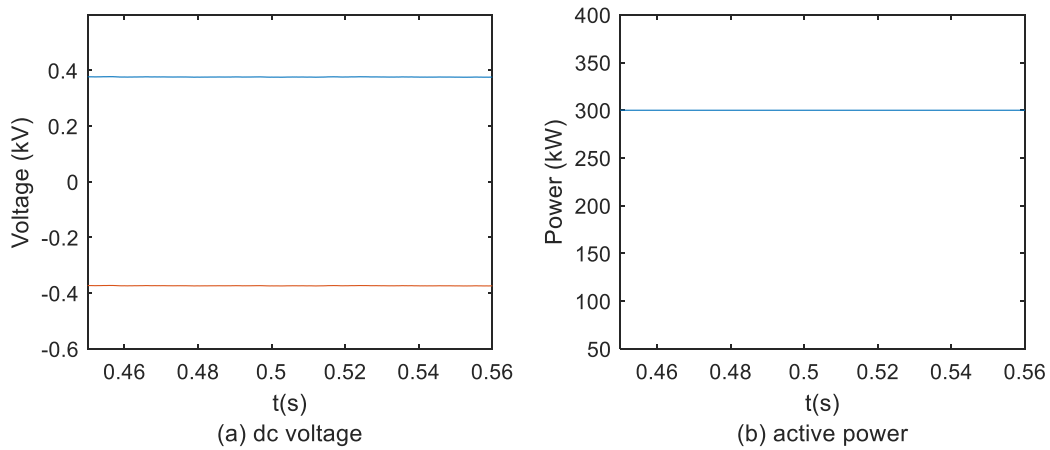
Fig. D.12 shows the DC voltages of and active power of the MVDC system. The DC voltage of the MVDC system is  $\pm 10$  kV. The waveform is shown in Fig. D.12(a). Thanks to the isolated transformer, the step-down ratio of the DC-DC converter is 25:1 (from  $\pm 250$  kV to  $\pm 10$  kV). The active power consumed by the load is 2 MW at the initial stage. At  $t = 0.5$  s, the active power is regulated to 1 MW. The waveform is shown in Fig. D.12(b).



App Figure D.12 - Waveforms of DC voltages and active power of the MVDC systems.

(3) Conversion of MVDC to LVDC

Fig. D.13 shows the voltages of the LVDC system and active power. The DC voltage of the LVDC system is  $\pm 375V$ . The waveforms are shown in Fig. A.13(a). The step-down ratio of the DC-DC converter is around 27:1 (from  $\pm 10\text{ kV}$  to  $\pm 0.375\text{ kV}$ ). The active power consumed by the load is 300 kW. The waveform is shown in Fig. A.13(b).



App Figure D.13 - Waveforms of DC voltages and active power of the LVDC systems.

## References

- [1] J. Yu, Future medium voltage distribution applications of power electronics, [Online]. Available: <https://cigre.org.uk/uncategorized/future-medium-voltage-distribution-applications-of-power-electronics/>
- [2] CIGRE TB 793, Medium voltage direct current (MVDC) grid feasibility study, 2020.
- [3] M. Salah Khalil, "International research and development trends and problems of HVDC cables with polymeric insulation," in IEEE Electrical Insulation Magazine, vol. 13, no. 6, pp. 35-47, Nov.-Dec. 1997.
- [4] U. Riechert, M. Eberhardt, J. Kindersberger and J. Speck, "Breakdown behaviour of polyethylene at dc voltage stress," ICSD'98. Proceedings of the 1998 IEEE 6th International Conference on Conduction and Breakdown in Solid Dielectrics (Cat. No.98CH36132), 1998, pp. 510-513.
- [5] U. Riechert, J. Kindersberger and J. Speck, "Effects of short-time voltage drops and polarity reversals on breakdown behaviour of cross-linked polyethylene," 1999 Eleventh International Symposium on High Voltage Engineering, 1999, pp. 216-219 vol.4.
- [6] S. Kikuchi, H. Mori, A. Mori, T. Sakurai and Y. Yagi, "Performance of an optimized XLPE material for controlling space charge in HVDC transmission cable system," 2017 IEEE Conference on Electrical Insulation and Dielectric Phenomenon (CEIDP), 2017, pp. 704-707, doi: 10.1109/CEIDP.2017.8257546.
- [7] Schichler, U., & Buchner, A. A. (2018). Anwendung von extrudierten AC-Kabeln für die Mittelspannungs-Gleichstromübertragung (MGÜ). Paper presented at VDE-Fachtagung Hochspannungstechnik 2018, Berlin, Germany.
- [8] Buchner, A. & Schichler, U. 2019, 'Application of Extruded MVAC Cables for DC Power Transmission', Contribution to Jicable 2019, Versailles, France, 23/06/19 - 27/06/19.
- [9] G. Chen, M. Hao, Z. Xu, A. Vaughan, J. Cao and H. Wang, "Review of high voltage direct current cables," in CSEE Journal of Power and Energy Systems, vol. 1, no. 2, pp. 9-21, June 2015,
- [10] J. L. Auge, C. Laurent, D. Fabiani and G. C. Montanari, "Investigating dc polyethylene threshold by space charge. Current and electroluminescence measurements," in IEEE Transactions on Dielectrics and Electrical Insulation, vol. 7, no. 6, pp. 797-803, Dec. 2000.
- [11] Giovanni Mazzanti; Massimo Marzinotto, "Space Charge in HVDC Extruded Insulation: Storage, Effects, and Measurement Methods," in Extruded Cables for High-Voltage Direct-Current Transmission: Advances in Research and Development, IEEE, 2013, pp.99-207.
- [12] W. Li et al., "State of the Art of Researches and Applications of MVDC Distribution Systems in Power Grid," IECON 2019 - 45th Annual Conference of the IEEE Industrial Electronics Society, Lisbon, Portugal, 2019, pp. 5680-5685
- [13] L. Qu, et al., Planning and analysis of the demonstration project of the MVDC distribution network in Zhuhai, Frontiers in Energy, vol. 13, pp. 120-130, 2019.
- [14] First five-terminal flexible DC power distribution demonstration project. [Online]. Available: <http://www.sgcio.com/news/zbcg/97234.html>
- [15] X. Wang, R. Chen, J. Ge, T. Cao, F. Wang and X. Mo, "Application of AC/DC Distribution Network Technology Based on Flexible Substation in Regional Energy Internet," 2019 IEEE Innovative Smart Grid Technologies - Asia (ISGT Asia), Chengdu, China, 2019, pp. 4340-4345
- [16] NR's MVDC Solution,  $\pm 10$ kV JiangDong MVDC for optimizing distribution network, [Online]. Available: <https://www.nrec.com/en/web/upload/2019/05/14/1557822630997rxt25.pdf>
- [17] C. Liang, J. Mengmeng, H. Qiang, Y. Xiaodong and L. Fei, "Engineering Simulation Analysis and Demonstration Application of Multi-terminal DC Distribution System," 2018 International Conference on Power System Technology (POWERCON), Guangzhou, 2018, pp. 2343-2349
- [18] Y. Liu, X. Cao and M. Fu, "The Upgrading Renovation of an Existing XLPE Cable Circuit by Conversion of AC Line to DC Operation," in IEEE Transactions on Power Delivery, vol. 32, no. 3, pp. 1321-1328, June 2017.
- [19] G. Bathurst, G. Hwang and L. Tejwani, "MVDC - The New Technology for Distribution Networks," 11th IET International Conference on AC and DC Power Transmission, Birmingham, 2015, pp. 1-5.
- [20] P. Schavemaker and L. Sluis, Electrical Power System Essentials. 2008
- [21] P. Le Métayer, et al., "Break-even distance for MVDC electricity networks according to power loss criteria," EPE 2021, accepted for publication.

- [22] ANGLE-DC, 2015 Electricity Network Innovation Competition, Ofgem, [Online]. Available: <https://www.ofgem.gov.uk/ofgem-publications/97841/anglesubmission-pdf>
- [23] Network Equilibrium, Western Power Distribution, United Kingdom [Online]. Available: <https://www.westernpower.co.uk/innovation/projects/network-equilibrium>
- [24] L. Zhang, J. Liang, W. Tang, G. Li, Y. Cai and W. Sheng, "Converting AC Distribution Lines to DC to Increase Transfer Capacities and DG Penetration," in IEEE Transactions on Smart Grid, vol. 10, no. 2, pp. 1477-1487, March 2019
- [25] Voltage Source Converter (VSC) HVDC for Power Transmission-Economic Aspects and Comparison With Other AC and DC Technologies, CIGRE Brochure 492, WG B4.46, 2012.
- [26] H. Lotfi and A. Khodaei, "AC Versus DC Microgrid Planning," in IEEE Transactions on Smart Grid, vol. 8, no. 1, pp. 296-304, Jan. 2017.
- [27] C-C Huang, M-J Chen, Y-T Liao, and C-N Lu, "DC microgrid operation planning," 2012 International Conference on Renewable Energy Research and Applications (ICRERA), Nagasaki, pp. 1-7, 2012.
- [28] Z. Wu, P. Liu, W. Gu, H. Huang, and J. Han, "A bi-level planning approach for hybrid AC-DC distribution system considering N-1 security criterion," Appl. Energy, vol. 230, pp. 417–428, Nov. 2018.
- [29] S. Parhizi, H. Lotfi, A. Khodaei, and S. Bahramirad, "State of the Art in Research on Microgrids: A Review," IEEE Access, vol. 3, pp. 890–925, 2015.
- [30] B. Aluisio, S. Bruno, L. De Bellis, M. Dicorato, G. Forte, and M. Trovato, "DC-Microgrid Operation Planning for an Electric Vehicle Supply Infrastructure," Applied Sciences, vol. 9, no. 13, p. 2687, Jul. 2019.
- [31] A. Zidan, H. A. Gabbar, and A. Eldessouky, "Optimal planning of combined heat and power systems within microgrids," Energy, vol. 93, pp. 235–244, 2015.
- [32] J. Decuir and P. Michael, "Draft IEEE standard for DC microgrids for rural and remote electricity access applications," 2017 IEEE Conference on Technologies for Sustainability (SusTech), Phoenix, AZ, pp. 1-5, 2017.
- [33] G. Van den Broeck, Jeroen Stuyts, and Johan Driesen, "A critical review of power quality standards and definitions applied to DC microgrids," Applied Energy, Vol. 229, pp. 281-288, 2018.
- [34] T. S. Ustun, C. Ozansoy, and A. Zayegh, "Modeling of a centralized microgrid protection system and distributed energy resources according to IEC 61850-7-420," IEEE Trans. Power Syst., vol. 27, no. 3, pp. 1560–1567, Aug. 2012.
- [35] H. J. Laaksonen, "Protection principles for future microgrids," IEEE Trans. Power Electron., vol. 25, no. 12, pp. 2910–2918, Dec. 2010.
- [36] D. Zhou, H. Wang and F. Blaabjerg, "Mission Profile Based System-Level Reliability Analysis of DC/DC Converters for a Backup Power Application," IEEE Trans. Power Electron., vol. 33, no. 9, pp. 8030-8039, Sept. 2018.
- [37] K. Ma, M. Liserre, F. Blaabjerg, and T. Kerekes, "Thermal loading and lifetime estimation for power device considering mission profiles in wind power converter," IEEE Trans. Power Electron., vol. 30, no. 2, pp. 590–602, Feb. 2015.
- [38] FIDES Guide 2009 Edition, "A reliability methodology for electronic systems," 2010.
- [39] G. Abeynayake, G. Li, T. Joseph, J. Liang and W. Ming, "Reliability and Cost-oriented Analysis, Comparison and Selection of Multi-level MVdc Converters," in IEEE Transactions on Power Delivery, doi: 10.1109/TPWRD.2021.3051531.
- [40] J. Sun, "Impedance-based stability criterion for grid-connected inverters," IEEE Trans. Power Electron., vol. 26, no. 11, pp. 3075–3078, Nov. 2011.
- [41] L. Harnefors, X. Wang, A. G. Yepes, and F. Blaabjerg, "Passivity-based stability assessment of grid-connected VSCs - An overview," IEEE J. Emerg. Sel. Topics Power Electron., vol. 4, no. 1, pp. 116–125, Mar. 2016.
- [42] M. Quester, F. Loku, V. Yellisetti and R. Puffer, "Online Impedance Measurement of a Modular Multilevel Converter," 2019 IEEE PES Innovative Smart Grid Technologies Europe (ISGT-Europe), Bucharest, Romania, 2019
- [43] L. Harnefors, M. Bongiorno, and S. Lundberg, "Input-admittance calculation and shaping for controlled voltage-source converters," IEEE Trans. Ind. Electron., vol. 54, no. 6, pp. 3323–3334, Dec. 2007.
- [44] X. Wang, L. Harnefors, and F. Blaabjerg, "Unified impedance model of grid-connected voltage-source

- converters," *IEEE Trans. Power Electron.*, vol. 33, no. 2, pp. 1775–1787, Feb. 2018.
- [45] K. Sharifabadi, L. Harnefors, H.-P. Nee, S. Norrga, and R. Teodorescu, *Design, Control, and Application of Modular Multilevel Converters for HVDC Transmission Systems*. Chichester, U.K.: Wiley, 2016.
- [46] M. Beza, M. Bongiorno, and G. Stamatiou, "Analytical derivation of the ac-side input admittance of a modular multilevel converter with open- and closed-loop control strategies," *IEEE Trans. Power Del.*, vol. 33, no. 1, pp. 248–256, Feb. 2018.
- [47] J. Sun and H. Liu, "Sequence impedance modeling of modular multilevel converters," *IEEE J. Emerg. Sel. Topics Power Electron.*, vol. 5, no. 4, pp. 1427–1443, Dec. 2017.
- [48] L. Bessegato, K. Ilves, L. Harnefors and S. Norrga, "Effects of Control on the AC-Side Admittance of a Modular Multilevel Converter," *IEEE Transactions on Power Electronics*, vol. 34, no. 8, pp. 7206-7220, Aug. 2019
- [49] M. Amin and M. Molinas, "Small-Signal Stability Assessment of Power Electronics Based Power Systems: A Discussion of Impedance- and Eigenvalue-Based Methods," *IEEE Transactions on Industry Applications*, vol. 53, no. 5, pp. 5014-5030, Sept.-Oct. 2017
- [50] G. Pinares and M. Bongiorno, "Modeling and Analysis of VSC-Based HVDC Systems for DC Network Stability Studies," in *IEEE Transactions on Power Delivery*, vol. 31, no. 2, pp. 848-856, April 2016, doi: 10.1109/TPWRD.2015.2455236.
- [51] D. Xue, J. Liu, Z. Liu, Y. Tu and T. Liu, "Modeling and Analysis of DC Terminal Impedance of Voltage-Source Converters With Different Control Modes," in *IEEE Transactions on Power Electronics*, vol. 35, no. 6, pp. 5883-5896, June 2020, doi: 10.1109/TPEL.2019.2953118.
- [52] Stamatiou, G., Beza, M., Bongiorno, M. and Harnefors, L. (2017), Analytical derivation of the DC-side input admittance of the direct-voltage controlled modular multilevel converter. *IET Gener. Transm. Distrib.*, 11: 4018-4030. <https://doi.org/10.1049/iet-gtd.2017.0278>
- [53] K. Ji, H. Pang, J. Yang and G. Tang, "DC Side Harmonic Resonance Analysis of MMC-HVDC Considering Wind Farm Integration," in *IEEE Transactions on Power Delivery*, vol. 36, no. 1, pp. 254-266, Feb. 2021, doi: 10.1109/TPWRD.2020.2982276.
- [54] Z. Li et al., "Accurate Impedance Modeling and Control Strategy for Improving the Stability of DC System in Multiterminal MMC-Based DC Grid," in *IEEE Transactions on Power Electronics*, vol. 35, no. 10, pp. 10026-10049, Oct. 2020, doi: 10.1109/TPEL.2020.2975619.
- [55] M. Nahalparvari, M. Asoodar, L. Bessegato, S. Norrga and H. -P. Nee, "Modeling and Shaping of the DC-Side Admittance of a Modular Multilevel Converter Under Closed-Loop Voltage Control," in *IEEE Transactions on Power Electronics*, vol. 36, no. 6, pp. 7294-7306, June 2021, doi: 10.1109/TPEL.2020.3041387.
- [56] R. T. Pinto, S. F. Rodrigues, P. Bauer and J. Pierik, "Comparison of direct voltage control methods of multi-terminal DC (MTDC) networks through modular dynamic models", *Proceedings of the 2011 14th European Conference on Power Electronics and Applications*, Birmingham, 2011, pp. 1-10.
- [57] P. Simiyu, "A Review of the DC Voltage Coordinated Control Strategies for Multi-terminal VSC MVDC Distribution Network. *The Journal of Engineering*, 2018.
- [58] P. Simiyu, A. Xin, L. Bibaya, V. Ndiyishimiye, G. Adwek and G. T. Bitew, "Modelling and Control of Multi-terminal MVDC Distribution Network," 2018 *International Conference on Power System Technology (POWERCON)*, Guangzhou, 2018, pp. 1-13.
- [59] S. Lin, L. Wang, D. Mu, L. Liu, K. Liao and Z. He, "Research on starting-up control strategy of VSC-HVDC system," in *IET Renewable Power Generation*, vol. 12, no. 16, pp. 1957-1965, 10 12 2018.
- [60] Ma Z, Jiang W. An adaptive droop voltage control for DC microgrid systems, *The 26th Chinese Control and Decision Conference (2014 CCDC)*. IEEE, 2014: 4512-4517.
- [61] N. R. Chaudhuri and B. Chaudhuri, "Adaptive Droop Control for Effective Power Sharing in Multi-Terminal DC (MTDC) Grids," *IEEE Transactions on Power Systems*, vol. 28, no. 1, pp. 21-29, Feb. 2013.
- [62] CIGRE B4.56 "Guidelines for the preparation of "connection agreements" or "grid codes" for multi-terminal DC schemes and DC grids", *Electra*, June 2016, pp. 53-55.
- [63] W. Leterme, I. Jahn, P. Ruffing, K. Sharifabadi, and D. Van Hertem, "Designing for High-Voltage dc Grid Protection: Fault Clearing Strategies and Protection Algorithms," *IEEE PES Magazine*, vol. 17, no. 3, pp. 73-81, May/June 2019
- [64] IEEE Std 1709TM-2018, IEEE Recommended Practice for 1 kV to 35 kV Medium-Voltage DC Power

Systems on Ships; IEEE, ISBN 978-1-5044-5201-4.

- [65] IEC Draft Specification on MicroGrids, Technical Requirements – Protection and Dynamic Control, IEC TS 62898-3-1 ED1, April 2019.
- [66] S. Fu, et al. "Research in system design of AC and DC distribution network based on flexible substation," *Journal of Physics: Conference Series*, vol. 1633, May 2020.
- [67] W. Li et al., "State of the Art of Researches and Applications of MVDC Distribution Systems in Power Grid," *IECON 2019 - 45th Annual Conference of the IEEE Industrial Electronics Society*, Lisbon, Portugal, 2019, pp. 5680-5685
- [68] M Babaei et al., "A Survey on Fault Detection, Isolation, and Reconfiguration Methods in Electric Ship Power Systems", *IEEE Access*, March 2018
- [69] I. Jahn, N. Johannesson, and S. Norrga, "Survey of Methods for Selective DC Fault Detection in MTDC Grids," in *Proc. IET ACDC*, Manchester, 14-16 Feb. 2017,
- [70] CIGRE TB 827, DC-DC converters in HVDC grids and for connections to HVDC systems, 2021.
- [71] C. Barker, C. Davidson, D. Trainer, and R. Whitehouse, "Requirements of DC-DC Converters to facilitate large DC Grids," *CIGRE, SC B4 HVDC and Power Electronics*, 2012 Paris Session
- [72] J. D. Páez, D. Frey, J. Maneiro, S. Bacha and P. Dworakowski, "Overview of DC–DC Converters Dedicated to HVdc Grids," in *IEEE Transactions on Power Delivery*, vol. 34, no. 1, pp. 119-128, Feb. 2019.
- [73] G. P. Adam, I. A. Gowaid, S. J. Finney, D. Holliday, and B. W. Williams, "Review of dc–dc converters for multi-terminal HVDC transmission networks," *IET Power Electronics*, vol. 9, no. 2, pp. 281–296, 2016
- [74] S. Cui, N. Soltau and R. W. De Doncker, "A High Step-Up Ratio Soft-Switching DC–DC Converter for Interconnection of MVDC and HVDC Grids," in *IEEE Transactions on Power Electronics*, vol. 33, no. 4, pp. 2986-3001, April 2018
- [75] P. Le Métayer, P. Dworakowski, and J. Maneiro, "Unidirectional thyristor-based DC-DC converter for HVDC connection of offshore wind farms," *EPE 2020*
- [76] G. J. Kish, "On the Emerging Class of Non-Isolated Modular Multilevel DC–DC Converters for DC and Hybrid AC–DC Systems," in *IEEE Transactions on Smart Grid*, vol. 10, no. 2, pp. 1762-1771, March 2019.
- [77] Jovcic, Dragan, P. Dworakowski, G. J. Kish, Ar Jamshidi Far, A. Nami Abb, A. Darbandi, and X. Guillaud. "Case Study of Non-Isolated MMC DC-DC Converter in HVDC Grids." (2019).
- [78] R. W. De Doncker, D. M. Divan, and M. H. Kheraluwala, "A three-phase soft-switched high power density DC/DC converter for high power applications," in *Conference Record of the 1988 IEEE Industry Applications Society Annual Meeting*, 1988, pp. 796–805 vol.1.
- [79] T. Luth, M. M. C. Merlin, T. C. Green, F. Hassan, and C. D. Barker, "High-frequency operation of a dc/ac/dc system for HVDC applications," *IEEE Trans. Power Electron.*, vol. 29, no. 8, pp. 4107–4115, Aug. 2014.
- [80] S. Cui, J. Hu, and R. W. De Doncker, "Fault-tolerant operation of a TLC-MMC hybrid dc-dc converter for interconnection of MVDC and HVDC grids," in *IEEE Trans. on Power Electronics*, vol. 35, pp. 83-93, 2019.
- [81] J. Hu, S. Cui, and R. W. De Doncker, "DC fault ride-through of a three-phase dual-active bridge converter for DC grids", in *IEEE International Power Electronics Conference (IPEC-ECCE Asia)*, 2018.
- [82] C. Barker, C. Davidson, D. Trainer, and R. Whitehouse, "Requirements of DC-DC Converters to facilitate large DC Grids," *CIGRE, SC B4 HVDC and Power Electronics*, 2012 Paris Session.
- [83] F. C. Schwarz and J. B. Klaassens, "A Controllable 45-kW Current Source for DC Machines," *IEEE Transactions on Industry Applications*, vol. IA-15, no. 4, pp. 437–444, Jul. 1979.
- [84] J. F. Lazar and R. Martinelli, "Steady-state analysis of the LLC series resonant converter," in *APEC 2001. Sixteenth Annual IEEE Applied Power Electronics Conference and Exposition (Cat. No.01CH37181)*, vol. 2, pp. 728–735, 2001.
- [85] L. H. Mweene, C. A. Wright, and M. F. Schlecht, "A 1 kW 500 kHz front-end converter for a distributed power supply system," *IEEE Transactions on Power Electronics*, vol. 6, no. 3, pp. 398–407, Jul. 1991.
- [86] R. W. A. A. De Doncker, D. M. Divan, and M. H. Kheraluwala, "A three-phase soft-switched high-power-density DC/DC converter for high-power applications," *IEEE Transactions on Industry Applications*, vol.

27, no. 1, pp. 63–73, Jan. 1991.

- [87] G. Xu, W. Yu, D. Griffith, N. Golmie and P. Moulema, "Toward Integrating Distributed Energy Resources and Storage Devices in Smart Grid," in *IEEE Internet of Things Journal*, vol. 4, no. 1, pp. 192-204, Feb. 2017.
- [88] J. J. Mesas, L. Monjo, L. Sainz and J. Pedra, "Study of MVDC system benchmark networks," 2015 International Symposium on Smart Electric Distribution Systems and Technologies (EDST), Vienna, 2015, pp. 235-240.
- [89] G. Byeon, S. Kim, J. Kim, J. Jeon and G. Kim, "Cooperative ESS management strategy for stable islanded operations in a bipolar-type LVDC system," 2015 International Symposium on Smart Electric Distribution Systems and Technologies (EDST), Vienna, 2015, pp. 290-295.
- [90] A. Agrawal and R. Gupta, "Hybrid DERs enabled residential microgrid system with MVDC and LVDC bus layout facilities," 2018 IEEMA Engineer Infinite Conference (eTechNXT), New Delhi, 2018, pp. 1-6.
- [91] M. R. Islam, M. A. Rahman, K. M. Muttaqi and D. Sutanto, "A New Magnetic-Linked Converter for Grid Integration of Offshore Wind Turbines Through MVDC Transmission," *IEEE Transactions on Applied Superconductivity*, vol. 29, no. 2, pp. 1-5, Art no. 5400905, March 2019.
- [92] M. Stieneker and R. W. De Doncker, "Medium-voltage DC distribution grids in urban areas", 2016 IEEE 7th International Symposium on Power Electronics for Distributed Generation Systems (PEDG 2016) in Vancouver, Canada, June 27-30, 2016
- [93] J. K. Steinke, P. Maibach, G. Ortiz, F. Canales, P. Steimer, "MVDC Applications and Technology", PCIM 2019, Nuremberg
- [94] "IEEE standard for power electronics open system interfaces in zonal electrical distribution systems rated above 100 kW," *IEEE Std 1826-2012*, pp. 1–46, June 2012.
- [95] Corti Matteo, "Introduction of DC and Storage Systems in Shipboard Electric Systems," Ph.D. dissertation, Energy Department, Politecnico di Milano, 2017.
- [96] R. Mo, R. Li and H. Li, "Isolated modular multilevel (IMM) DC/DC converter with energy storage and active filter function for shipboard MVDC system applications," 2015 IEEE Electric Ship Technologies Symposium (ESTS), 2015, pp. 113-117.
- [97] X. Xiang, X. Zhang, G. P. Chaffey and T. C. Green, "An Isolated Resonant Mode Modular Converter With Flexible Modulation and Variety of Configurations for MVDC Application," in *IEEE Transactions on Power Delivery*, vol. 33, no. 1, pp. 508-519, Feb. 2018
- [98] B. Zhao, Q. Song, J. Li, and W. Liu, "High-Frequency-Link DC Transformer Based on Switched Capacitor for Medium-Voltage DC Power Distribution Application," *IEEE Trans. Power Electron.*, vol. 31, no. 7, pp. 4766–4777, Jul. 2016.
- [99] Y. Shi and H. Li, "Isolated Modular Multilevel DC–DC Converter with DC Fault Current Control Capability Based on Current-Fed Dual Active Bridge for MVDC Application," in *IEEE Transactions on Power Electronics*, vol. 33, no. 3, pp. 2145-2161, March 2018.
- [100] R. Mo, H. Li and Y. Shi, "A Phase-Shifted Square Wave Modulation (PS-SWM) for Modular Multilevel Converter (MMC) and DC Transformer for Medium Voltage Applications," in *IEEE Transactions on Power Electronics*, vol. 34, no. 7, pp. 6004-6008, July 2019.
- [101] X. Xiang, X. Zhang, T. Luth, and T. C. Green, "A Compact Modular Multilevel DC–DC Converter for High Step-Ratio MV and HV Use", *IEEE Trans. Power Electron.*, vol. 65, no. 9, pp. 7060–7071, Sep. 2018.
- [102] B. Zhao, Q. Song, J. Li, and X. Xu, "Comparative Analysis of Multilevel-High-Frequency-Link and Multilevel-DC-Link DC–DC Transformers Based on MMC and Dual-Active Bridge for MVDC Application", *IEEE Trans. Power Electron.*, vol. 33, no. 3, pp. 2035–2049, Mar. 2018.
- [103] D. Yadeo, P. Chaturvedi and S. K. Saketi, "A New Five Level Dual Active Bridge DC-DC Converter for Solid State Transformer", 2018 IEEE International Conference on Power Electronics, Drives and Energy Systems (PEDES), Chennai, India, 2018, pp. 1-5.
- [104] S. Kim, H. Kang, H. Cha, S. Jeong and H. Kim, "Double step-down dual active bridge DC-DC converter," 2015 9th International Conference on Power Electronics and ECCE Asia (ICPE-ECCE Asia), Seoul, 2015, pp. 777-784.
- [105] B. Wu, M. Narimani, *High-Power Converters and AC Drives*, 2nd Edition. Wiley-IEEE Press. January, 2017.
- [106] X. Feng, J. Liu, and F. C. Lee, "Impedance specifications for stable DC distributed power systems," in

IEEE Transactions on Power Electronics, vol. 17, no. 2, pp. 157-162, March 2002.

- [107] Girinon, S., et al. "Analytical input filter design in DC distributed power systems approach taking stability and quality criteria into account." 2009 13th European Conference on Power Electronics and Applications, IEEE, 2009.
- [108] P. Magne, B. Nahid-Mobarakeh and S. Pierfederici, "General Active Global Stabilization of Multiloads DC-Power Networks," in IEEE Transactions on Power Electronics, vol. 27, no. 4, pp. 1788-1798, April 2012.
- [109] M. E. Baran and N. R. Mahajan, "DC distribution for industrial systems: opportunities and challenges", in IEEE Transactions on Industry Applications, vol. 39, no. 6, pp. 1596-1601, Nov.-Dec. 2003
- [110] X. Yang, H. Hu, Y. Ge, S. Aatif, Z. He and S. Gao, "An Improved Droop Control Strategy for VSC-Based MVDC Traction Power Supply System", in IEEE Transactions on Industry Applications, vol. 54, no. 5, pp. 5173-5186, Sept.-Oct. 2018
- [111] J. F. Hansen and F. Wendt, "History and State of the Art in Commercial Electric Ship Propulsion, Integrated Power Systems, and Future Trends," in Proceedings of the IEEE, vol. 103, no. 12, pp. 2229-2242, Dec. 2015
- [112] Z. Shajari, J. M. Guerrero and M. H. Javidi, "Operation Management for Next-Generation of MVDC Shipboard Microgrids," 2020 International Conference on Smart Energy Systems and Technologies (SEST), Istanbul, Turkey, 2020, pp. 1-6
- [113] P. K. Steimer and O. Apeldoorn, "Medium Voltage Power Conversion Technology for efficient Windpark Power Collection Grids," in 2nd IEEE International Symposium on Power Electronics for Distributed Generation Systems, Hefei, 2010.
- [114] P. C. Kjaer, "MF transformer-based series-resonant converter for DC wind turbine", ECPE Workshop "New Technologies for Medium-Frequency Solid-State Transformers", Lausanne, 14-15 February 2019
- [115] H. Siddique and R. W. De Doncker, "Evaluation of DC Collector-Grid Configuration for Large Photovoltaic Parks," IEEE Transaction on Power Delivery, vol. 33, no. 1, pp. 311-320, 2018.
- [116] E. Wesoff, "First Solar Postpones Its Move to a Medium-Voltage DC Utility Solar Architecture", Greentech Media, 13.02.2017.
- [117] Z. Ma, et al., "Study on the Feasibility of MVDC", CIGRE WG C6.31, CIGRE Paris Session 2018.
- [118] MVDC Technology Study – Market Opportunities and Economic Impact, TNEI, 2015.02.
- [119] G. F. Reed, B. M. Grainger, A. R. Sparacino and Z. Mao, "Ship to Grid: Medium-Voltage DC Concepts in Theory and Practice," in IEEE Power and Energy Magazine, vol. 10, no. 6, pp. 70-79, Nov.-Dec. 2012
- [120] D. Dong et al., "Control and operation of medium-voltage high-power bi-directional resonant DC-DC converters in shipboard dc distribution systems," 2016 IEEE Energy Conversion Congress and Exposition (ECCE), Milwaukee, WI, 2016, pp. 1-9
- [121] "IEEE Recommended Practice for 1 kV to 35 kV Medium-Voltage DC Power Systems on Ships," in IEEE Std 1709-2018 (Revision of IEEE Std 1709-2010), 27 Sept. 2018.
- [122] D. Bosich, A. Vicenzutti, R. Pelaschiar, R. Menis and G. Sulligoi, "Toward the future: The MVDC large ship research program," 2015 AEIT International Annual Conference (AEIT), 2015, pp. 1-6
- [123] VDE|ETG Studie Gleichspannung in der elektrischen Energieverteilung, 2019.
- [124] EN 50123: Railway applications – Fixed installations – D.C. switchgear.
- [125] EN 50328: Railway applications – Fixed installations – Electronic power converters for substations.
- [126] A. Gómez-Expósito, J. M. Mauricio, and J. M. Maza-Ortega, "VSC-based MVDC Railway Electrification System," IEEE Trans. Power Del., vol. 29, no. 1, pp. 422–431, Feb. 2014.
- [127] C. Yuan, M. A. Haj-ahmed, and M. S. Illindala, "Protection Strategies for Medium-Voltage Direct-Current Microgrid at a Remote Area Mine Site", IEEE Transactions on Industry Applications, vol. 51, no. 4, pp. 2846 – 2853, July/August 2015